HOKKAIDO UNIVERSITY

Title	Geomorphological Study on the Periglacial Slope Deposits in the Northern Hidaka Mountains, Hokkaido, Japan
Author(s)	Yamamoto, Kenshiro
Citation	Environmental science, Hokkaido University : journal of the Graduate School of Environmental Science, Hokkaido University, Sapporo, 14(1), 17-89
Issue Date	1991-09-30
Doc URL	http://hdl.handle.net/2115/37262
Type	bulletin (article)
File Information	14(1)_17-89.pdf

Instructions for use

Hokkaido University Collection of Scholarly and Academic Papers : HUSCAP

Environ. Sci., Hokkaido University	14 (1)	17~89	Sept. 1991

Geomorphological Study on the Periglacial Slope Deposits in the Northern Hidaka Mountains, Hokkaido, Japan

Kenshiro Yamamoto
Laboratory of Fundamental Research, Division of Environmental Structure,
Graduate School of Environmental Science,
Hokkaido University

Contents

Part I MACRO FABRICS OF THE PERIGLACIAL SLOPE DEPOSITS

I. INTRODUCTION

I—1. Significance and Purpose of the Study

Smooth and gently inclined crest and mountain slopes usually composed of coarse rubbly deposits have been generally regarded as fossil periglacial slopes in Central and Northern Japan. However, sedimentological characteristics such as fabrics, clast size and shape and textural properties of these slope deposits have not been examined in detail.

Furthermore, the discussion on the periglacial slope formation in Holocene has been lacked except in a few studies, although much attention has been paid for the periglacial slope formation in the last glacial time.

It is certain that the present periglacial slope processes work dominantly only in the areas above the timber line. However, there is a good possibility that the periglacial mass movement such as solifluction occurred in Holocene on the lower mountain slopes in Northern Japan, especially in Hokkaido.

The purposes of this study are 1) to identify periglacial slope deposits on the basis of a clast fabric analysis; 2) to describe the sedimentological characteristics of periglacial slope deposits; and 3) to determine the periods of solifluction since the last glacial time by using different tephra layers.

For these purposes, I have chosen the eastern slope of the Northern Hidaka Mountains for the study area, since the "fossil periglacial slope" has been widely recognized there, and besides many Holocene tephra layers are intercalated in the slope deposits.

I will discuss the macro fabrics of slope deposits in Part I, which is composed of Chapters I to IV. Part II, which is composed of Chapters V to IX, will be devoted to the description of sedimentological characteristics and the periods of solifluction.

After summarizing, in the First Chapter, the previous studies on periglacial slope deposits in Japan from the view-points of chronological and quantitative studies, the Second Chapter introduces the methods of macro fabric measurement, and discusses the relation among each parameter.

The Third Chapter treats the effects of clast size and shape on the macro fabrics in the slope deposits.

The Forth Chapter compares the macro fabrics of periglacial slope deposits and non-periglacial ones by two- and three-dimensional fabric analyses. The comparison leads to the general conclusion of Part I, which proves that the three-dimensional fabric analysis is the best method to distinguish the periglacial slope deposits from non-periglacial ones.

The Fifth Chapter describes the topographical and geological settings of the study area, and the Sixth Chapters introduces the measuring methods of the quantitative and chronological characteristics of the periglacial slope deposits.

The Seventh Chapter summarizes the results of the measurements of quantitative characteristics and the Eighth Chapter describes and discusses the periods of periglacial mass movement in the study area.

The Ninth Chapter is the last one in which I discuss both macro fabrics of periglacial slope deposits and the effects of rock types on the sedimentary characteristics and the periods of solifluction.

I−2. Review of Chronological and Quantitative Studies on the Fossil Periglacial Slope Deposits in Japan

A chronological approach to fossil periglacial slope formation in Japan was opened by the application of tephrochronology in the 1960's. Wako (1961, 1963, 1966) took notice of gentle slopes which continues smoothly to some fluvial terraces in Northeastern Hokkaido. Later, he found similar gentle slopes in Northeastern Honshu, and concluded that they are cryopediments (Wako, 1963) which were formed chiefly by solifluction and related processes under the cold climate of the late Pleistocene (Wako, 1966).

The idea of cryopediment formation in Northern Japan was indirectly supported by the discoveries of fossil periglacial phenomena: for example, Suzuki et al. (1964) reported the cryoturbation in tephra layers and argued its significance.

The cryopediment studies by Wako were the first application of tephrochronology to the chronological study of the fossil periglacial slopes. Such studies based on tephrochronology were widely attempted later in the Northern half of Japan (e.g., Koaze et al, 1974; Hirakawa, 1977; Inoue et al, 1981), and especially in cooperation with tephrochronological studies of glaciation (e.g., Kobayashi, 1965; Ono and Hirakawa, 1975). They also contributed to the reconstruction of climatic and morphogenetic environments of the Last Glacial and Holocene ages (e.g., Machida, 1980; Nogami et al, 1980; Ono, 1984; Iwata, 1986).

Tamura and Miura (1968, 1971) recognized various kinds of phenomena which indicate former mass movements on tephra profiles in the northern margin of the Kitakami Highlands, northeastern Japan. In that area, the tephra horizons which indicated the periods of slope instability were investigated by means of the recognition of the lack of marker-tephras whose ages range from about 100,000 y.B.P. (or older than this age) to 1, 000 y.B.P.. The periods of slope instability were considered to be mostly related to the cold climate in the late Pleistocene.

Since then, chronological studies of fossil periglacial slope formation in reference to climatic change have received much attention in Quaternary geomorphology. Numbers of such studies have been accumulated in several tephra-covered areas, particularly in the Kitakami Highlands and their environs (Sugawara, 1973; Iso, 1974; Endo, 1977; Higaki, 1980; Inoue et al., 1981; Sawaguchi, 1984; Saijo, 1987).

In several mountains in the north and west of the Kanto Plain, smooth crest- and upper side-slopes composed of coarse rubbly deposits were proved to have been formed under periglacial condition of mostly Last Glacial and partly early Postglacial ages (e.g., Shimizu, 1983; Takada, 1986). The discussion is based on the facies observation of slope deposits, marker-tephra findings in the deposits, and the morphological studies of the slopes.

Coarse colluvial materials intercalated in peaty deposits are also indicative of an unstable condition of slopes surrounding the peat swamp. Using radiocarbon dating and pollen analysis of many horizons of peat in several locations in Northeastern Honshu,

Miyagi et al. (1971, 1981) and Nakayama and Miyagi (1984) discussed the history of mass movement and climatic changes in late Quaternary.

Higaki (1987) defined seven slope units which constitute the watershed in the Kitakami Highlands through morphological observation, and clarified the processes and age of the formation of each unit in terms of tephrochronology and facies analysis of the slope deposits. His study indicated the significance of cryogenic slope processes which prevailed in the early and later periods of the Last Glacial age as well as in older ages compared with the Last Interglacial.

In a similar way, I investigated the gentle slopes stretching behind fluvial terraces around Mt. Syokanbetsudake, West-Central Hokkaido (Yamamoto, 1987). The gentle slopes were classified into two surfaces (gentle slopes I and II). They were considered to have been formed under a colder climatic condition than at present, based on the sedimentological data involving fabric analysis. The formation age of gentle slope I was estimated to be older than 40,000 or 40,000−20,000 y.B.P., and that of gentle slope II, between 20,000 and 5,000 y.B.P., respectively.

Furthermore, I examined the ages and processes concerning the formation of fossil periglacial slopes, ranging from 500 m to 1,600 m in altitude in the Hidaka Mountains, East-Central Hokkaido, through both tephrochronological observation and sedimentological analysis of deposits (Yamamoto, 1989a).

Shimizu (1989) also studied in detail the facies of slope deposits which are, or not, associated with tephra of various modes of occurrence in the mountain slopes adjacent to the area studied by Yamamoto (1989a). The conclusion of these studies suggested that the periglacial slope formation ceased in the later time in the higher altitude according to a time-lag in Postglacial warming.

Win Maung and Toyoshima (1989) made another contribution to the interpretation of the mode of occurrence of slope deposits with intercalated tephra layers, and discussed the denudation of terrace scarps by certain periglacial processes in the early and late periods of the Last Glacial age in the area of western Sendai, Northern Honshu.

A gentle mountain slope which has the appearance of "fossil periglacial slope" was also reported in the Southwestern Japan. Akagi (1965) investigated piedmont gentle slopes in parts of Southwestern and Central Japan. He regarded them as the pediments which were formed under a somewhat drier climate. But, Tsurumi and Nogami (1965) refuted his conclusion on the basis of the tephrochronological data.

Tanaka et al. (1982, 1986) and Nomura and Tanaka (1989) surveyed several types of piedmont gentle slopes in the inland of Hyogo Prefecture, Southwestern Honshu, where the prevalence of periglacial environment in the Last Glacial age had been considered doubtful. Analyzing marker-tephras intercalated in colluvial deposits as well as the deposits and the slope forms, they concluded that most slopes which they investigated were formed under the influence of periglacial processes in the Last Glacial age.

Oguchi (1986) recognized smooth depositional slopes and debris slopes on the caldera wall of the Aso volcano, central Kyusyu, and concluded that they were formed by the periglacial slow mass movement.

The slope deposits discussed in these four examples (Akagi, 1965; Tanaka et al., 1982;

1986; Nomura and Tanaka, 1989; Oguchi, 1986) are located at an altitude lower than the estimated forest limit during the Last Glacial age inferred by Kaizuka (1969), Koaze (1972), Ohmori (1979) and Ono (1984). The detailed examination of the slope deposits, by the methods including fabric analysis, will be necessary to evaluate their conclusions.

Although many studies mentioned above were aimed to estimate the formation age of fossil periglacial slopes in reference to the climatic change, there were no studies except ours (Yamamoto, 1989a, 1990) that examined sedimentologically in detail the deposits on the slopes which were regarded as fossil periglacial ones.

II. MEASURING METHODS OF MACRO FABRICS

II−1. Two-Dimensional Vector Analysis

II−1−1. Vector magnitude method

Vector magnitude method (Krumbein, 1931) which is applied to the orientation measurement of clasts is as follows:

$$\text{N}-\text{S component}=\Sigma n \cos 2\theta$$
$$\text{E}-\text{W component}=\Sigma n \sin 2\theta$$
$$r=(\Sigma n \sin 2\theta)+(\Sigma n \cos 2\theta)$$
$$\text{Vector Magnitude}(\%)=r/\Sigma n \times 100$$
$$\text{Vector Mean(degree)}=1/2 \arctan (\Sigma n \sin 2\theta)/(\Sigma n \cos 2\theta)$$

(where n is the number of observations. North is defined as 0 degree and the degree is calculated clockwise.)

These calculations are performed on either grouped or ungrouped data. The vector mean is interpreted as a measure of the central tendency of the distribution, such as the preferred orientation direction of the long axes of clasts.

The vector magnitude varies from 0 per cent to 100 per cent. A random distribution of orientations will give a magnitude of 0 per cent. Contrary to this, a case of 100 per cent means that all observed vectors have exactly the same phase, or in the case of grouped data, they all lie within the same azimuth group.

I will use the abbreviations "V. Me." and "V. Mg.", instead of Vector Mean and Vector Magnitude, respectively.

II−1−2. Vector strength method

Vector strength method is proposed by Thomas (1967). This method has an advantage which is easier for calculation of fabric data than other methods. The method of calculations is as follows:

$$\text{Vector Strength}(\%)=100-[(X-X1)+(X-X2)+X-X3)+\cdots+(X-Xn)]\times 100/K$$

where:—

$$X=(X1+X2+X3+\cdots Xn)/n$$

X1, X2, X3,…Xn= Azimuths of observed distribution

and for common sample size, k equals:

where n=10, k=450

n=25, k=1125

n=50, k=2250

n=100, k=4500

Although this method is available for samples with concentrated orientation, it is useless for those with random orientation.

In the following description, "V. St." is used as an abbreviation of Vector Strength.

II—2. Three-Dimensional Vector Analysis

II—2—1. Eigen value method

This analytical procedure was proposed by Scheidegger(1965). It can be briefly summarized as follows:

Individual observations are regarded as unit vectors. The attitude of the ith observation of N observations is given by direction cosines li, mi, ni. A 3×3 matrix of the sums of cross products of the direction cosines is constructed as follows:

$$a=\begin{pmatrix} \Sigma li\times li & \Sigma li\times mi & \Sigma li\times ni \\ \Sigma mi\times li & \Sigma mi\times mi & \Sigma mi\times ni \\ \Sigma ni\times li & \Sigma ni\times mi & \Sigma ni\times ni \end{pmatrix}$$

A normalized form of this matrix

$$A=a/N$$

was termed the orientation tensor by Scheidegger(1965). Three eigenvectors [v1, v2, v3] and the corresponding eigen values [$\lambda 1$, $\lambda 2$, $\lambda 3$] are computed. Eigen vector v1 is an estimate of the distribution mean, and eigen vector v3 is an estimate of the pole to the best-fit girdle to the distribution, provided that the data do not form an axially symmetric cluster.

Eigen values $\lambda 1$, $\lambda 2$, and $\lambda 3$ have the property

$$\lambda 1+\lambda 2+\lambda 3=N.$$

They are more useful in a normalized form

$$Si=\lambda\ i/N$$

so that

$$S1+S2+S3=1.$$

In referring to S1, a high value means a high degree of vector concentration.

II—2—2. Logarithmic ratio plot method

Logarithmic ratio plot method was proposed by Woodcock (1977). This method uses a graph with a plot of ln(S2/S3) against ln(S1/S2). On the graph, the axial girdles (=the

x-axis) plot where S2/S3, that is, along the line ln(S2/S3)=0. The axial clusters (=the y-axis) plot where S1=S2, that is, along the line ln(S1/S2)=0. The remainder of the graph is occupied by plots that have both girdle and cluster tendencies. These can be quantified by a parameter, K, where

$K=\ln(S1/S2)/\ln(S2/S3)$.

K gives the gradient of straight lines radiating from the origin. Points that have equal girdle and cluster tendencies are plotted on the lines where K=1, that is, where S1/S2=S2/S3. Girdle plots are below this line in the field where $0 \leqq K < 1$, and cluster plots are above, where $1 < K \leqq \infty$.

Uniform distributions are plotted at the graph's origin, random distributions are near the origin, and those with increasingly strong preferred orientation are progressively farther from the origin. Thus, a parameter C, where

$C=\ln(S1/S3)$,

is a measure of the strength of the preferred orientation.

A logarithmic ratio plot provides a convenient representation of distribution shape that is comparable in form to strain plots.

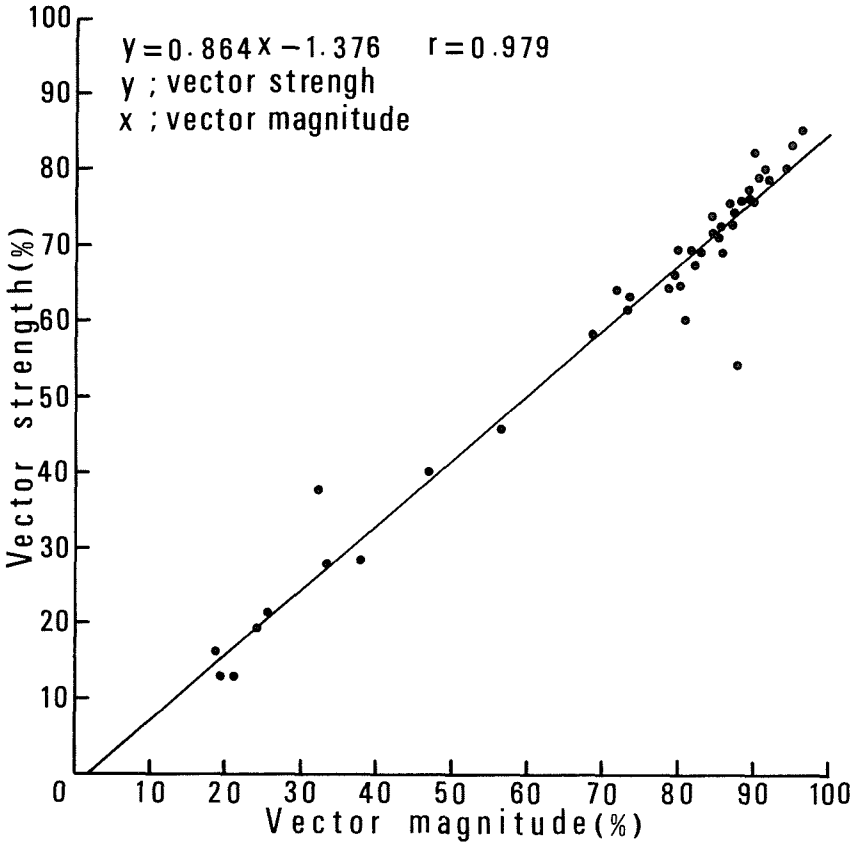

Figure 1 Relationship between vector strength(%) and vector magnitude(%).
Data from slope deposits in the Northern Hidaka Mountains and fan deposits in the Tokachi Plain.

Vector magnitude, S1 and C values become larger for a stronger fabric (=have a good preferred orientation), smaller values for a weaker fabric (=have no good preferred orientation).

II–3. Discussion: Relation among the individual fabric strengths

Figure 1 shows a relation between V.St.(%) and V.Mg.(%). Both values of V.St. and V.Mg. are derived from data of the fossil periglacial slope and fan deposits described in the following chapter (see Tables 13 and 14). These two values are closely correlated with each other, and the regression coefficient is quite high. The result indicates that V.St. can be transformed into V.Mg. by a regression equation shown in Figure 1.

Figure 2 shows a relation between V.Mg. and S1 for five grouped data. Lines from 1 to 5 show a linear regression of each grouped datum. Grouped data of 1 and 2 are of periglacial origin: 1 is 2,350 clasts' fabrics described in the next chapter (see Table 4), and 2 is those measured in order of an a-axis length (See Table 1). Grouped data from 3 to 5 are of non-periglacial origin and were calculated by Mills (1983, 1984, 1986): 1, 2 and 3 are mudflow deposits, volcanic mud flow deposits at Mt. St. Helens and soil creep deposits, respectively. The figure indicates that there is a wide overlap of V.Mg. between periglacial

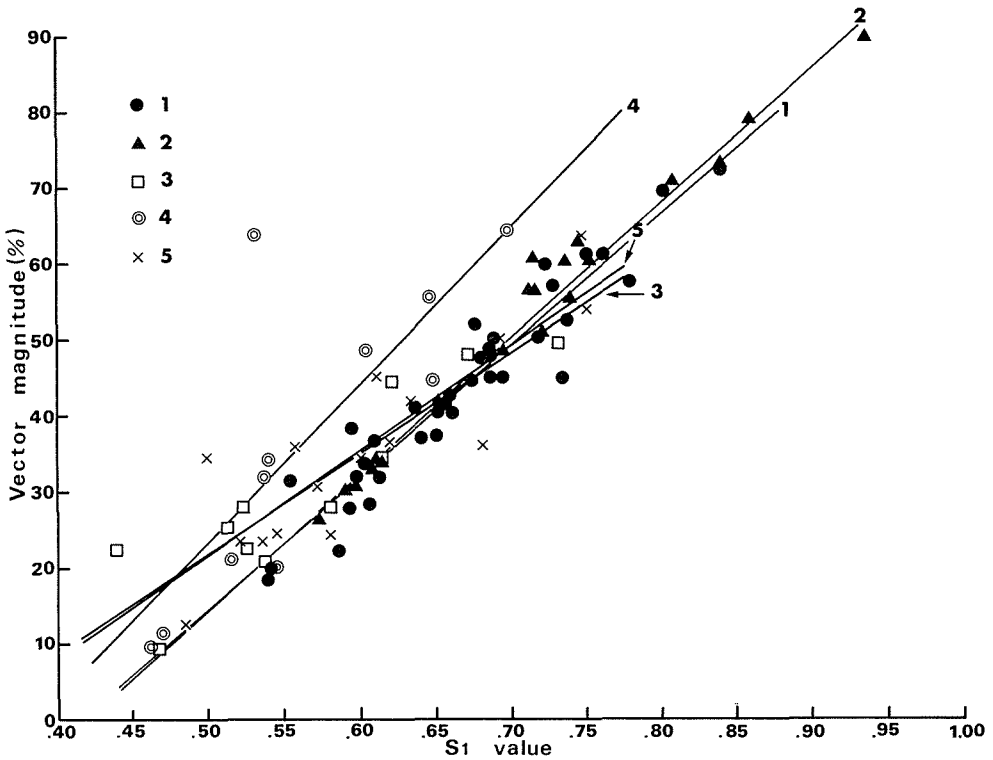

Figure 2 Relationship between vector magnitude(%) and S1 value.
Data source; 1: Yamamoto (1989b, data listed in Table 4), 2: Yamamoto (1989b, data listed in Table 1), 3: Mills (1986), 4: Mills (1984), 5:Mills (1983).

and non-periglacial deposits, but that there is a small overlap of SI between the former and the latter. This fact suggests that the distinction of periglacial slope deposits from non-periglacial slope deposits is possible by the three-dimensional fabric analysis.

III. MACRO FABRICS AFFECTED BY CLAST SIZE AND SHAPE

III−1. Introduction

The azimuths and dips of clasts, commonly referred to as fabrics, have been utilized in numerous geomorphic and sedimentological studies in order to determine flow direction and sedimentary processes in various environments. Although the fabrics of fluvial and glacial sediments have been studied extensively, slope deposits especially under the periglacial environment have received less attention. Under such conditions, there is a considerable difference in opinion as to the significance of fabrics in viscous fluid deposits.

Drake (1974) insisted that the clast shape influences its fabrics in viscous fluid deposits. In contrast to this, Mills (1977) indicated that there is little relation between the clast fabric and the clast size or shape in viscous fluid deposits.

Although many investigators (e.g., Holmes, 1941; Harrison, 1957; Anderson and King, 1968; Kruger, 1970) agreed with Drake, there seems to be no consensus among investigators as to the nature of this relationship. The contradiction between Drake and Mills is probably due to a shortage of the number of investigated clasts, since an apparent orientation preference may arise by chance when the sampling number is small.

Few fabric studies have been done in Japan on slope deposits, except for two- and three-dimensional fabric analyses of some slope deposits (Yamamoto, 1989a; 1989b; 1990).

The purpose of this chapter is (1) to determine the processes related to material transportation on the slope by means of two- and three-dimensional fabric analyses and (2) to evaluate the influence of clast size and shape in slope deposits. For this purpose, I selected the eastern slope in the Northern Hidaka Mountains, Hokkaido, Japan, and measured the orientation and the shape of clasts which were excavated from the slope deposits.

III−2. Relation between Fabrics and Clast Size and Shape

III−2−1. Measuring site and methods

The study site is located at approximately 3km northeast of Nissho Pass in central Hokkaido (Figure 3). The altitude of the site is 498m a.s.l. The slope angle is 14 degrees, and the slope orientation (north is defined as 0 degree, and calculated in clockwise) is 3 degrees. Slope deposits, more than 1−5m thick, are derived from the granite basement and are underlain by Ta-d pumice which fell at about 9,000 y.B.P. They are poorly sorted and composed of angular-subangular gravels (Photo 1). Two- and three-dimensional fabric analyses supported the idea that the slope deposits are of periglacial origin, probably transported by solifluction (Yamamoto, 1989a; 1990).

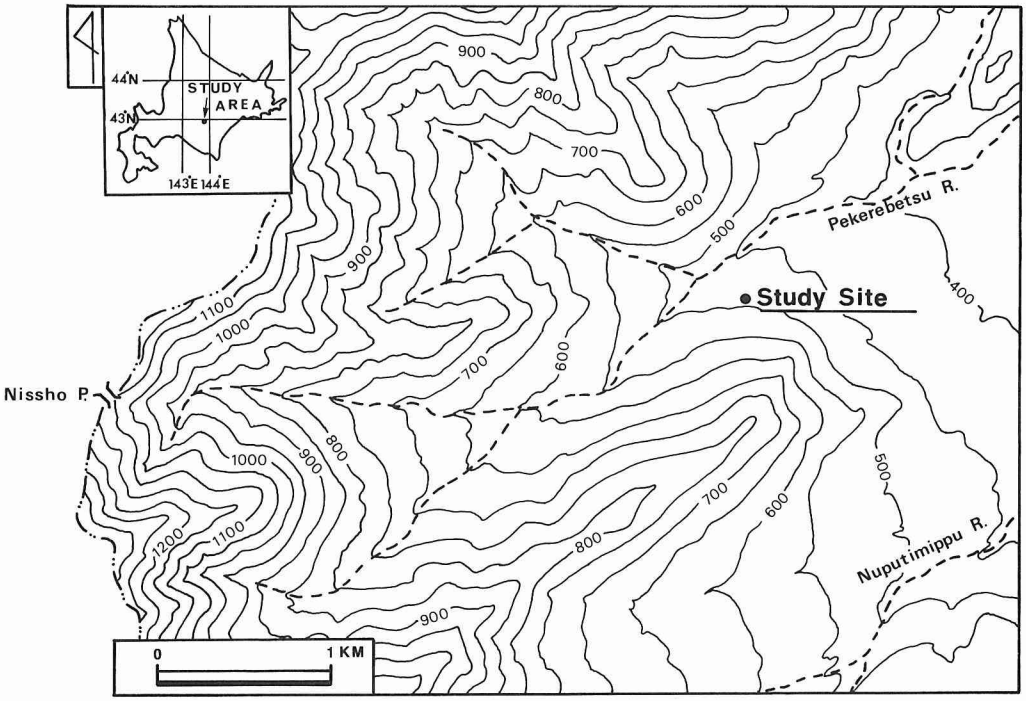

Figure 3 Map showing study site.

Photo. 1 Section at Loc.42.
Slope deposits, more than 1–5 m thick, are underlain by Ta-d.
Measure is 1 m long.

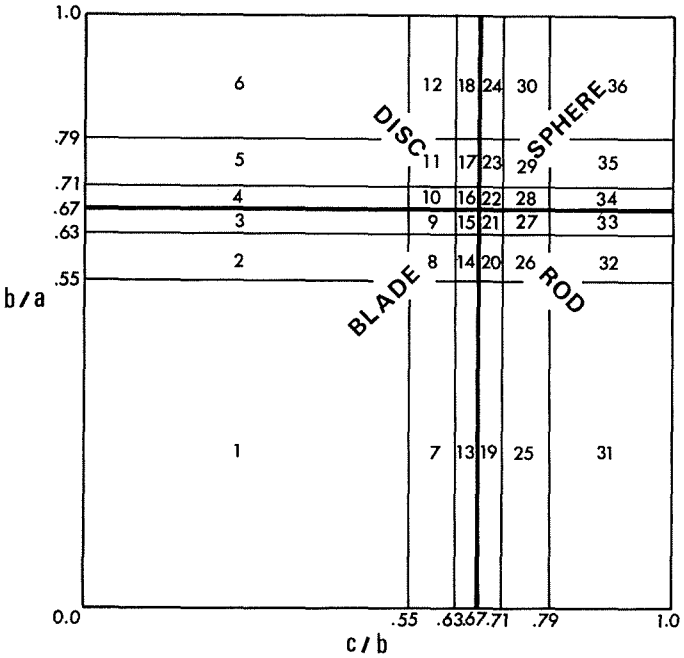

Figure 4 Categorical subdivisions of clast shape based on axis ratio of b/a and c/b.
Blade, Disc, Rod, and Sphere are subdivided by Zingg (1935).
Numbers indicate category subdivisions proposed by Drake (1974).

Azimuths and dips of the a-axis (long axis) of clasts were measured at the depth of 2–3 meters below the base of Ta-d horizon, and a total of 2,350 clasts, with the length of the a-axis over 2 cm, was measured. The mean orientation and fabric strength were calculated by Krumbein's vector magnitude and Scheidegger's eigen value methods.

The relationship of clast shape to fabric was investigated by applying Drake's (1974) method. First, the clast shape was classified by an axial ratio into four types: Blade, Disc, Rod and Sphere which are defined by Zingg (1935). Secondly, the clast shape was classified by the detailed axial ratio into Drake's categories (Figure 4). The fabric characteristics of each category were evaluated separately.

The relationship of axial length to fabric was also investigated. The correlation between the fabric and the a-axis length was calculated in order to determine whether any significant relationship existed. A total of 2,350 clasts was classified by the length of the a-axis into 20 classes and the fabric characteristics of each class were evaluated separately. Although statistically the difference of the number of clasts measured in each category and class influence significance level of fabric strength value are related to the null hypothesis that deposits have a random fabric (=have no preferred orientation), the difference dose not have any influence at all on the fabric characteristics theoretically (Curray, 1956; Anderson and Stephens, 1972).

Table 1 Characteristics of the fabrics in each class of a-axis length.

Clast size		N	Clast shape				Clast fabric analysis								
Length of a-axis (cm)	Class mark (cm)		B(%)	D(%)	R(%)	S(%)	two-dimension V.Mg. (%)	$\Delta\theta$H1 (°)	three-dimention S1	S2	S3	C	K	$\Delta\theta$H2 (°)	$\Delta\theta$P (°)
2≦a <3	2.5	111	6.3	41.4	12.6	39.6	29.5	1.1	.588	.317	.095	1.827	0.513	1.4	− 5.6
3≦a <4	3.5	437	11.6	41.2	18.8	28.6	33.9	0.9	.610	.306	.084	1.982	0.535	1.9	− 6.2
4≦a <5	4.5	412	11.4	45.0	22.5	21.1	33.6	3.9	.616	.295	.089	1.932	0.615	3.5	− 5.9
5≦a <6	5.5	331	15.7	45.0	19.0	20.2	33.3	0.0	.600	.299	.101	1.786	0.638	2.0	− 8.8
6≦a <7	6.5	199	13.1	46.2	19.6	21.1	26.8	5.0	.572	.323	.105	1.697	0.508	4.8	− 9.0
7≦a <8	7.5	172	11.6	45.9	26.9	15.7	30.5	5.4	.596	.312	.092	1.862	0.533	5.0	− 8.1
8≦a <9	8.5	123	13.0	52.0	22.0	13.0	48.6	2.6	.691	.235	.074	2.241	0.930	1.8	− 5.6
9≦a <10	9.5	103	20.4	38.8	29.1	11.7	41.3	1.6	.655	.256	.085	2.042	0.829	2.3	−10.4
10≦a <11	10.5	64	23.4	35.9	29.7	10.9	56.2	1.1	.711	.213	.076	2.238	1.167	0.2	−10.4
11≦a <12	11.5	61	27.9	45.9	16.4	9.8	56.3	3.8	.716	.176	.111	1.860	3.265	2.9	−14.4
12≦a <13	12.5	49	26.5	49.0	16.3	8.2	62.5	1.0	.744	.170	.086	2.163	2.150	1.4	− 9.9
13≦a <14	13.5	43	32.6	34.9	30.2	2.3	60.1	2.5	.735	.182	.083	2.179	1.786	2.3	−13.0
14≦a <15	14.5	31	25.8	38.9	19.4	16.1	60.4	5.7	.720	.194	.086	2.122	1.612	7.4	−10.2
15≦a <16	15.5	31	32.3	41.9	19.4	6.5	70.6	6.5	.808	.138	.054	2.709	1.863	7.3	− 5.3
16≦a <18	17.0	49	32.7	44.9	20.4	2.9	50.7	0.7	.718	.225	.057	2.528	0.847	2.4	−12.1
18≦a <20	19.0	31	38.7	29.0	29.0	3.2	54.8	9.9	.737	.214	.049	2.717	0.833	8.9	−14.5
20≦a <24	22.0	30	36.7	30.0	30.0	3.3	78.7	13.9	.857	.104	.039	3.083	2.182	12.7	−14.7
24≦a <28	26.0	26	57.7	11.5	30.8	0.0	59.3	1.3	.752	.186	.062	2.486	1.285	0.7	−15.4
28≦a <32	30.0	21	52.4	28.6	19.0	0.0	72.3	7.5	.833	.136	.031	3.291	1.224	6.7	−10.4
32≦a	58.8	26	46.2	19.2	30.8	3.8	89.4	2.1	.929	.046	.025	3.625	4.860	1.6	− 2.3

N: number of observations, B: Blade, D: Disc, R: Rod, S: Sphere, V.Mg: Vector Magnitude, $\Delta\theta$H1: deviation of Vector Mean from slope orientation, $\Delta\theta$H2: deviation of V 1 azimuth from slope orientation, $\Delta\theta$p: deviation of V1 plunge from slope angle (−: upslope imbrication).

Table 2 Rerationship between each fabric strength and length of a-axis (class mark, cm).

y	x : length of a-axis (class mark, cm) equation of regression	
	linear regression	correlation
V.Mg.	y =1.132x +35,533	0.812
S_1	y =0.0016x +0.897	0.796
C	y =0.0564x +3.051	0.796

V.Mg.: vector magnitude (%).

III−2−2. Relationship between macro fabrics and clast size

Table 1 shows that the fabric characteristics of each class divided by the length of the a-axis. It indicates that the changes in vector magnitude, S1 and C, are closely related to the increase in the a-axis length.

The correlation between each fabric strength and the length of the a-axis (by class mark, see Table 1) is summarized in Table 2. All regression correlations show quite high

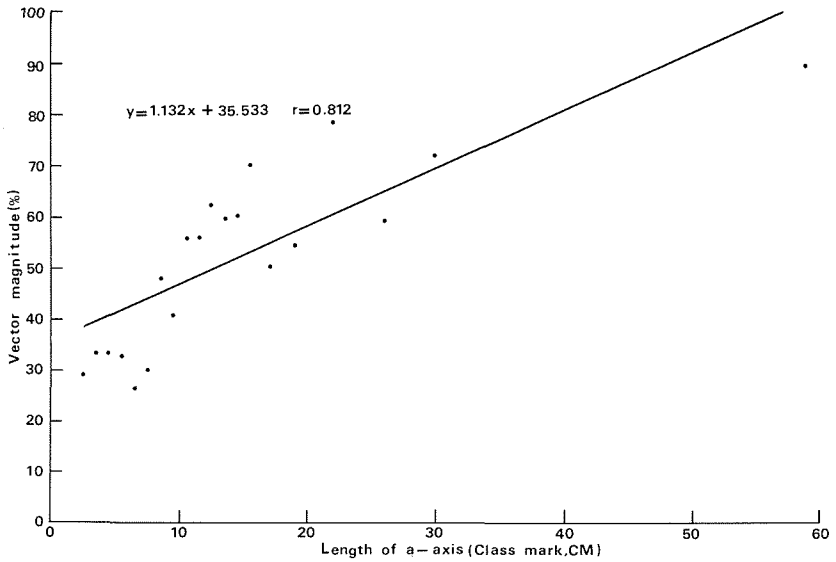

Figure 5 Plots of vector magnitude as a function of a-axis length.

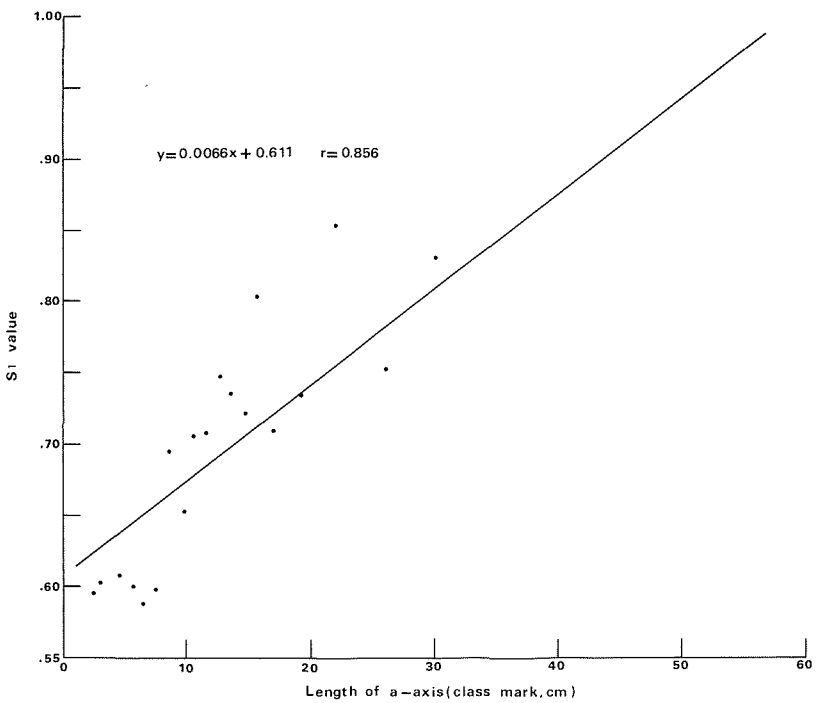

Figure 6 Plots of S1 value as a function of a-axis length.

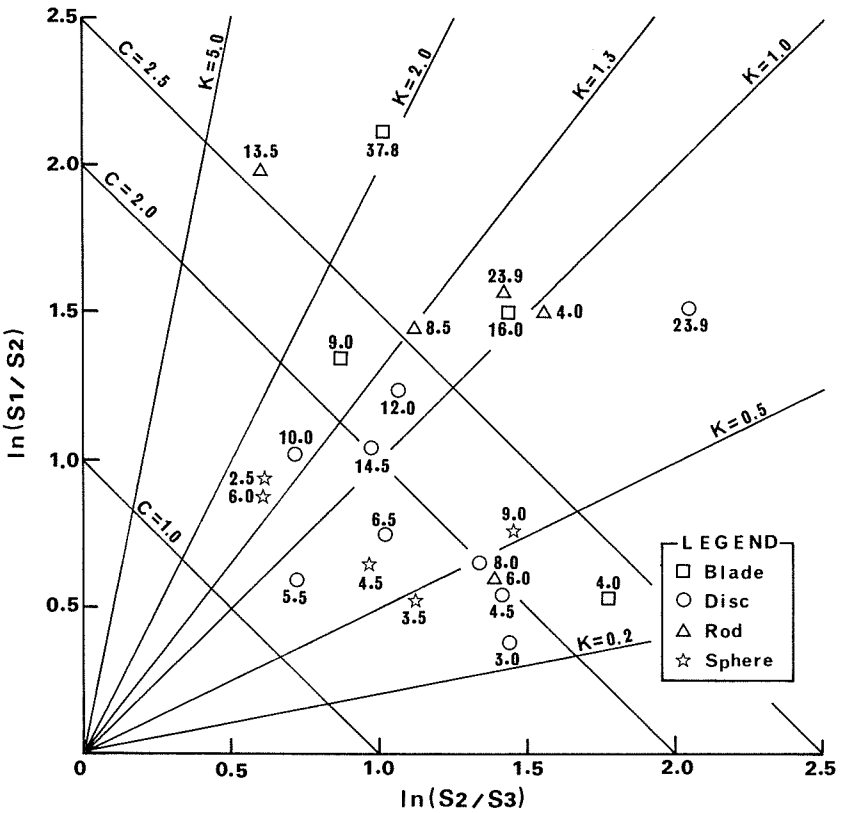

Figure 7 Logarithmic ratio plot of eigen values of each datum in classes classified by a-axis length.
Figure beside the symbol means class mark of a-axis length.

values. Figure 5 shows the correlation between the vector magnitude and the length of the a-axis, and Figure 6 shows the correlation between S1 value and the length of the a-axis. These figures indicate that the length of the a-axis is closely related to each fabric strength.

Figure 7 shows logarithmic ratio plots which were derived from the data listed in Table 1. The plots shown in Figure 7 range from the axial cluster to the transition girdle and cluster, and are distributed in a range with about $C>3.0$. The plots indicate that the class with a longer a-axis length has a higher C value.

This result indicates that the fabric strength increases as a function of the length of the a-axis.

The size and shape of clasts are mutually related with each other as shown in Table 1: clasts with a long a-axis have a tendency with a high content of Blade and Rod. In order to evaluate whether the size or shape affects more strongly to the clast fabrics, the changes in each fabric strength of clasts with the same shape against the a-axis length are analyzed (Table 3).

Table 3 Fabrics related to the increasing a-axis length in each clast shape.

Clast shape (Crake's category number)	Clast size		N	Clast fabric analysis									
	Length of a-axsis (cm)	Class mark (cm)		Two-dimension V.Mg. (%)	$\Delta\theta$H1 (°)	Three-dimensdon S1	S2	S3	C	K	$\Delta\theta$H2(°)	$\Delta\theta$P(°)	
Clade (1,7,13)	2≦ a <6	4.0	29	28.7	0.6	.592	.349	.059	2.299	0.299	1.8	− 5.4	
	6≦ a <12	9.0	26	68.3	11.8	.730	.190	.080	2.216	1.544	14.6	−15.5	
	12≦ a <20	16.0	17	66.4	3.0	.783	.175	.042	2.913	1.059	0.9	−11.6	
	20≦ a	37.8	23	80.2	4.7	.865	.101	.034	3.244	1.961	6.4	− 8.4	
Disk (6)	2≦ a <4	3.0	65	21.2	4.1	.541	.369	.090	1.788	0.273	4.9	−10.3	
	4≦ a <5	4.5	66	24.1	2.2	.579	.337	.084	1.935	0.390	3.5	− 3.4	
	5≦ a <6	5.5	43	38.8	5.8	.548	.304	.148	1.313	0.815	1.2	− 9.6	
	6≦ a <7	6.5	45	30.8	5.9	.616	.292	.092	1.902	0.646	15.7	− 9.8	
	7≦ a <9	8.0	49	27.6	5.2	.603	.314	.083	1.981	0.491	6.4	− 9.4	
	9≦ a <11	10.0	28	48.2	5.3	.651	.234	.115	1.736	1.442	0.1	−10.4	
	11≦ a <13	12.0	20	56.2	17.7	.719	.209	.072	2.300	1.165	13.7	−12.2	
	13≦ a <16	14.5	18	54.7	17.5	.673	.237	.090	2.007	1.080	19.2	− 8.1	
	16≦ a	23.9	16	68.1	14.9	.800	.177	.023	3.522	0.750	9.8	−14.1	
Rod (31)	3≦ a <5	4.0	28	61.9	4.7	.786	.176	.038	3.027	0.975	4.0	− 5.6	
	5≦ a <7	6.0	21	23.5	0.9	.594	.325	.081	1.991	0.434	2.2	−11.1	
	7≦ a <10	8.5	18	65.7	7.1	.761	.181	.058	2.574	1.264	6.9	−11.1	
	10≦ a <17	13.5	19	72.0	10.3	.823	.114	.063	2.567	3.360	6.0	−10.3	
	17≦ a	23.9	18	67.3	7.0	.795	.165	.040	2.985	1.117	4.6	−11.7	
Sphere (24,30,36)	2≦ a <3	2.5	24	31.7	0.9	.625	.243	.132	1.554	1.543	4.9	3.6	
	3≦ a <4	3.5	57	23.2	13.2	.562	.330	.108	1.647	0.478	9.6	− 2.5	
	4≦ a <5	4.5	45	27.2	18.7	.581	.303	.116	1.617	0.673	16.9	−12.2	
	5≦ a <7	6.0	40	37.1	0.3	.609	.253	.138	1.486	1.453	2.2	− 8.8	
	7≦ a	9.0	23	38.0	1.1	.637	.294	.069	2.224	0.534	4.3	− 2.2	

N: number of observations, V.Mg.: Vector Magnitude, $\Delta\theta$H1: deviation of Vector Mean from slope orientation, $\Delta\theta$H2: deviation of V 1 azimuth from slope orientation, $\Delta\theta$p: deviation of V1 plunge from slope angle (−: upslope imbrication).

Clasts are classified into 4 shapes based on Drake's definition. Drake's category numbers 1, 7 and 13 represent Blade type; the number 6, Disc type; the number 31, Rod type; and the numbers 24, 30, and 36, Sphere type. Classification of the a-axis length in each clast shape was done at random in order to obtain a sufficient number of samples in each class. The class mark in the longest a-axis class is a mean value of measured clasts, and in the classes with a shorter a-axis than the class mentioned above, the median is adopted as the class mark. It is recognized that the class with a longer a-axis has a higher fabric strength than the class with a shorter a-axis.

Figures 8, 9 and 10 show that the changes in each fabric strength against those of a -axis in different shapes. Vector magnitude shown in Figure 8 ranges from about 20% to 80%. The peak value of Blade, Disc and Sphere except Rod appeared in the class with the longest a-axis. Though the vector magnitude of Blade and Rod shows a higher value than that of Disc and Sphere in a range of the shorter a-axis length (less than about 20 cm), it is as much as the latter in a range of the longer a-axis (more than about 20 cm). Such tendencies of the changes in vector magnitude are also recognized in S1 and C values shown in Figures 9 and 10, respectively.

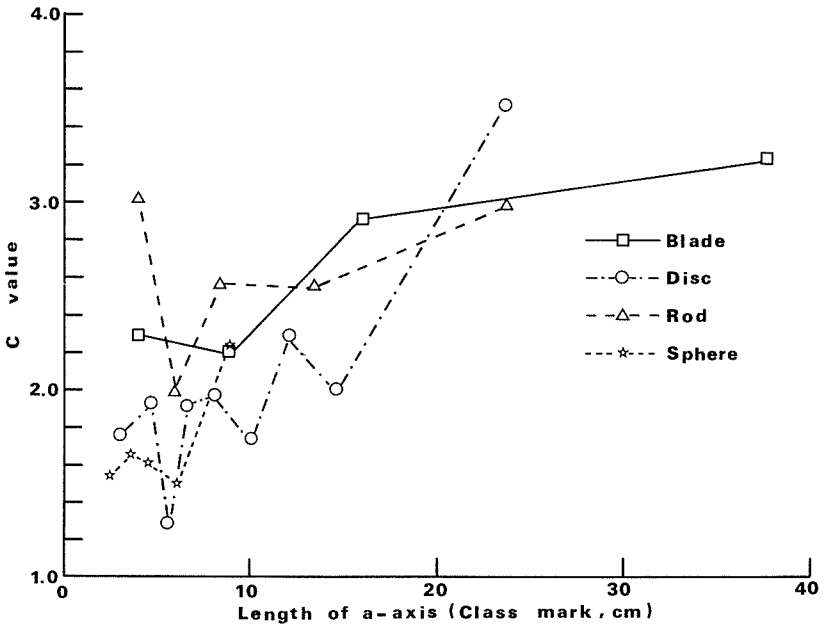

Figure 8 Changes in C value related to a-axis length.

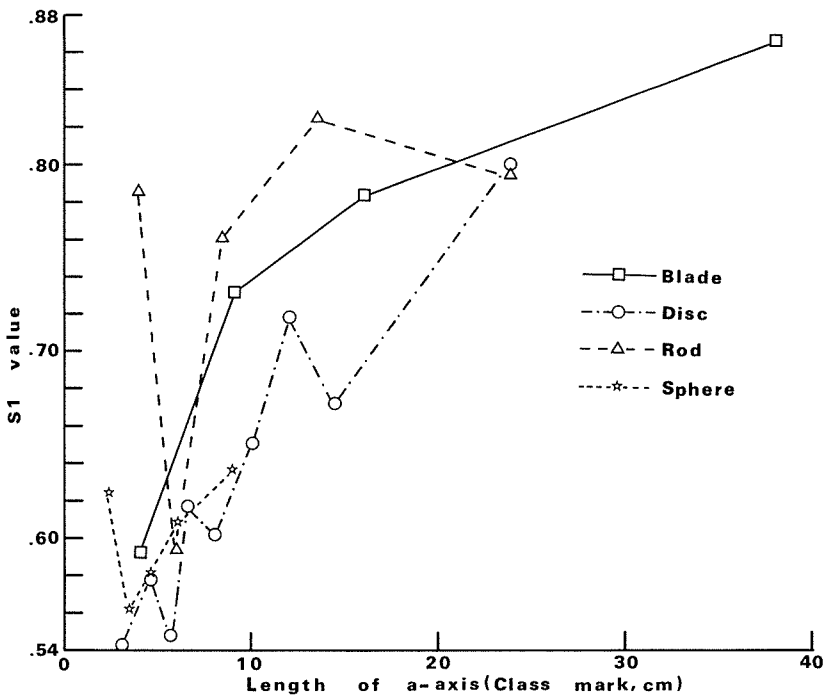

Figure 9 Changes in S1 value related to a-axis length.

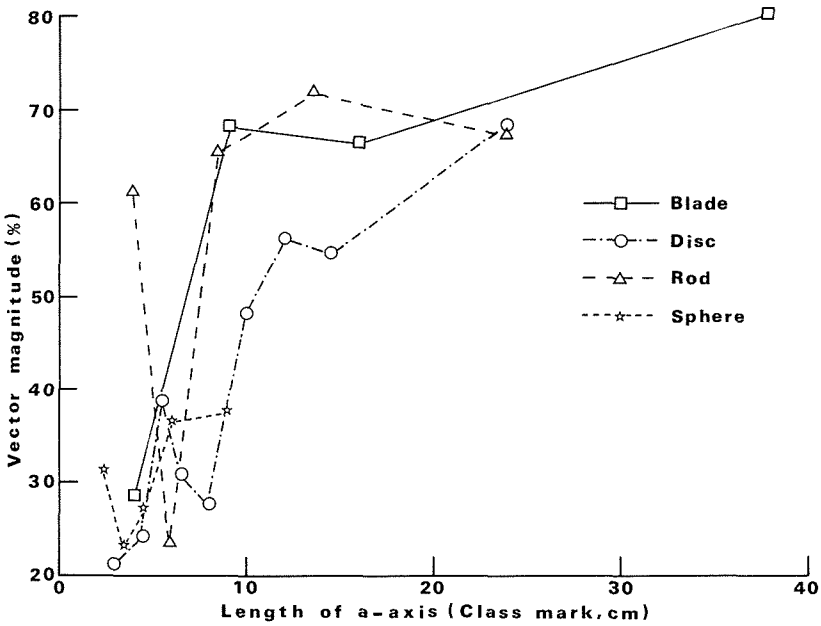

Figure 10 Changes in vector magnitude(%) related to a-axis length.

III−2−3. Relationship between macro fabrics and clast shape

Figure 12 and Table 4 shows the fabric characteristics in each Drake's category, and indicates that the vector magnitude ranges from 18.4 to 72.2; S1 value from 0.534 to 0.833; and C value from 1.369 to 3.320. Table 5 shows the interval estimates of each fabric strength population mean in the different clast shape. There is no overlap between two interval estimates of each fabric strength for both Blade and Sphere at a 90% confidence interval, and each fabric strength average of Blade and Rod is higher than that of Disc and Sphere.

Figure 11 shows the population mean and range of vector magnitude in each clast shape. Means of Rod's vector magnitude and S1 value are higher than those of Disc's and Sphere's, and are near those of Blade's.

In order to evaluate the clast shape influences on the fabric strength, Welch's statistical test which examines the difference among the above population mean is attempted (Table 6). The null hypothesis —no significance difference— is rejected in each statistical test. The result indicates that Blade and Rod have a stronger fabric than Disc and Sphere do. As the clasts of Blade and Rod have a lower b/a-axis ratio, the clasts with a lower b/a-axis ratio likely have a stronger fabric than clasts with a higher one. Wilcoxen's rank sum test supports this hypothesis (Table 7): all null hypotheses are rejected in each test composed of clast shape separated by the b/a-axis ratio, while they are significant in each test separated by the c/b-axis ratio.

The changes in each fabric strength of clasts with the same a-axis length against the b/a-axis ratio are analyzed (Tables 8 and 9). Table 8 shows a case of clasts with the a

Table 4 Characteristics of the fabrdcs classified by Crake's category.

Drake's category number	N	Clast size		Clast fabric analysis								
		length of a-axis		two-dimension		three-dimension						
		Av. (cm)	Sd. (cm)	V.Mg. (%)	$\Delta\theta$H1(°)	S1	S2	S3	C	K	$\Delta\theta$H2(°)	$\Delta\theta$P(°)
1	56	14.7	9.37	59.7	3.5	.720	.210	.070	2.334	1.118	3.3	−12.5
2	82	10.3	8.28	45.3	4.7	.687	.263	.050	2.630	0.575	6.2	−11.6
3	57	9.9	6.59	48.0	2.2	.685	.254	.061	2.418	0.698	0.1	− 7.9
4	72	7.8	4.11	37.1	2.8	.636	.291	.073	2.166	0.565	3.1	−10.8
5	167	8.1	6.09	42.8	1.1	.659	.261	.080	2.103	0.788	0.8	− 7.6
6	370	7.5	4.91	33.8	1.0	.602	.300	.098	1.820	0.620	3.4	− 9.1
7	35	21.3	28.40	50.0	2.9	.687	.244	.069	2.299	0.820	3.4	− 7.7
8	52	10.0	11.15	45.1	7.0	.733	.221	.046	2.758	0.771	14.0	−16.2
9	37	7.7	4.08	50.3	7.5	.715	.222	.063	2.427	0.933	7.7	− 9.5
10	48	8.1	4.86	37.5	3.6	.650	.254	.096	1.912	0.969	5.2	−12.0
11	94	6.1	4.23	44.4	6.3	.672	.255	.073	2.215	0.774	6.3	− 7.0
12	150	5.7	4.71	19.9	2.3	.534	.331	.136	1.369	0.539	3.1	− 1.8
13	17	13.8	21.50	72.2	10.8	.833	.135	.032	3.259	1.269	11.4	−11.6
14	32	7.4	4.32	60.9	8.8	.760	.192	.048	2.769	0.987	9.2	− 7.4
15	25	12.8	16.82	61.3	0.0	.751	.191	.058	2.577	1.149	1.6	− 7.2
16	22	6.2	2.87	41.0	12.9	.635	.281	.084	2.021	0.676	11.6	− 0.9
17	35	6.4	5.70	28.7	2.6	.609	.326	.065	2.245	0.385	2.8	− 8.5
18	46	5.6	2.80	40.0	1.6	.662	.252	.086	2.045	0.891	5.6	−12.7
19	19	13.2	10.06	68.9	5.7	.800	.143	.057	2.644	1.868	5.6	− 5.9
20	25	6.3	3.99	32.4	8.7	.594	.331	.075	2.068	0.394	9.9	− 8.3
21	19	7.4	6.90	57.7	0.2	.777	.195	.028	3.320	0.712	0.1	− 3.1
22	17	6.3	2.90	52.4	7.3	.731	.213	.056	2.559	0.930	6.4	− 6.4
23	33	6.6	6.42	48.1	1.9	.685	.242	.073	2.234	0.871	2.2	− 8.6
24	55	5.5	3.18	38.5	5.7	.593	.274	.133	1.498	1.060	3.6	− 6.6
25	46	11.0	7.26	44.5	4.0	.692	.244	.064	2.373	0.783	3.6	− 8.2
26	69	9.8	22.61	51.8	5.9	.675	.222	.103	1.874	1.463	6.3	−10.5
27	43	6.2	3.84	36.3	7.3	.606	.276	.118	1.632	0.932	10.2	− 5.7
28	36	5.7	2.68	21.8	0.8	.586	.365	.049	2.490	0.235	2.5	−13.7
29	60	5.6	2.47	47.3	3.8	.678	.250	.061	2.418	0.698	4.9	− 8.6
30	53	4.9	2.15	32.3	3.3	.611	.297	.092	1.895	0.613	3.5	− 6.5
31	112	10.5	7.78	56.9	0.3	.728	.206	.066	2.393	1.120	1.4	− 9.5
32	105	6.5	3.65	41.0	2.3	.656	.269	.075	2.169	0.697	1.4	− 7.6
33	66	6.6	3.40	40.8	11.8	.653	.277	.070	2.233	0.624	13.1	− 2.3
34	39	5.5	2.11	18.4	6.0	.540	.350	.109	1.597	0.372	2.2	− 3.5
35	70	6.0	3.83	27.9	0.2	.591	.329	.080	2.000	0.415	1.1	− 9.8
36	86	4.6	1.75	31.2	5.2	.555	.311	.134	1.418	0.685	0.9	− 5.2

N: number of observations, Av.: average length of a-axis in each category, Sd.: standard deviation of length of a-axis in each category, V.Mg.: Vector Magnitude, $\Delta\theta$H1: deviation of Vector Mean from slope orientation, $\Delta\theta$H2: deviation of V 1 azimuth from slope orientation, $\Delta\theta$p: deviation of V1 plunge from slope angle (−: upslope imbrication).

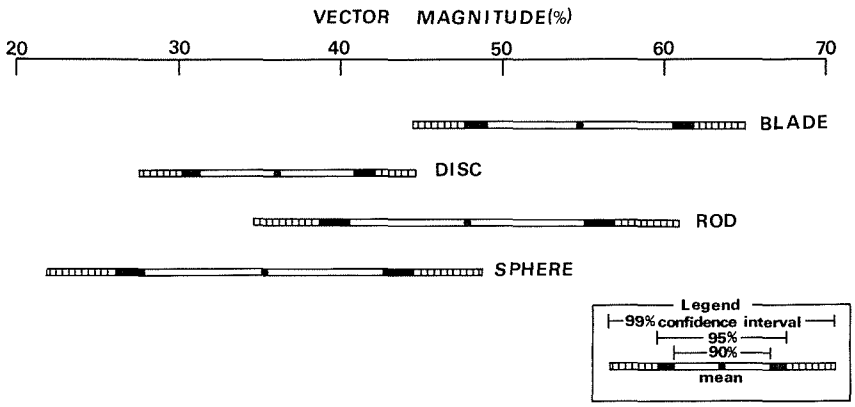

Figure 11 Population mean and range of vector magnitude in each clast shape at different confidence interval.

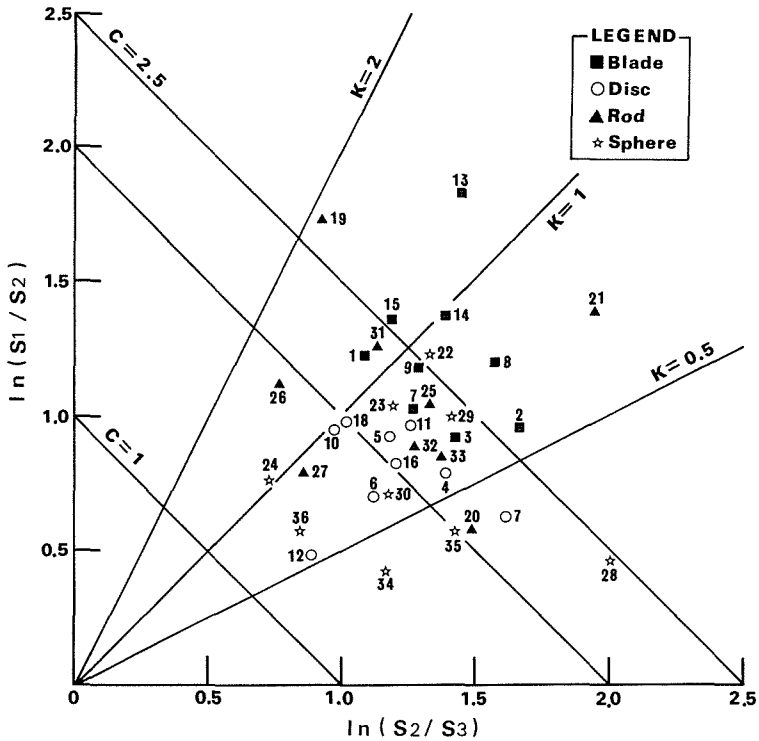

Figure 12 Logarithmic ratio plot of eigen values for each grouped Number beside the symbol means Drake's category subdivisions in Figure 4.

Table 5 Interval estimates of each fabric strength population mean in each clast shape at different confidence interval.

Clast shape	Fabric strength	Av.	s.	confidence interval 90%	95%	99%
Blade	V.Mg.	54.8	9.22	49.03 ≦μ≦0.9483	47.66 ≦μ≦ 61.84	44.44 ≦μ≦ 65.06
	S1	0.939	0.0151	0.9297≦μ≦0.9483	0.9274≦μ≦0.9506	0.9222≦μ≦0.9558
	C	4.070	0.4324	3.6505≦μ≦4.4903	3.5499≦μ≦4.5909	3.3131≦μ≦4.8277
Disc	V.Mg.	36.1	7.73	31.34 ≦μ≦ 40.92	30.19 ≦μ≦ 42.07	27.49 ≦μ≦ 44.78
	S1	0.905	0.0195	0.8932≦μ≦0.9176	0.8904≦μ≦0.9204	0.8836≦μ≦0.9272
	C	3.372	0.3583	3.0007≦μ≦3.7429	2,9118≦μ≦3.8318	2.7025≦μ≦4.0411
Rod	V.Mg.	47.8	11.82	40.48 ≦μ≦ 55.14	38.72 ≦μ≦ 56.90	34.59 ≦μ≦ 61.03
	S1	0.923	0.0222	0.9097≦μ≦0.9371	0.9064≦μ≦0.9404	0.8986≦μ≦0.9482
	C	3.769	0.5834	3.2952≦μ≦4.2422	3.1817≦μ≦4.3557	2.9147≦μ≦4.6227
Sphere	V.Mg.	35.3	12.04	27.86 ≦μ≦ 42.79	26.07 ≦μ≦ 44.58	21.86 ≦μ≦ 48.79
	S1	0.905	0.0318	0.8856≦μ≦0.9250	0.8808≦μ≦0.9298	0.8697≦μ≦0.9409
	C	3 * 441	0.7330	2.9867≦μ≦3.8953	2.8776≦μ≦4.0044	2.6214≦μ≦4.2606

Av.: sample mean, s,: sample standard deviatiion.

Table 6 Welch's statistical test among population mean of each fabric strength in clast shape.

Vector magnitude	S_1 value	C value
(1)H_0 : Blade=Disc H_1 : Blade>Disc	(5)H_0 : Blade=Disc H_1 : Blade>Disc	(9)H_0 : Blade=Disc H_1 : Blade>Disc
T=4.642 with DF=16	T=2.999 with DF=13	T=3.601 with DF=15
$t_{16}(.005)=2.921$ ∴reject H_0	$t_{13}(.01)=2.650$ ∴reject H_0	$t_{15}(.005)=2.947$ ∴reject H_0
(2)H_0 : Blade=Sphere H_1 : Blade>Sphere	(6)H_0 : Blade=Sphere H_1 : Blade>Sphere	(10)H_0 : Blade=Sphere H_1 : Blade>Sphere
T=3.844 with DF=15	T=2.871 with DF=18	T=4.247 with DF=19
$t_{15}(.005)=2.947$ ∴reject H_0	$t_{18}(.01)=2.552$ ∴reject H_0	$t_{19}(.005)=2.861$ ∴reject H_0
(3)H_0 : Rod=Disc H_1 : Rod>Disc	(7)H_0 : Rod=Disc H_1 : Rod>Disc	(11)H_0 : Rod=Disc H_1 : Rod>Disc
T=2.481 with DF=14	T=1.831 with DF=15	T=1.740 with DF=13
$t_{14}(.05)=1.761$ ∴reject H_0	$t_{15}(.05)=1.753$ ∴reject H_0	$t_{13}(.1)=1.350$ ∴reject H_0
(4)H_0 : Rod=Sphere H_1 : Rod>Sphere	(8)H_0 : Rod=Sphere H_1 : Rod>Sphere	(12)H_0 : Rod=Sphere H_1 : Rod>Sphere
T=2.221 with DF=16	T=1.400 with DF=27	T=1.240 with DF=18
$t_{16}(.05)=1.746$ ∴reject H_0	$t_{27}(.1)=1.314$ ∴reject H_0	$t_{18}(.1)=1.330$ ∴significant H_0

H_0 : statistical hypothesis. H_1 : alternative hypothesis, T:calculated statistical testing value in each case, DF : degree of freedom=15, level of significance=0.05.

Table 7 Wilcoxen's rank sum test among population mean of each fabric strength.

Vector magnitude	S_1 value	C value
effect of b/a		
(1)-a H_0 : Blade+Rod=Disc+Sphere H_1 : Blade+Rod≠Disc+Sphere $W=217,252<W_{18,18}(.01)<414$ ∴reject H_0	(1)-b H_0 : Blade+Rod=Disc+Sphere H_1 : Blade+Rod≠Disc+Sphere $W=236,252<W_{18,18}(.01)<414$ ∴reject H_0	(1)-c H_0 : Blade+Rod=Disc+Sphere H_1 : Blade+Rod≠Disc+Sphere $W=248,252<W_{18,18}(.01)<414$ ∴reject H_0
(2)-a H_0 : Blade=Disc H_1 : Blade≠Disc $W=45,56<W_{9,9}(.01)<115$ ∴reject H_0	(2)-b H_0 : Blade=Disc H_1 : Blade≠Disc $W=48,56<W_{9,9}(.01)<115$ ∴reject H_0	(2)-c H_0 : Blade=Disc H_1 : Blade≠Disc $W=49,56<W_{9,9}(.01)<115$ ∴reject H_0
(3)-a H_0 : Rod=Sphere H_1 : Rod≠Sphere $W=63,66<W_{9,9}(.1)<105$ ∴reject H_0	(3)-b H_0 : Rod=Sphere H_1 : Rod≠Sphere $W=58,62<W_{9,9}(.05)<109$ ∴reject H_0	(3)-c H_0 : Rod=Sphere H_1 : Rod≠Sphere $W=73,66<W_{9,9}(.1)<105$ ∴reject H_0
effect of c/b		
(4)-a H_0 : Blade+Disk=Rod+Sphere H_1 : Blade+Disc≠Rod+Sphere $W=304,280<W_{18,18}(.1)<386$ ∴significant H_0	(4)-b H_0 : Blade+Disk=Rod+Sphere H_1 : Blade+Disc≠Rod+Sphere $W=308,280<W_{18,18}(.1)<386$ ∴significant H_0	(4)-c H_0 : Blade+Disk=Rod+Sphere H_1 : Blade+Disc≠Rod+Sphere $W=358,280<W_{18,18}(.1)<386$ ∴significant H_0
(5)-a H_0 : Blade=Rod H_1 : Blade≠Rod $W=68,66<W_{9,9}(.1)<105$ ∴significant H_0	(5)-b H_0 : Blade=Rod H_1 : Blade≠Rod $W=66,66<W_{9,9}(.1)<105$ ∴significant H_0	(5)-c H_0 : Blade=Rod H_1 : Blade≠Rod $W=67,66<W_{9,9}(.1)<105$ ∴significant H_0
(6)-a H_0 : Disc=Sphere H_1 : Disc≠Sphere $W=83,66<W_{9,9}(.1)<105$ ∴significant H_0	(6)-b H_0 : Disc=Sphere H_1 : Disc≠Sphere $W=91,66<W_{9,9}(.1)<105$ ∴significant H_0	(6)-c H_0 : Disc=Sphere H_1 : Disc≠Sphere $W=83,66<W_{9,9}(.1)<105$ ∴significant H_0

W : calculated statistical testing value in each each case, $W18,18(.01)$: statistical testing value with level of significance = 0.01 ; 18 indicates the number of samples.

-axis length ranging from 3.0 cm to 3.9 cm, and Table 9 shows a case, ranging from 7.0 cm to 8.9 cm. In both cases, Blade and Rod have a stronger fabric than Disc and Sphere do, and that clasts with a lower b/a-axis ratio have a stronger fabric than clasts with a higher one.

Figure 13 shows that the changes in each fabric strength against b/a-axis ratio, separated by c/b-axis ratio (more or less than 0.67) and a-axis length ($3.0 \leqq a \leqq 3.9$ cm or $7.0 \leqq a \leqq 8.9$ cm) based on the data listed in Tables 8 and 9. This figure suggests the following:

First, the changes in each fabric strength of clasts with the same a-axis length are similar to each other. This result indicates that c/b-axis ratio cannot influence the fabric strength.

Second, the changes in each fabric strength of clasts with the same c/b-axis ratio, that is, comparison for straight line against dotted line shows almost similar changes. This feature suggests that a small difference of the length of a-axis also cannot influence the fabric strength.

Figure 14 illustrates that the changes in each fabric strength against b/a-axis ratio separated by a-axis length ($3.0 \leqq a \leqq 3.9$ cm or $7.0 \leqq a \leqq 8.9$ cm) based on the data listed in Tables 8 and 9. Each fabric strength is closely related to the decrease of a-axis length, and the highest value of fabric strength appears in a range of b/a-axis ratio less than 0.55.

Table 8 Fabrics of clasts with a-axis length ranging from 3.0 to 3.9 cm.

Drake's category number	N	Clast fablic analysis								
		two-dimension		three-dimension						
		V.Mg. (%)	$\Delta\theta$H1 (°)	S1	S2	S3	C	K	$\Delta\theta$H2(°)	$\Delta\theta$P(°)
1, 7,13	9	69.6	8.3	.797	.163	.040	3.004	1.119	9.3	0.0
2, 8,14	17	51.1	9.6	.711	.231	.058	2.496	0.820	12.5	− 8.8
3, 9,15	11	60.3	20.9	.677	.257	.066	2.325	0.716	26.4	− 7.1
4,10,16	30	31.7	6.6	.626	.305	.070	2.203	0.484	4.0	− 4.3
5,11,17	41	34.3	4.2	.640	.272	.088	1.979	0.760	3.9	−12.9
6,12,18	66	31.9	1.5	.587	.297	.116	1.623	0.720	3.2	− 8.2
19,25,31	31	64.1	11.1	.777	.180	0.43	2.885	1.027	10.3	− 5.6
20,26,32	26	48.5	2.4	.693	.204	.103	1.901	1.795	5.9	− 6.9
21,27,33	18	31.6	7.3	.634	.325	.041	2.738	0.322	31.9	− 8.3
22,28,34	11	55.4	22.8	.679	.241	.080	2.143	0.939	16.7	− 2.7
23,29,35	16	51.7	3.7	.681	.276	.043	2.759	0.485	6.1	− 6.4
24,30,36	14	41.2	17.4	.640	.283	.077	2.124	0.625	12.5	0.3
1-3, 7-9,13-15	37	57.5	12.2	.712	.216	.072	2.296	1.085	15.1	− 6.3
4-6,10,12,16-18	137	31.5	0.7	.608	.293	.099	1.814	0.677	0.9	− 8.7
19-21,25-27,31-33	75	48.1	10.5	.702	.228	.070	2.307	0.954	11.8	− .2
22-24,28-30,34-36	41	41.9	1.5	.648	.277	.075	2.149	0.655	1.4	− 2.3
1,7,13,19,25,31	40	62.6	6.4	.767	.184	.049	2.744	1.086	5.8	− 4.3
2,8,14,20,26,32	43	48.5	2.5	.688	.225	.087	2.066	1.176	1.3	− 7.9
3,9,15,21,27,33	29	27.4	2.9	.568	.379	.053	2.364	0.206	6.5	− 7.2
4,10,16,22,28,34	41	33.5	4.9	.630	.293	.077	2.100	0.573	3.1	− 3.5
5,11,17,23,29,35	57	38.7	1.6	.647	.275	.078	2.115	0.680	0.8	−10.8
6,12,18,24,30,36	80	31.0	2.0	.593	.295	.112	1.667	0.720	5.2	− 7.4

N: number of observations, V.Mg.: Vector Magnitude, $\Delta\theta$H1: deviation of Vector Mean from slope orientation, $\Delta\theta$H2: deviation of V 1 azimuth from slope orientation, $\Delta\theta$p: deviation of V1 plunge from slope angle (−: upslope imbrication).

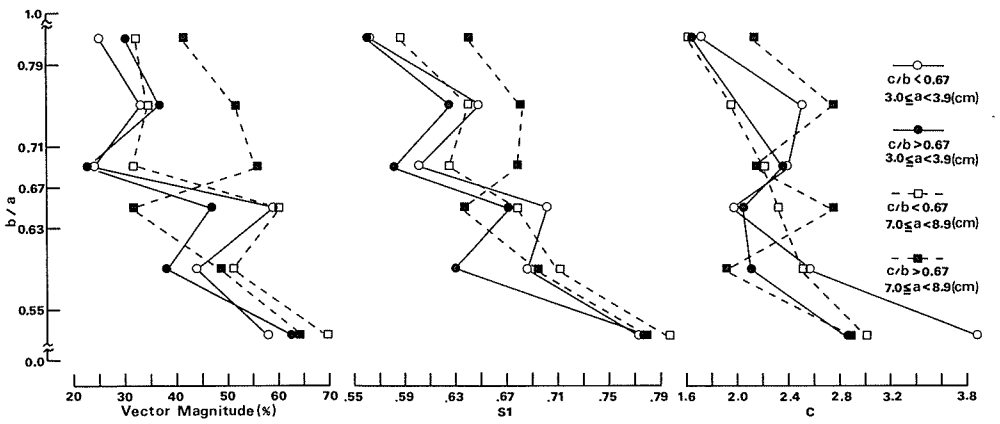

Figure 13 Changes in each fabric strength variable of clasts separated by c/b-axis ratio with same a-axis length related to b/a-axis ratio.

Table 9 Fabrics of clasts with a-axis length ranging from 7.0 to 8.9 cm.

Drake's category number	N	Clast fabric analysis								
		two-dimension		three-dimension						
		V.Mg. (%)	$\Delta\theta$H1 (°)	S1	S2	S3	C	K	$\Delta\theta$H2(°)	$\Delta\theta$P(°)
1, 7,13	8	57.6	10.9	.773	.212	.015	3.883	0.500	9.7	3.2
2, 8,14	25	43.9	6.8	.687	.261	.052	2.574	0.604	7.7	− 9.7
3, 9,15	17	59.0	8.4	.707	.194	.099	1.961	1.931	10.1	− 3.3
4,10,16	15	24.3	25.6	.603	.342	.055	2.395	0.310	26.1	−14.4
5,11,17	66	33.2	10.8	.640	.307	.053	2.502	0.416	10.2	− 6.1
6,12,18	94	25.3	2.1	.561	.338	.101	1.709	0.420	1.3	− 5.7
19,25,31	21	62.6	13.4	.776	.179	.045	2.859	1.053	15.5	− 4.8
20,26,32	36	37.9	6.4	.629	.293	.078	2.094	0.573	9.1	− 6.7
21,27,33	24	47.0	2.3	.670	.243	.087	2.041	0.983	3.2	− 5.3
22,28,34	22	22.8	8.1	.580	.364	.056	2.340	0.250	11.1	− 8.8
23,29,35	45	36.8	1.7	.627	.291	.082	2.039	0.602	2.3	− 8.5
24,30,36	55	30.2	12.3	.559	.332	.109	1.634	0.467	12.6	− 2.1
1-3, 7-9,13-15	50	48.9	7.7	.702	.230	.068	2.343	0.910	9.0	− 5.2
4-6,10,12,16-18	175	26.7	3.7	.586	.334	.080	1.994	0.391	2.4	− 5.2
19-21,25-27,31-33	81	44.1	1.6	.664	.259	.077	2.162	0.770	1.4	− 5.5
22-24,28-30,34-36	122	30.1	3.6	.580	.328	.092	1.839	0.448	2.2	− 5.7
1,7,13,19,25,31	29	57.2	7.5	.753	.210	.037	3.009	0.736	9.4	− 2.4
2,8,14,20,26,32	61	40.4	10.7	.652	.278	.070	2.240	0.614	8.5	− 8.0
3,9,15,21,27,33	41	49.0	4.3	.683	.223	.094	1.980	1.305	6.3	− 4.3
4,10,16,22,28,34	37	19.5	5.8	.565	.379	.056	2.306	0.210	5.3	−10.7
5,11,17,23,29,35	111	34.2	6.9	.633	.302	.065	2.285	0.478	7.0	− 7.1
6,12,18,24,30,36	149	26.3	3.8	.557	.338	.105	1.669	0.429	5.6	− 4.4

N: the number of observations, V.Mg.: Vector Magnitude, $\Delta\theta$H1: deviation of Vector Mean from slope orientation, $\Delta\theta$H2: deviation of V 1 azimuth from slope orientation, $\Delta\theta$p: deviation of V1 plunge from slope angle (−: upslope imbrication).

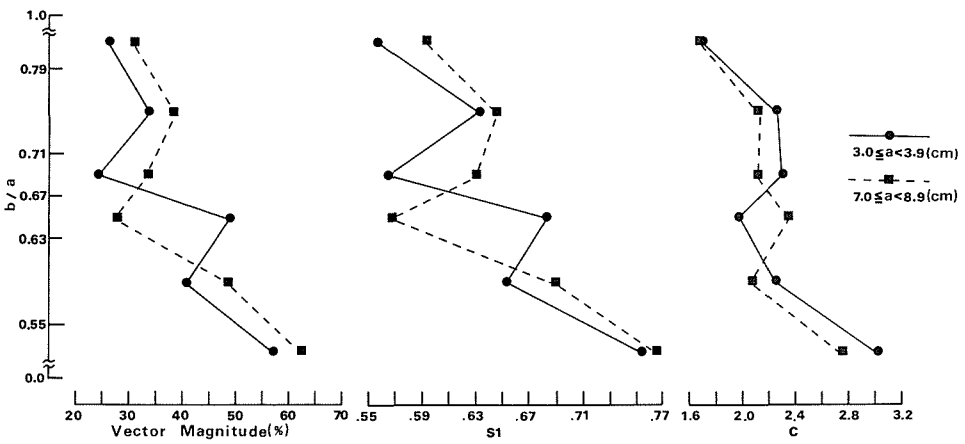

Figure 14 Changes in each fabric strength variable of clasts with same a-axis length related to b/a-axis ratio.

III—3. Discussion: Effects of clast size and shape on macro fabrics

Fabric data from the fossil solifluction deposits indicate that the clast shape and size exert a strong influence on its fabric strength. Using Zingg's shape definition, clasts of Blade and Rod have a stronger fabric strength than those of Disc and Sphere.

Welch's statistical test for a population mean of each fabric strength indicates that the fabric strength of Blade and Rod are significantly different from those of Disc and Sphere. Wilcoxen's rank sum test demonstrates that b/a-axis ratio influences its fabric strength, while c/b-axis ratio has no relation to the latter. This result supports the idea that Blade - and Rod-type clasts are more likely to be elongated to the flow direction in viscous fluids than Disc- and Sphere-type clasts (Drake, 1974).

A linear regression between a-axis size and its fabric strength shows a strong relation among them: clasts with a longer a-axis and a lower b/a-axis ratio have a stronger fabric than clasts with a shorter a-axis and a higher b/a-axis ratio.

These findings may be attributed to the difference of velocity of clasts' movement in viscous fluids. Since the movement velocity of clasts with a shorter a-axis is faster than that of clasts with a longer a-axis, the former can move through the openings among the latter, and may change its flow direction easily. This may be the reason why clasts with a shorter a-axis have a weaker fabric.

The analyses of the changes in each fabric strength of clasts with the same a-axis length against b/a-axis ratio show that fabrics are similar to each other in spite of different c/b-axis ratio, and that b/a-axis ratio less than 0.55 has the strongest fabric. This result indicates that c/b-axis ratio has little effect on its fabrics, and that clasts with a longer a-axis length have probably stronger fabrics.

When the changes in each fabric strength of clasts with the same shape are analyzed against a-axis length, clasts of Blade or Rod type have a stronger fabric than those of Disc or Sphere type in a range of shorter a-axis length. On the other hand, fabric strength of each clast shape is closely similar to each other in a range of longer a-axis length. Taking these results into consideration, azimuths and dips of a-axis of clasts with longer one must be measured in order to gain a stronger fabric in periglacial slope deposits. Clasts with b/a-axis ratio less than 0.55 might be added under the condition with much investigating time.

IV. MACRO FABRICS OF SLOPE DEPOSITS

IV—1. Macro Fabrics of Periglacial Slope Deposits

Figure 15 shows all V.Mg.(%) data of the slope deposits which have been reported hitherto. Straight lines and solid circles indicate the range of V.Mg. and the mean value of V. Mg., respectively. Numbers 1 to 11 on the right-hand site of each straight line correspond to a reference which is descrbeded bellow :

1: Original data are from McArthur (1981): Fossil periglacial slope deposits, which were probably transported in the late Pleistocene along the upper Derwent Valley in the

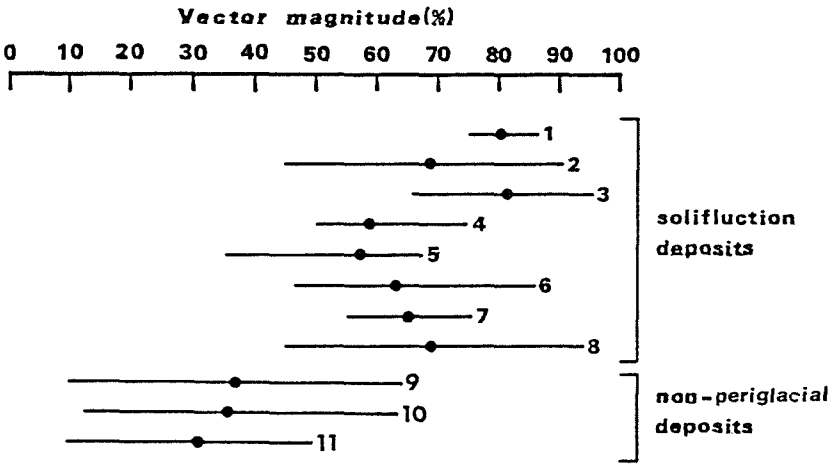

Figure 15 Ranges of vector magnitude(%) of solifluction and non-periglacial deposits.
Vector strength values (%) of sample Nos.1-3 were altered for vector magnitude(%) by regression equation shown in Figure 1. Solid circles reveal mean value of vector magnitude in each sample. Data source; 1: McArthur (1981), 2: Thomas (1967), 3: Yamamoto (1987), 4:Watson, E. (1969), 5: Harris and Wright (1980), 6: Willson (1981), 7: Shakesby (1981), 8: Watson E. and S. (1967), 9: Mills (1984, volcanic mudflow deposits), 10: Mills (1983, soil creep deposits), 11: Mills (1986, mudflow deposits).

Southern Pennines, England. These deposits, which were resulted from the congelifractates from the retreating sandstone escarpments, appeared to have been accumulated on the terraces along the Derwent Valley. Thirty-five to forty clasts were measured at four sites. V.St. ranging from 63.3 to 71.2 (mean value: 67.8), I transformed them to V.Mg. by the regression equation shown in Figure 1. It ranges from 44.9 to 86.3 (mean value: 80.0; standard deviation : 4.73).

2: Original data are from Thomas (1967). Thirty-three to sixty clasts were measured at four sites of solifluction lobes in Keswick, Cumbria. V.St., ranging from 37.6 to 76.7 (mean value: 57.7), I transformed them to V.Mg. by the regression equation shown in Figure 1. It ranges from 45.1 to 90.4 (mean value: 68.4; standard deviation: 18.95).

3: Original data are from Yamamoto (1987). Over 70 clasts were measured at 14 sites of the fossil periglacial slope deposits which developed behind the fluvial terraces around Mt. Syokanbetsudake, Hokkaido. V.St., ranging from 55.4 to 81.4 (mean value: 68.8), I transformed them to V.Mg. by the regression equation shown in Figure 1. It ranges from 65.7 to 95.8 (mean value: 81.2; standard deviation: 9.02).

4: Original data were from Watson (1969). Fossil periglacial slope deposits, which were probably transported in the late Divensian, in the Nant Iago Valley, Central Wales. These deposits, which were composed of coarse gravelly head of 1−6 m thickness, appeared to have accumulated on the terraces along the Nant Iago Valley. Fifty to one hundred clasts of head deposits were measured at six sites. V.Mg. ranges from 35.3 to 67. 5 (mean value: 59.2; standard deviation: 9.84).

5: Original data are from Harris and Wright (1980). Fossil periglacial slope deposits, which were transported by solifluction in the late Devensian, at Pontypridd, South Wales. The number of measuring sites was six, but the number of observed clasts was not described. V.Mg. ranges from 35.3 to 67.5 (mean value: 57.3; standard deviation: 12.08).

6: Original data are from Willson (1981). Fifty clasts with length of a-axis ranging from 2 cm to 12 cm were measured at eight sites of solifluction lobes at Edale, North Derbyshire. The lobes, which were composed mainly of silt, lie on the terraces along the Edale River. V.Mg. ranges from 46.5 to 85.7 (mean value: 62.8; standard deviation: 13.46).

7: Original data are from Shakesby (1981). Fossil periglacial slope deposits, which were probably transported mainly during the Loch Lomond Stadial (corresponding to Younger Dryas Stadial), near Woolhope in South Wales. The deposits were composed of sediment of 1.5 m thickness comprising Silurian rock fragments in a fine matrix. Fifty clasts with elongated shape were measured at four sites except ML and LL sites. V.Mg. ranges from 55.2 to 75.0 (mean value: 65.0; standard deviation: 10.32).

8: Original data are from Watson, E. and S.(1967). Fossil periglacial slope deposits, which were the deposits of the Last Glacial age, at Morfa-Bychan, near Aberystwyth. The deposits were composed of coarse gravelly head of 1−4 m thickness. Fifty clasts with a/b-axis ratio showing a value of over 1.5 were measured at 27 sites. V.Mg. ranges from 44.9 to 93.7 (mean value: 68.7; standard deviation: 12.95).

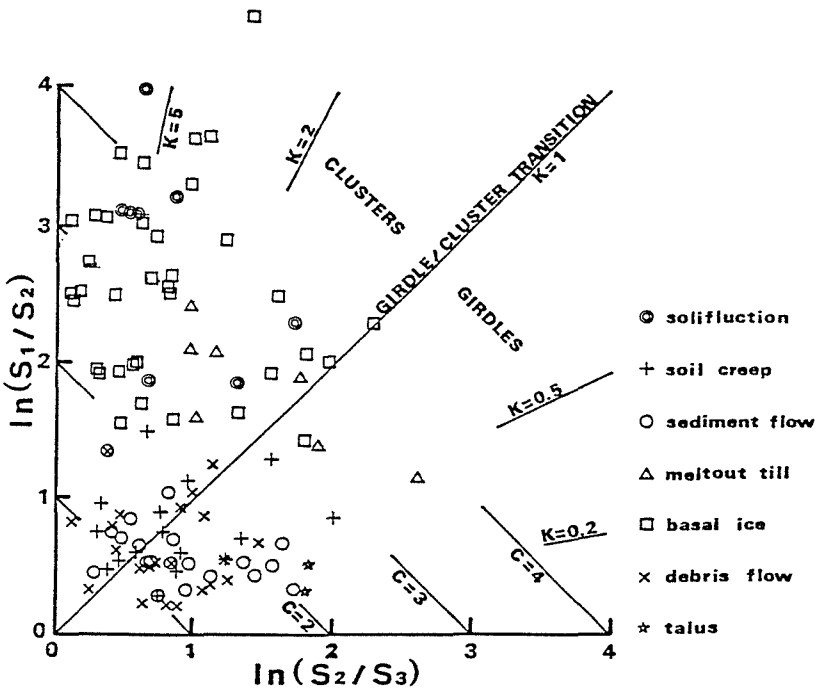

Figure 16 Logarithmic ratio plot of eigen values of various deposits.
Data source; solifluction: Nelson (1985), soil creep: Mills (1983), sediment flow, meltout till, and basal ice: Lawson (1979), debris flow: Mills (1984, 1986), talus: Giardino and Vitek (1985), and Takada (1987).

Figure 16 illustrates the logarithmic ratio plot of eigen values from various types of deposits described above. Solifluction deposits in this figure are originated from the data of Nelson (1985), which are briefly summarized below:

Fifty clasts with a length of a-axis ranging from 10 cm to 35 cm and an a/b-axis ratio showing the value of over 2 were measured in 10 cm−40 cm depth from the surface at eight solifluction lobes on the north-fcing side slope of a cryoplanation terrace near Eagle Summit, Alaska. The lobes lie at an altitude between 1,100 and 1,200 m a.s.l.; late-lying snowbanks upslope provided moisture for mass movement. Except for small Pleistocene cirque glaciers, the area had not been glaciated. The lobes are composed predominantly of silt, but contain numerous angular cobbles and blocks derived from the underlying schist. S1 ranges from 0.811 to 0.971 (mean value: 0.905; standard deviation: 0.056); C ranges from 2.539 to 4.480 (mean value: 3.604; standard deviation: 0.588); and K ranges from 1.345 to 8. 097 (mean value: 4.430; standard deviation: 2.540).

IV−2. Macro Fabrics of Non-Periglacial Slope Deposits

Numbers 9 to 11 shown in Figure 15 correspond to the data of non-periglacial slope deposits:

9: Original data are from Mills(1984). Volcanic mudflow deposits, which were resulted from the 18 May 1980 Mount St. Helens avalanche and eruption, along the North Fork of the Toutle River, Washington. Most deposits were no more than several meters thick, and were composed of subangular pebble and cobble gravels with abundant silt and clay in matrix. Twenty-five to fifty clasts with the a/b-axis ratio showing the value of over 1. 5 were measured at 11 sites. V.Mg. ranges from 9.8 to 64.1 (mean value: 36.8; standard deviation: 19.68).

10: Original data are from Mills (1983). Clast fabrics of soil creep deposits, which were transported under the non-periglacial environment in the Last Glacial age, were measured in the upper 20 cm of soil on the forested hill slopes in Giles County, Virginia. The major bedrock formations underlying the measuring sites were hematite-cemented sandstone in Silurian and silica-cemented orthoquartzite in Ordovician. At measuring sites the percentage of silt and clay in the less than 2 mm fraction varied only from 40 to 68%. Twenty-five or fifty clasts with both a/b-axis ratio showing values of over 1.5 in length of a-axis ranging from 2 cm to 10 cm were measured at sixteen sites. V.Mg. ranges from 12.4 to 63.7 (mean value: 35.6; standard deviation: 13.10).

11: Original data are from Mills (1986). Alluvial fan deposits (piedomont-cove), which were widespread along the piedmont slopes in the Great Smoky Mountains, southern Appalachian Mountains. The deposits, which were composed largely of bouldery diamictons lacking sorting and stratification, spread near the mouth of first- or second-order stream valley. Twenty-five or fifty clasts with both a/b-axis ratio showing values of over 1.5 and length of a-axis ranging from 2 cm to 15 cm were measured at 11 sites. V. Mg. ranges from 18.5 to 31.9 (mean value : 24.5; standard deviation: 5.56).

Non-periglacial slope deposits, that is, soil creep and sediment flow deposits, meltout till, basal ice and talus deposits shown in Figure 16, were derived from data of the following

articles. Their measuring methods and results are as follows:

Soil creep deposits: Original data are from Mills (1983). Measuring methods are the same as those mentioned in the section V.Mg.. S1 ranges from 0.484 to 0.751 (mean value: 0.624; standard deviation: 0.095); C ranges from 0.904 to 2.856 (mean value: 1.662; standard deviation: 0.604); and K ranges from 0.435 to 2.880 (mean value: 1.164; standard deviation: 0.953).

Sediment flow deposits: Original data are from Lawson (1979). The deposits, which were accompanied with saturated water and shear plane, and were transported by gravity to downslope near the Matanuska Glacier, Alaska, have no relations to glacial deposits. Twenty-five clasts with a/b-axis ratio showing a value of over 2 and b/c-axis ratio showing one over 1, or a/b-axis ratio showing one over 1 and a/c-axis ratio showing one over 2, or a/b/c-axis ratio showing the ratio of over 3/2/1 were measured at 20 sites. S1 ranges from 0.487 to 0.698 (mean value: 0.567; standard deviation: 0.052); C ranges from 0. 808 to 2.309 (mean value: 1.539; standard deviation: 0.388); and K ranges from 0.210 to 3. 627 (mean value: 0.899; standard deviation: 0.795).

Meltout till: Original data are from Lawson (1977). Measuring methods are the same as those of sediment flow deposits mentioned above, and the measuring was done at seven sites near the Matanuska Glacier, Alaska, except for No. 41072, for the reason that S3 shows an impossible value theoretically. S1 ranges from 0.748 to 0.887 (mean value: 0.882; standard deviation: 0.052); C ranges from 2.603 to 3.727 (mean value: 3.276; standard deviation: 0.362); and K ranges from 0.210 to 3.627 (mean value: 0.889; standard deviation: 0.795).

Basal ice deposits: Original data are from Lawson (1977). Thirty-eight samples were obtained at 17 sites of the Matanuska Glacier. Measuring methods are the same as the sediment flow deposits mentioned above. S1 ranges from 0.743 to 0.963 (mean value: 0.879; standard deviation: 0.062); C ranges from 2.016 to 6.203 (mean value: 3.332; standard deviation: 0.837); and K ranges from 0.810 to 25.961 (mean value: 5.704; standard deviation: 5.732).

Mudflow deposits: Original data are from Mills (1984; 1986). Measuring methods are the same as those mentioned in the section V.Mg. Measuring was done at 22 sites. S1 ranges from 0.438 to 0.729 (mean value: 0.556; standard deviation: 0.079); C ranges from 0. 561 to 2.402 (mean value: 1.453; standard deviation: 0.455); and K ranges from 0.255 to 6. 755 (mean value: 1.252; standard deviation: 1.467).

Talus deposits: Original data are from Takada (1987) and Giardino and Vitek (1985). The former measured 50 to 100 clasts with a/b-axis ratio showing a value of over 1.5 in the Mikuni Mountains, Japan. S1 equals 0.561, C equals 2.187 and K equals 0.224. The latter measured 100 clasts with both a/b-axis ratio showing a value of over 2 and length of a-axis showing those of over 10 cm in 1 m depth from the surface area of 1−2 m^2 of the talus slope in Mt. Mestas, Colorado. S1 equals 0.553, C equals 2.124 and K equals 0.171.

IV−3. Discussion and Conclusions

The range of V.Mg. of the solifluction deposits and that of non-periglacial deposits are

overlapped with each other (Figure 15). This result suggests that, although it is difficult to recognize periglacial slope deposits only by means of an analysis of V.Mg., the mean values of V.Mg. is useful for the separation of the periglacial and non-periglacial slope deposits. However, the lowest value of the means of V.Mg. in solifluction deposits shows 57.3%, while the highest value of those in non-periglacial deposits shows 36.8%: these two values have a difference of about 20%.

Furthermore, Table 10 shows the interval estimates of V.Mg. population mean for both solifluction deposits and non-periglacial deposits. It is recognized that not all of the interval estimates at a 95% confidence interval show overlaps. Table 11 shows the results of Welch's statistical test which is to test the difference among population means of V.Mg. for cases of recognized overlaps of interval estimates at a 95% confidence interval listed in Table 10. The null hypothesis, that is, no significance difference, was rejected in each statistical test. This result indicates that solifluction deposits have higher V.Mg. than non-periglacial slope deposits do.

These characteristics are in accordance with those based on results of distribution of logarithmic ratio plot of eigen values both of solifluction deposits and non-periglacial slope deposits shown in Figure 16. Plots of soil creep, sediment flow, mudflow and talus deposits indicate low values both of C and K compared with those of solifluction deposits. This result leads to the conclusions that (1) the fabrics of solifluction deposits except glacial deposits have a higher C value than the deposits formed under different environ-

Table 10 Interval estimates of vector magnitude population mean for both solifluction and non-periglacial deposits.

	solifluction deposits	1 (n=4)	2 (n=4)	3 (n=14)	4 (n=6)	5 (n=6)	6 (n=8)	7 (n=4)	8 (n=27)	1-8 (n=73)	12 (n=24)	13 (n=16)	14 (n=19)	12-14 (n=59)
nonperiglacial deposits	confidence interval (%)	999590	999590	999590	999590	999590	999590	999590	999590	999590	999590	999590	999590	999590
9 (n=11)	99	+	−	+	−	−	−	−	+	+	+	+	+	+
	95	+	−	+	−	−	+	−	+	+	+	+	+	+
	90	+	−	+	+	−	+	+	+	+	+	+	+	+
10 (n=16)	99	+	−	+	−	−	+	−	+	+	+	+	+	+
	95	+	−	+	+	+	+	+	+	+	+	+	+	+
	90	+	+	+	+	+	+	+	+	+	+	+	+	+
11 (n=12)	99	+	−	+	+	−	+	−	+	+	+	+	+	+
	95	+	−	+	+	+	+	+	+	+	+	+	+	+
	90	+	+	+	+	+	+	+	+	+	+	+	+	+
9-11 (n=38)	99	+	−	+	+	−	+	−	+	+	+	+	+	+
	95	+	−	+	+	+	+	+	+	+	+	+	+	+
	90	+	+	+	+	+	+	+	+	+	+	+	+	+
15 (n=8)	99	+	−	+	+	+	+	+	+	+	+	+	+	+
	95	+	+	+	+	+	+	+	+	+	+	+	+	+
	90	+	+	+	+	+	+	+	+	+	+	+	+	+

+ : no overlap, − : overlap between two interval estimates. Numbers 1 to 15 correspond to those shown in Figure 21.

Table 11 *Results of Welch's statistical test population mean of both solifluction and non-periglacial deposits.*

(1) $H_0: \mu 2=\mu 9$, $H_1: \mu 2>\mu 9$, t3(.05)=2.353	T=3.271 with DF=3 ∴ reject H_0
(2) $H_0: \mu 2=\mu 10$, $H_1: \mu 2>\mu 10$, t4(.05)=2.132	T=3.273 with DF=4 ∴ reject H_0
(3) $H_0: \mu 2=\mu 11$, $H_1: \mu 2>\mu 11$, t3(.05)=2.353	T=3.845 with DF=3 ∴ reject H_0
(4) $H_0: \mu 2=\mu 9\text{-}11$, $H_1: \mu 2>\mu 9\text{-}11$, t3(.05)=2.353	T=3.466 with DF=3 ∴ reject H_0
(5) $H_0: \mu 4=\mu 9$, $H_1: \mu 4>\mu 9$, t15(.05)=1.753	T=3.126 with DF=15 ∴ reject H_0
(6) $H_0: \mu 5=\mu 9$, $H_1: \mu 5>\mu 9$, t15(.05)=1.753	T=2.675 with DF=15 ∴ reject H_0
(7) $H_0: \mu 7=\mu 9$, $H_1: \mu 7>\mu 9$, t11(.05)=1.796	T=3.586 with DF=11 ∴ reject H_0

H_0: statitsical hypothesis. H_1: alternative hypothesis, T: calculated statistical testing value in each case. DF: degree of freedom. t3(.05): statistical testing value with degree of freedom=3, level of significance=0.05. $\mu 2$: sample number which equals to one shown in Table 10.

ments; (2) the solifluction deposits are plotted in a zone with C ranging over about 2.5, and K ranging over about 1.3 by the logarithmic ratio plot; and (3) it is, therefore, possible to distinguish solifluction deposits from non-periglacial slope deposits by means of the logarithmic ratio plot.

Part II QUANTITATIVE CHARACTERISTICS AND PERIODS OF MASS MOVEMENT OF PERIGLACIAL SLOPE DEPOSITS IN THE HIDAKA MOUNTAINS

V. REGIONAL SETTINGS OF STUDY AREA

V−1. Introduction

The study area occupies the northern part of the Hidaka Mountains which forms the backbone range of Hokkaido. The range trends in north-south direction between Cape Erimo to the south and Mt. Sahorodake (1,059 m a.s.l., Photo 2) to the north, about 250 km apart. The study area covers the eastern slope of the range, stretching from Mt. Sahorodake in the northern margin, through the Karikachi Pass (644 m a.s.l.), Mt. Odassyu (1,097 m a.s.l., Photo 3), the Nissho Pass (1,106 m a.s.l., Photo 4), Mt. Pekerebetsudake (1,532 m a.s.l., Photo 5) and Mt. Memurodake (1,753 m a.s.l.), to Mt. Tsurugi (1,205 m a.s.l.) in the southern margin.

Three year (1944−1946) weather record at the top of Mt. Sahorodake (1,053 m a.s.l.), located in the northern margin of the study area, gives the mean annual temperature of 0.4 ℃, and the mean January and July temperature, −14.3 ℃ and 14.0 ℃, respectively (Asai et al., 1986). The mean annual temperature and the mean annual precipitation measured at the meteorological observatory of Shintoku (178 m a.s.l.), near Mt. Shintoku (455 m a.

Photo. 2 Mt. Sahorodake (A; 1,059 m) viewed from the southeast (April, 1987).

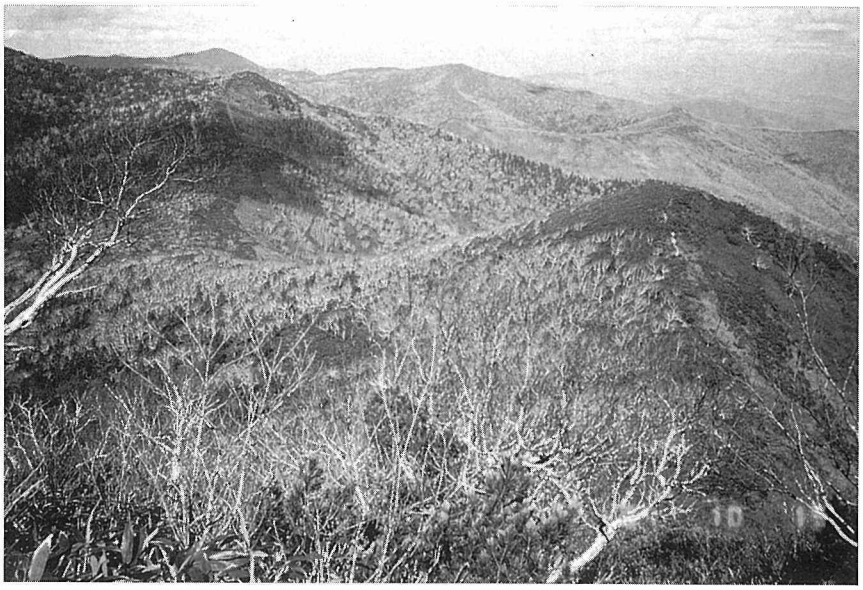

Photo. 3 Southern mountain slopes of Mt. Odassyu (1,097 m), viewed from the top (October, 1987).

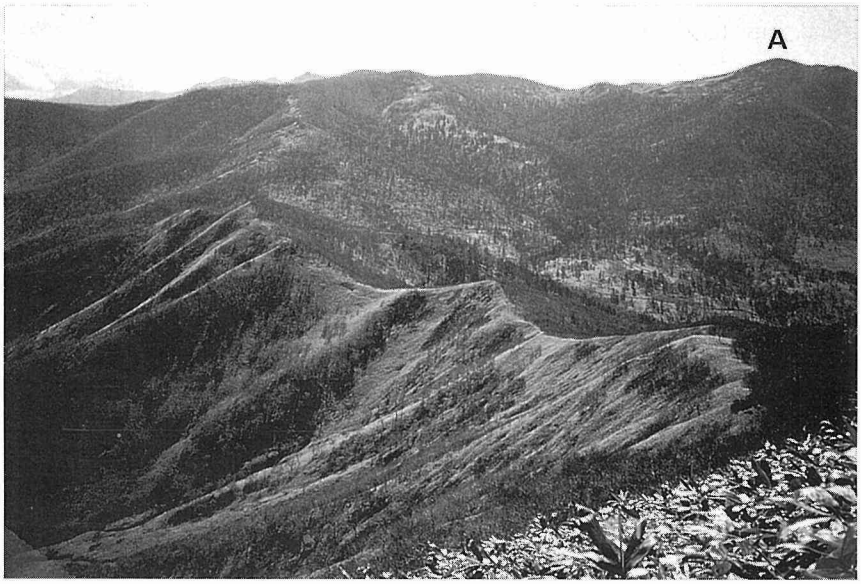

Photo. 4 Mt. Pekerebetsudake (A; 1,532 m) viewed from the southeast (October, 1987).

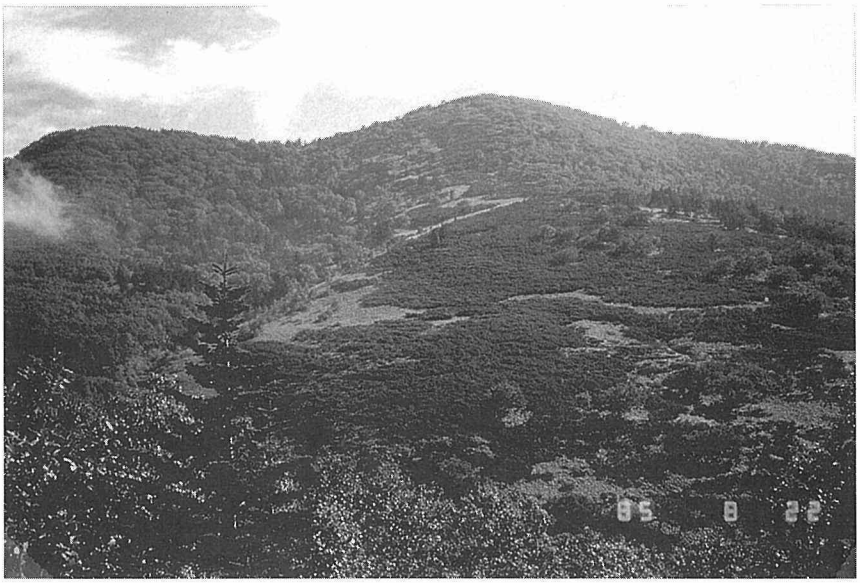

Photo. 5 Smooth and gently inclined crest and mountain slopes around the Nissho Pass (1,106 m) viewed from the south (August, 1985).

s.l.) in the study area, are 7.0 and 1,144 mm between 1966−1975, respectively. The mean January and July temperature are −6.5 and 19.6 between 1966−1975. Precipitation is distributed relatively uniformly throughout the year. The mean maximum snow depth is 57 cm in January, 85 cm in February and 78 cm in March between 1966−1975 (The Ministry of Agriculture and Forestry and The Meteorological Agency, 1978).

According to Tsujii and Miki (1988), the natural vegetation of Mt. Sahorodake mainly involves of subalpine and montane belts. The subalpine belt occupies a comparatively narrow area above 950 m a.s.l., and consists of *Pinus pumila* spreading only on the ridge and north- and west-facing mountain slopes, *Sasa kurilensis* covering comparatively wide areas around the south- and east-facing mountain slopes, *Alnus maximowiczii* communities and *Betula ermanii* forests. The distribution of *Pinus pumila* to the lower altitudes is explained by the effect of the strong north-westerly prevailing wind in winter.

The montane belt occupies areas between 550 m and 950 m a.s.l., and consists mainly of *Betula ermanii* and *Picea jezoensis* communities.

V−2. Topography and Geology

Eastern slopes of the Northern Hidaka Mountains is chosen for the study area. Firstly because the "fossil periglacial slopes" have been widely recognized there, and secondly because that parts of the Hidaka Mountains are composed of different rock types.

Figure 17, a map of the study area, indicates the geology and localities for the

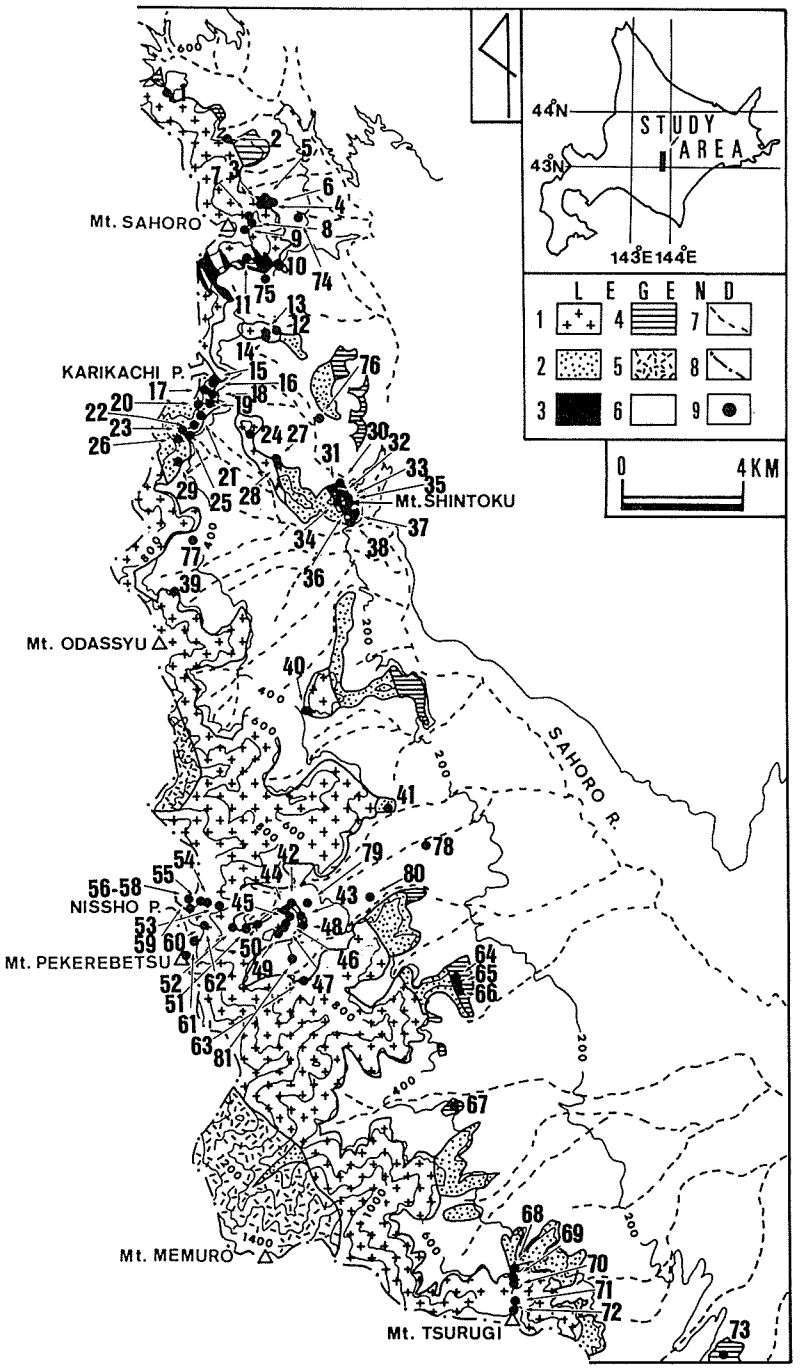

Figure 17 Map showing the study area.
1: Granitic rocks, 2: Hornfels, 3: Gabbro, 4: Shale(The Hidaka Group), 5: Migmatite, 6: Fans, fluvial terraces and river-bed gravel, 7: River, 8: Main ridge, 9: Observation locality.

collection of sedimentological data. The study area is composed of (1) the mountain slopes of the Northern Hidaka Mountains, stretching from north to south with the altitude ranging from 600 m to 1,600 m a.s.l., (2) gentle piedmont slopes bellow 600 m a.s.l., on which many tributaries of the Sahoro River flow in the direction from southwest to northeast, and (3) several isolated hills dominating the piedmont slopes.

Eastern slopes of the Hidaka Mountains are composed both of metamorphic and plutonic rocks such as hornfels, migmatite, granite and gabbro. Hills are chiefly composed of hornfels and shale (the Hidaka Group). Hornfels has a well-developed schistosity along the contact with granitic rocks. All of these rocks are formed in the Pre-cretaceous period (Hashimoto, 1954, 1971; Konoya et al., 1969).

Mountain slopes of the Hidaka Mountains are widely covered with solifluction deposits. They are poorly dissected and densely covered with Sasa (swale bamboo). Such properties give them the smoothness and many author have regarded them as "fossil periglacial slopes" (Ono and Hirakawa, 1975; Hirakawa, 1976, 1977; Yamamoto, 1989a, 1990).

The author restricts the present study only to the slopes composed of granitic rocks, hornfels and shale which are rich in many exposures compared with other rock areas.

Up to now, only a few studies have been done to evaluate the effects of the basement rocks on the development of periglacial slopes. For example, Shimizu (1983) indicated in the Chichibu Mountains, Central Honshu, that the inactive block field develops in a different manner in granite and sedimentary rock areas respectively. The present study area, which includes mountain slopes composed of granite, hornfels and shale, is favorable for the examination of effects of rock types on the periglacial slope formation.

VI. MEASURING METHODS OF THE PERIGLACIAL SLOPE DEPOSITS

VI−1. Macro Fabrics of Slope Deposits

Azimuth and dip of a-axis of clasts were measured at 34 sites of different rock types as indicated in Figure 17. Macro fabrics were measured in different layers separated by tephra layers in many sites; therefore, a total of 59 data were obtained.

Table 12 shows a relationship between length of a-axis and fabrics at two locations: Loc.42 in the granite area and Loc.30 in the shale area shown in Figure 17. In each class which is separated by the a-axis length, 50 clasts were measured. Totally, 150 clasts were measured for the class with a-axis longer than 8 cm in Loc. 42. Table 12 reveals that clasts with longer a-axis show a higher V.Mg. and thus a lesser deviation was seen from the direction of the maximum dip of each slope compared with those with a shorter one.

These results agree well with the idea mentioned in section III−3−1: the azimuths and dips of a-axis of clasts with a longer one should be measured in order to gain a stronger fabric in periglacial slope deposits. In the present study, clasts with length of a-axis at least 8 cm long were selected for measurement, under the assumption that clasts with the length of a-axis over 8 cm show fully strong fabrics.

In a similar way, fabrics of fan deposits were measured at seven sites by the same

methods mentioned above in order to compare these with those of mountain slope deposits.

Table 12 Relationship between length of a-axis and fabric.

Longost Axis(cm)	Granite Stones (Loc.42) Vector Mean (°)	Granite Stones (Loc.42) Vector Magitude (%)	Shale Stones (Loc.30) Vector Mean (°)	Shale Stones (Loc.30) Vector Magitude (%)
8> a	167.2	32.3	83.6	54.1
8≦ a <16	173.3	72.4	———	———
16≦ a <32	175.9	88.2	———	———
32≦ a	176.1	89.7	———	———
8≦ a	175.5	79.1	93.2	73.1

Fifty clasts were measured in each class. Totally, one hundred fifty clasts were measured for the class with a-axis longer than 8 cm in Loc. 42.

VI−2. Grain Size Distribution of Slope Deposits

Grain size distributions were measured at 34 sites in the study slopes. Slope deposits in the granite area are sampled from the horizon below Ta-d pumice and those of hornfels and shale are below To-c2 pumice. Sample was collected from a nearly vertical section with 2 m×4 m on each exposure. The mean and standard deviation of the mean particle size, the skewness, the sorting and the kurtosis by Inman's method were calculated from its textural properties separated by all component and matrix one (-1ϕ). Furthermore, weight percentage of each component such as gravel (-1ϕ>), sand (from -1ϕ to 4ϕ), silt (from 4ϕ to 8ϕ) and clay (8ϕ), was calculated in each rock area.

VI−3. Clast Size and Shape of Slope Deposits

Average length of long axis of the 20 largest clasts (we will abbreviate this "Av.M.A."), average length of long axis of clasts (we will abbreviate this "Av.A."), roundness of clasts, and average ratios of b-axis length against a-axis length of clasts and that of c-axis against b-axis (we will abbreviate them "b/a" and "c/b", respectively) were measured in the same horizons mentioned in section VI−2 in order to describe clast size and shape of slope deposits.

Av.M.A. is defined as an average length of long axis of the 20 largest clasts measured in the order of their size in a nearly vertical section with 2m×4m on each exposure, and Av.A. is defined as the average length of long axis of 50 clasts with a long axis of at least longer than 2 cm in the same sections mentioned above. The parameters b/a and c/b are defined as the average ratio of 50 clasts in the same sections, and roundness measured by Cailleux's method is defined as the average one of 50 clasts with a long axis of at least longer than 5 cm in the same sections.

VI—4. Joint Density of each Bedrock

A joint density is defined as the average number of joints intersecting a circular line 1m long on each bedrock surface by five measurings. The joint density of different lithologic types was measured at six sites as follows: Locations 44 and 48 in the granite area, Locations 18 and 20 in the hornfels area and Locations 10 and 37 in the shale area, as indicated in Figure 17.

VI—5. Stratigraphy of the Periglacial Slope Deposits

VI—5—1. Distribution and age of tephra layers in the study area

Using the estimated or recorded age of tephras described in the previous studies which summarized tephrochronology in Hokkaido (Tephra Layers Naming Committee in Hokkaido, 1982), now Holocene tephra layers fell in the study area are outlined here.

Figure 18 shows a distribution of tephra layers in the study area and columnar sections at points A and B. The C-14 age of the Tarumai d pumice fall deposits (Ta-d) erupted from Mt. Tarumai volcano is believed to be about 9,000 y.B.P., although there is a possibility that the age of Ta-d becomes slightly younger (Umetsu, 1987). This pumice appears as reddish-brown, and is widespread in the study area. The C-14 age of the Tarumai c1 pumice fall deposits (Ta-c1), which appears as white, also erupted from Mt.

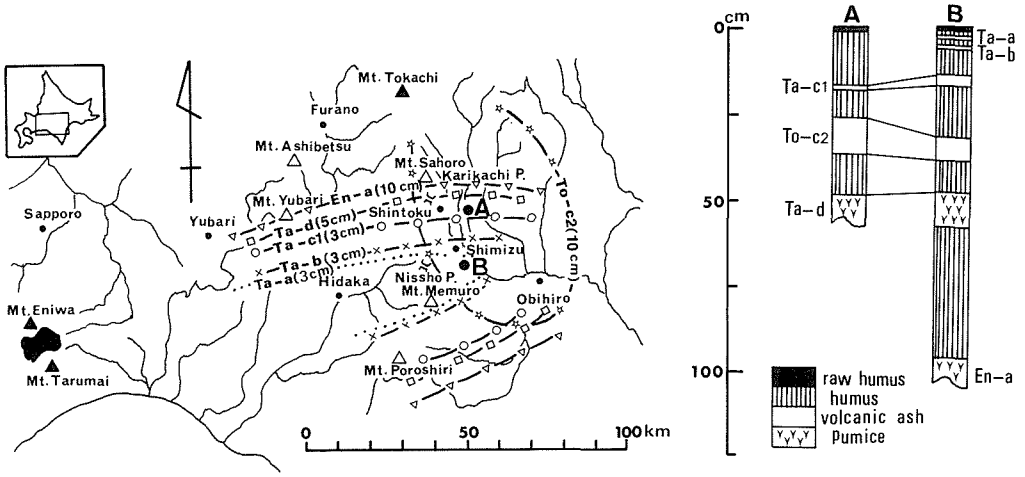

Figure 18 Distribution of tephra layers in the study area and columnar sections at points A and B(after Tephra Layers Naming Committee in Hokkaido, 1982, and Kondo and Doi, 1987).

Tarumai volcano is about 2,000 y.B.P. This pumice spreads in a zone between around Mt. Tsurugi and the Nissho Pass in the study area. This pumice is in accordance with that named To-c1 in the Tokachi plain (Kondo and Doi, 1986).

Both of Tarumai b pumice fall deposits (Ta-b), which fell in the year 1669 A.D. and Tarumai a pumice fall deposits (Ta-a), which fell in the year 1739 A.D., also cover the southern part of the study area with a few centimeters in thickness. Distributions and thickness both of Ta-a and Ta-b are similar to those of Ta-c1.

The C-14 age of the Tokachi c2 pumice fall deposits (To-c2), which appears as white, erupted from Mt. Tokachidake volcano, is about 3,000 y.B.P. To-c2 is widespread with more than a few centimeters in thickness in the study area.

Point A is located approximately 8 km southeast of Karikachi Pass. It has Ta-c1 with 2 cm thickness, To-c2 with 10 cm thickness and Ta-d with more than 8 cm thickness from the upper to the lower (Photo 6). Point B is located approximately 7 km southeast of Nissho Pass. At this point, Ta-a, Ta-b, Ta-c1, To-c2 and Ta-d are found at depth of 3−4 cm, 5−6 cm, 17−21.5 cm, 32−39 cm and 47−60 cm, respectively.

These Holocene tephras suffered the Holocene pedogenesis and formed the andsol (so -called Kuroboku soil in Japan) together with the uppermost tephra of the Last Glacial age, mostly between 7,000 y.B.P. and 3,000 y.B.P. (Kondo, 1985). The period of pedogenesis is also used to determine the ages of mass movement in the Holocene.

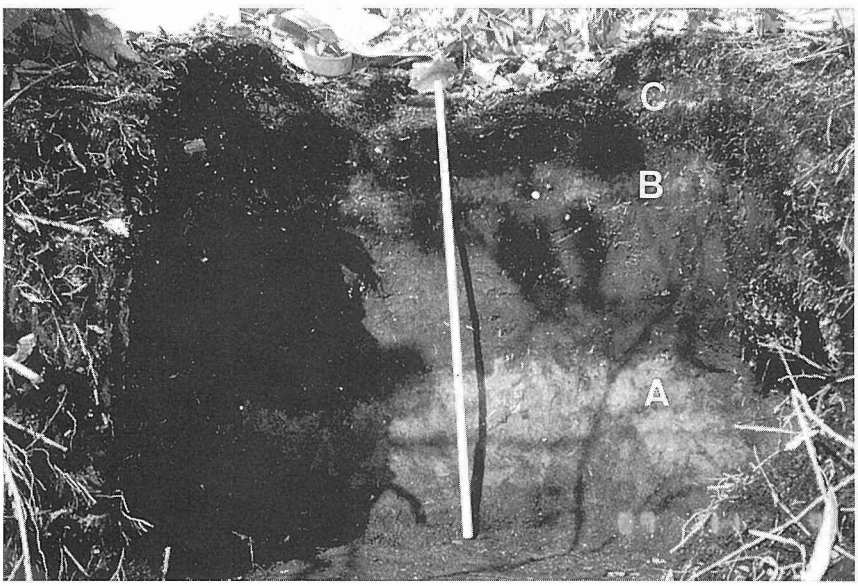

Photo. 6 Section at point A.
Exposure shows Ta-c1 with 2 cm thick (C), To-c2 with 10 cm thick (B) and Ta -d with more than 8 cm thick (A) from the upper to the lower. Measure is 1 m long.

VI—5—2. Division of the stages of mass movement by tephra layers and Kuroboku soil

Figure 19 shows schematic columnar sections showing the periods of mass movement on mountain slopes in the study area. The ages of the pumice layers and Kuroboku horizon mentioned above allow us to classify the following five stages of mass movement on the slopes:

Stage 1: Before the fall of Ta-d or before 9,000 y.B.P.: slope deposits are overlain by Ta-d.

Stage 2: During or shortly after the fall of Ta-d or around 9,000 y.B.P.: slope deposits are mixed with Ta-d, or a thin slope deposit overlies Ta-d.

Stage 3: Before the fall of To-c2 (before 3,000 y.B.P.) or Ta-c1 (before 2,000 y.B.P.): slope deposits are overlain by To-c2 or Ta-c1.

Stage 4: After the fall of To-c2 (after 3,000 y.B.P.) or Ta-c1 (after 2,000 y.B.P.): slope deposits are interstratified with To-c2 or Ta-c1.

Stage 5: After the formation of the Kuroboku horizon (after about 7,000 y.B.P.): slope deposits are mixed with the Kuroboku soil.

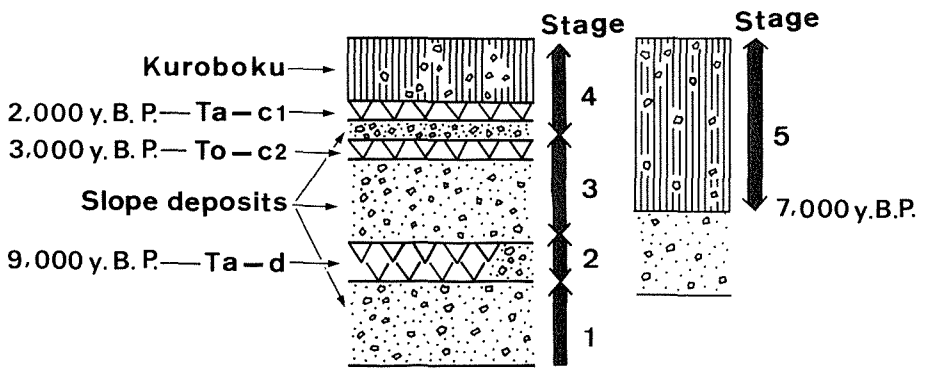

Figure 19 Schematic columnar sections showing the stages of mass movement on mountain slopes in the study area.

VII. QUANTITATIVE CHARACTERISTICS OF SLOPE DEPOSITS AND JOINT DENSITY OF EACH BEDROCK

VII—1. Macro Fabrics of Slope Deposits

Table 13 summarizes macro fabrics of slope deposits in each tephra horizon mentioned above, and Table 14 shows those of fan deposits. Figure 20 illustrates the a-axis orientation of clasts by a rose diagram of both deposits. It shows that all slope deposits have a better preferred orientation than fan deposits do: V.Mg. of slope deposits exceeds 40%, while that of fan deposits is below 40%. This result indicates that the macro fabrics such as V.Mg. is sufficiently useful to distinguish the slope deposits from fan deposits in the

Table 13 Characteristics of clast fabric of slope deposits in the study area.

Loc.	Rock	Stage	Alti-tude (m)	Slope angle (°)	Slope ort. (°)	two-dimension V.Me. (°)	V.Mg. (%)	χ^2	three-dimension S1	S2	S3	C	K	Horizon
1	Gr.	5	563	14	27	24.3	74.2	38.5	.960	.027	.013	4.302	4.892	Kuroboku
2☆	Gr.	1	552	16	342	159.6	85.2	73.8	.928	.052	.020	3.837	3.016	under Ta-d
3☆	Gr.	2	611	13	82	84.8	84.2	70.1	.901	.056	.043	3.042	10.523	under Ta-d
3☆	Gr.	2				85.1	83.7	70.0	.890	.058	.052	2.840	25.053	over Ta-d
4	Gr.	3	620	11	76	84.8	84.2	72.5	.950	.033	.017	4.023	5.068	under To-c2
5☆	Gr.	1	572	13	77	90.6	80.3	53.2	.910	.060	.030	3.412	3.923	under Ta-d
6☆	Gr.	1	516	15	96	56.4	89.1	76.9	.917	.061	.022	3.730	2.658	under Ta-d
7☆	Gr.	1	828	22	3	74.3	87.6	72.5	.934	.052	.014	4.200	2.201	under Ta-d
8	Gr.	5	834	23	79	89.3	61.2	31.3	.937	.047	.016	4.070	2.776	Kuroboku
9☆	Gr.	1	850	22	91	61.4	85.0	69.7	.924	.055	.021	3.784	2.930	under Ta-d
11☆	Gr.	1	477	19	33	29.7	81.5	64.7	.904	.059	.037	3.196	5.849	under Ta-d
12☆	Gr.	4	488	14	170	177.9	81.8	64.8	.920	.051	.029	3.45.7	5.124	under Ta-d
12☆	Gr.	4				176.7	62.5	36.7	.901	.066	.033	3.411	3.771	between Ta-d & Ta-c1
12☆	Gr.	4				179.9	48.4	22.1	.851	.110	.039	3.083	1.973	over Ta-c1
13☆	Gr.	1	417	17	107	107.5	87.0	74.9	.967	.053	.030	3.420	5.009	under Ta-d
14	Gr.	4	360	10	171	179.9	48.4	22.1	.913	.070	.017	3.9384	1.815	over To-c2
24☆	Gr.	2	335	16	130	126.5	90.2	80.4	.922	.053	.025	3.608	3.801	under Ta-d
24☆	Gr.	2				124.9	88.9	77.2	.920	.051	.025	3.608	3.801	over Ta-d
39	Gr.	3	530	13	23	19.1	80.4	60.9	.951	.027	.022	3.766	17.376	under buried soil
40☆	Gr.	1	399	11	161	159.6	79.7	63.6	.910	.055	.032	3.348	5.181	under Ta-d
42☆	Gr.	1	498	14	3	175.3	79.1	61.3	.914	.048	.038	3.180	12.614	under Ta-d
43☆	Gr.	1	522	15	6	4.8	91.1	77.1	.941	.040	.019	3.903	4.242	under Ta-d
45☆	Gr.	2	748	30	100	96.3	94.9	85.1	.949	.029	.022	3.860	9.387	under Ta-d
45☆	Gr.	2				94.1	93.8	82.7	.950	.028	.022	3.765	14.611	over Ta-d
46	Gr.	2	760	21	8	172.3	84.2	70.2	.931	.048	.021	3.792	3.585	under Ta-d
47☆	Gr.	2	751	24	177	176.5	82.3	67.3	.899	.084	.017	3.968	1.484	under Ta-d
47☆	Gr.	2				177.4	79.4	62.4	.911	.076	.013	4.250	1.407	over Ta-d
49	Gr.	2	733	17	149	165.1	87.5	70.0	.928	.053	.019	3.888	2.789	under Ta-d
50☆	Gr.	2	862	22	2	177.5	89.3	75.8	.937	.042	.021	3.798	4.677	under Ta-d
50☆	Gr.	2				180.9	86.1	74.1	.939	.033	.028	3.513	20.379	over Ta-d
51	Gr.	1	860	20	353	1.7	91.9	81.9	.966	.023	.011	4.435	5.065	under Ta-d
52	Gr.	2	837	23	170	177.2	83.9	69.0	.920	.051	.029	3.457	5.120	under Ta-d
53	Gr.	2	961	24	153	162.1	96.4	90.6	.971	.020	.009	4.681	4.859	under Ta-d
54	Gr.	1	982	24	6	8.2	78.5	58.2	.919	.067	.014	4.184	1.672	under Ta-d
55	Gr.	1	1011	20	352	11.5	77.3	57.1	.911	.059	.030	3.413	4.049	under Ta-d
56	Gr.	1	1023	14	339	66.8	84.3	70.	.921	.057	.022	3.734	2.923	under Ta-d
57☆	Gr.	1	1082	17	221	37.3	84.1	73.6	.921	.061	.018	3.935	2.224	under Ta-d
58	Gr.	1	1110	16	247	70.7	81.9	65.2	.929	.040	.031	3.400	12.334	under Ta-d
59	Gr.	1	1040	23	130	124.3	82.1	65.0	.920	.064	.016	4.052	1.923	under Ta-d
60	Gr.	3	1122	20	61	59.2	69.2	48.1	.901	.061	.038	3.166	5.693	under Ta-c1
61	Gr.	3	1327	20	11	8.9	67.3	44.2	.906	.067	.027	3.513	2.865	under Ta-c1
62	Gr.	3	1508	21	352	168.4	68.7	70.1	.900	.060	.040	3.114	6.687	under Ta-c1
63	Gr.	2	607	14	347	139.8	86.7	70.1	.928	.053	.019	3.889	2.790	under Ta-d
68	Gr.	2	432	11	2	178.2	84.3	69.2	.933	.047	.020	3.843	3.499	under Ta-d
69	Gr.	1	527	16	320	144.3	82.3	65.2	.930	.048	.022	3.744	3.800	under Ta-d
70	Gr.	1	561	15	352	8.9	81.3	63.1	.927	.042	.031	3.398	10.279	under Ta-d
71	Gr.	3	1033	20	201	28.2	60.3	32.1	.905	.058	.037	3.197	6.106	under To-c2
72	Gr.	2	1107	21	41	30.4	63.2	36.9	.912	.048	.040	3.127	16.178	under Ta-d

Table 13 (continued)

15☆	Ho.	4	451	15	201	16.2	92.4	81.9	.936	..051	.013	4.277	2.129	under To-c2
15☆	Ho.	4				17.5	90.0	81.5	.920	.043	.017	3.991	2.047	under To-c2
16	Ho.	4	452	14	153	142.5	83.7	71.1	.921	.057	.022	3.734	2.922	under buried soil
16	Ho.	4				140.3	82.1	70.5	.942	.047	.029	3.461	6.167	over buried soil
17☆	Ho.	4	460	19	81	80.2	95.9	88.3	.966	.028	.006	5.081	2.299	under To-c2
17☆	Ho.	4				79.1	95.8	88.1	.955	.032	.012	4.377	3.327	over To-c2
19☆	Ho.	4	422	15	181	175.6	89.0	79.3	.922	.055	.021	3.782	2.928	under To-c2
19☆	Ho.	4				170.2	87.1	74.8	.941	.034	.025	3.628	10.799	over To-c2
21	Ho.	5	390	16	30	34.2	62.1	36.7	.890	.066	.044	3.007	6.424	Kuroboku
22	Ho.	4	408	16	189	17.5	90.9	81.8	.950	.038	.012	4.372	2.792	over To-c2
23☆	Ho.	4	419	17	152	151.5	86.8	73.3	.901	.060	.039	3.140	6.289	under To-c2
23☆	Ho.	4				154.9	84.9	70.0	.889	.068	.043	3.029	5.608	over To-c2
25☆	Ho.	4	401	18	169	170.9	91.9	84.6	.952	.030	.018	3.968	6.769	under To-c2
25☆	Ho.	4				162.2	84.1	68.3	.947	.034	.019	3.909	5.717	over To-c2
26☆	Ho.	4	397	18	247	62.0	68.8	37.4	.899	.075	.026	3.543	2.345	under buried soil
26☆	Ho.	4				63.3	65.2	42.2	.906	.072	.022	3.718	2.136	over buried soil
27	Ho.	5	251	14	36	29.6	85.2	73.8	.904	.076	.020	3.811	1.855	Kuroboku
28☆	Ho.	4	300	13	89	94.9	89.8	80.7	.922	.055	.023	3.691	3.234	under To-c2
28☆	Ho.	4				90.8	82.4	60.7	.916	.054	.030	3.419	4.816	over To-c2
29☆	Ho.	4	502	19	77	77.5	93.6	83.1	.940	.048	.012	4.361	2.146	under To-c2
29☆	Ho.	4				76.5	92.8	81.0	.942	.042	.016	4.075	3.223	over To-c2
10☆	Sh.	4	474	18	177	175.0	87.9	73.7	.918	.058	.026	3.564	3.645	under To-c2
10☆	Sh.	4				172.0	67.3	46.1	.870	.091	.039	3.105	2.665	over To-c2
30☆	Sh.	4	353	30	95	93.2	73.1	52.3	.896	.062	.038	3.160	5.456	under To-c2
30☆	Sh.	4				90.1	64.5	40.6	.890	.064	.046	2.963	7.972	over To-c2
31☆	Sh.	4	366	33	101	97.1	79.9	59.7	.903	.051	.048	2.935	47.424	under To-c2
31☆	Sh.	4				96.4	69.9	47.0	.889	.063	.048	2.919	9.735	over To-c2
33	Sh.	3	397	25	60	53.5	85.2	71.3	.922	.051	.027	3.531	4.551	under To-c2
34☆	Sh.	4	411	31	356	171.9	76.6	47.1	.907	.075	.018	3.920	1.747	under Ta-d
34☆	Sh.	4				172.3	62.1	37.1	.891	.063	.046	2.964	8.424	between Ta-d & To-c2
34☆	Sh.	4				168.3	50.2	23.6	.860	.082	.058	2.696	6.787	over To-c2
35☆	Sh.	4	403	29	359	1.6	46.4	20.6	.848	.101	.051	2.811	3.114	under To-c2
35☆	Sh.	4				4.7	47.1	23.2	.861	.113	.026	3.500	1.382	over To-c2
36☆	Sh.	4	394	19	3	0.3	56.0	29.8	.873	.078	.049	2.880	5.195	under To-c2
36☆	Sh.	4				185.4	53.3	27.9	.869	.077	.054	2.778	4.608	over To-c2
38☆	Sh.	4	278	18	6	4.0	86.2	72.8	.919	.065	.016	4.051	1.890	under To-c2
38☆	Sh.	4				178.8	66.3	44.7	.866	.094	.040	3.075	2.599	over To-c2
41☆	Sh.	4	478	17	104	100.9	78.6	55.0	.891	.061	.048	2.921	11.187	under To-c2
41☆	Sh.	4				109.0	68.1	44.0	.870	.075	.055	2.761	7.901	over To-c2
64	Sh.	2	410	14	190	177.4	62.1	37.7	.901	.056	.043	3.042	10.523	under Ta-d
65☆	Sh.	4	415	19	159	162.9	85.1	68.9	.933	.052	.013	4.273	2.083	under To-c2
65☆	Sh.	4				153.6	62.3	34.7	.891	.076	.033	3.296	2.951	over To-c2
66	Sh.	1	398	17	162	170.2	59.2	33.0	.878	.071	.051	2.846	7.598	under Ta-d
67	Sh.	3	480	14	6	20.3	80.4	63.0	.914	.050	.036	3.234	8.832	between Ta-d & To-c2
73	Sh.	4	301	13	140	142.3	81.8	64.0	.927	.043	.030	3.431	8.530	under Ta-d

Slope ort.: slope orientation. V.Me.: vector mean, V.Mg.: vector magnitude. χ^2: chi-sluare value (degree of freedom is 8). Stages 1 to 5 correspond to those illustrated in Fig. 19. Star on the right-hand side of locality number means samples whose sedimeneary characeeviseics such as clast size and shape, and grain size distributions were mesured.

Table 14 Characteristics of clast fabric of fan deposits in the study area. Measuring methods are the same as in Table 13.

Loc.	Altitude	Slope angle	Slope ort.	two-dimension			three-dimension					investigated horizon
	(m)	(deg.)	(deg.)	V.Me. (deg.)	V.Mg. (%)	χ^2	S_1	S_2	S_3	C	K	
74	460	8	93	58.9	25.3	6.3	.631	.243	.126	1.611	1.452	under Ta-d
75	387	6	132	6.0	32.8	10.7	.599	.261	.140	1.454	1.334	under Ta-d
76	239	4	222	175.6	18.5	2.8	.633	.270	.097	1.876	0.832	under Ta-d
77	343	5	72	75.2	31.9	20.3	.656	.254	.090	1.986	0.914	under Ta-d
78	284	5	14	90.0	20.1	4.6	.691	.211	.098	1.953	1.546	between En-a and Ta-d
79	450	4	52	166.5	25.5	6.3	.551	.315	.134	1.414	0.654	under Ta-d
80	396	4	72	3.1	23.8	5.2	.621	.275	.104	1.787	0.838	under Ta-d
81	626	8	19	161.2	18.5	3.1	.571	.302	.127	1.503	0.736	under Ta-d

study area.

When we plot the values of V.Mg. of slope and fan deposits in the study area on the diagram shown in Figure 15, we obtain Figure 21.

In Figure 21, numbers from 12 to 14 correspond to slope deposits and number 15 is fan deposits in the study area. The sampling procedures are briefly summarized below:

12: Data are derived from slope deposits in the granite area. Twenty-four samples in different layers were obtained from 17 sites. In each site, fifty clasts with the length of a -axis over 8 cm were measured. V.Mg. ranges from 48.4 to 94.9 (mean value: 83.1; standard deviation: 9.81).

13: Data are derived from slope deposits in the hornfels area. Sixteen samples in different layers were obtained from eight sites. V.Mg. ranges from 65.2 to 95.9 (mean value: 87.0; standard deviation: 8.77).

14: Data are derived from slope deposits in the shale area. Nineteen samples in different layers were obtained from nine sites. V.Mg. ranges from 46.4 to 87.9 (mean value: 67.4; standard deviation: 12.98).

15: Data are derived from fan deposits in the study area. Measuring was done at eight sites. V.Mg. ranges from 18.5 to 31.9 (mean value: 30.5; standard deviation: 12.51).

Figure 22 shows a logarithmic ratio plot of slope deposits in order to evaluate the difference of macro fabrics between slope deposits in the study area and other various deposits. In this figure, the data of slope deposits are grouped into different rock types as follows:

Slope deposits in the granite area: S1 ranges from 0.851 to 0.950 (mean value: 0.919; standard deviation: 0.021); C ranges from 2.840 to 4.250 (mean value: 3.583; standard deviation: 0.365); and K ranges from 1.407 to 25.053 (mean value: 6.551; standard deviation: 6.084).

Slope deposits in the hornfels area: S1 ranges from 0.899 to 0.966 (mean value: 0.928; standard deviation: 0.002); C ranges from 3.029 to 5.081 (mean value: 3.812; standard deviation: 0.506); and K ranges from 2.047 to 10.799 (mean value: 4.051; standard deviation: 2.456).

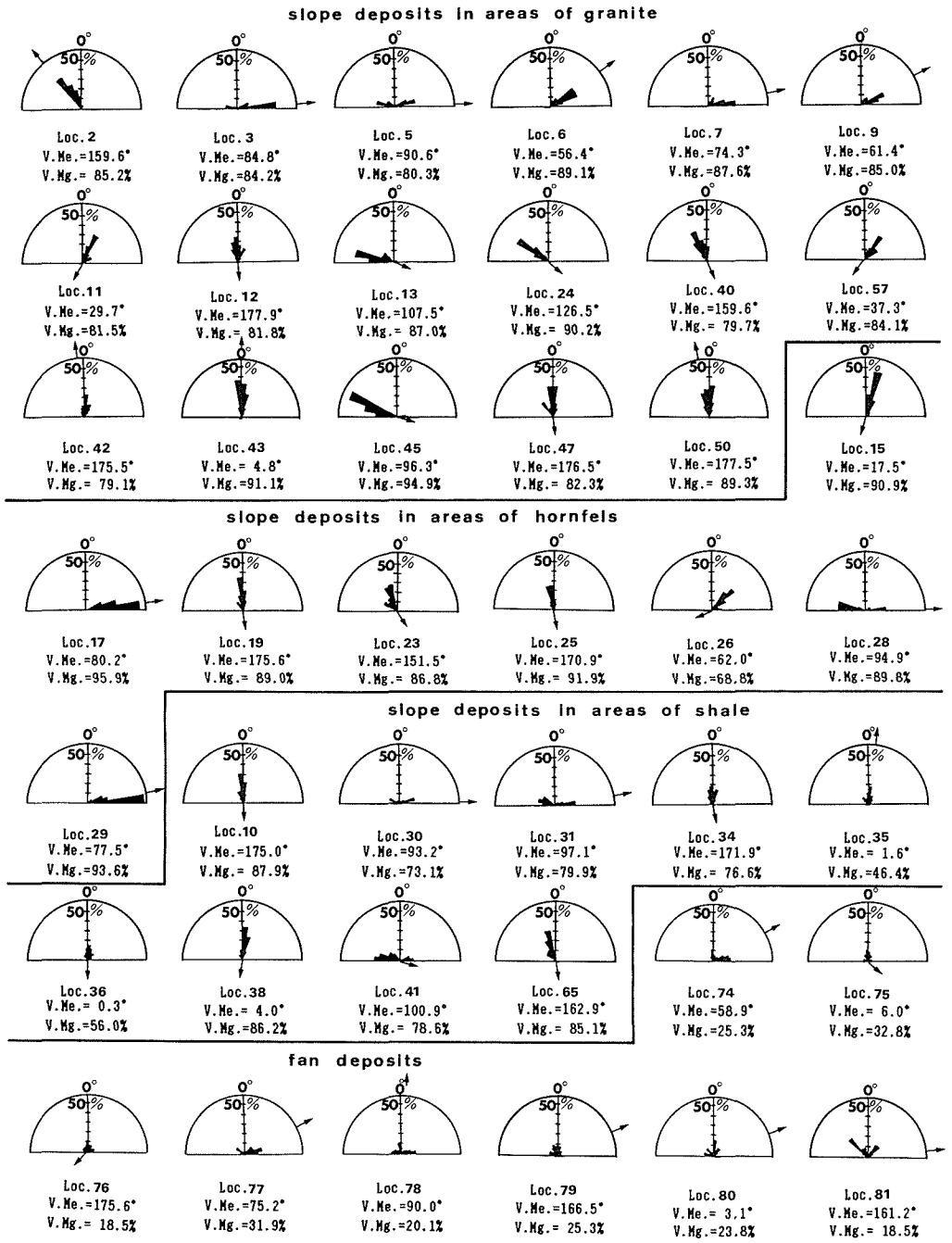

Figure 20 Clast orientation at each locality in the study area.
Arrow indicates direction of maximum dip. V.Me.: Vector Mean (degree), V.Mg.: Vector Magnitude(%).

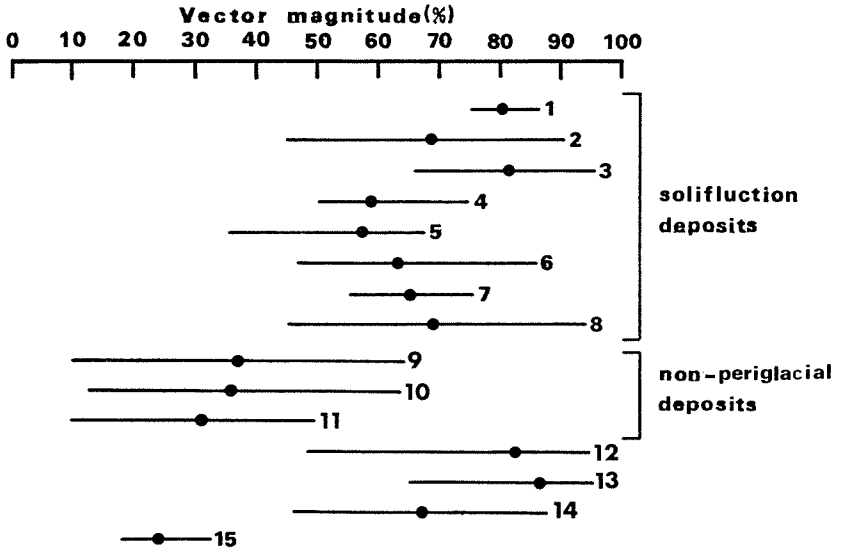

Figure 21 Ranges of vector magnitude(%) of slope and fan deposits in the study area.
Numbers 1 to 11 correspond to those shown in Figure 15. Numbers 12 to 15: data of the study area; 12: slope deposits in the granite area, 13: slope deposits in the hornfels area, 14: slope deposits in the shale area, 15: fan deposits.

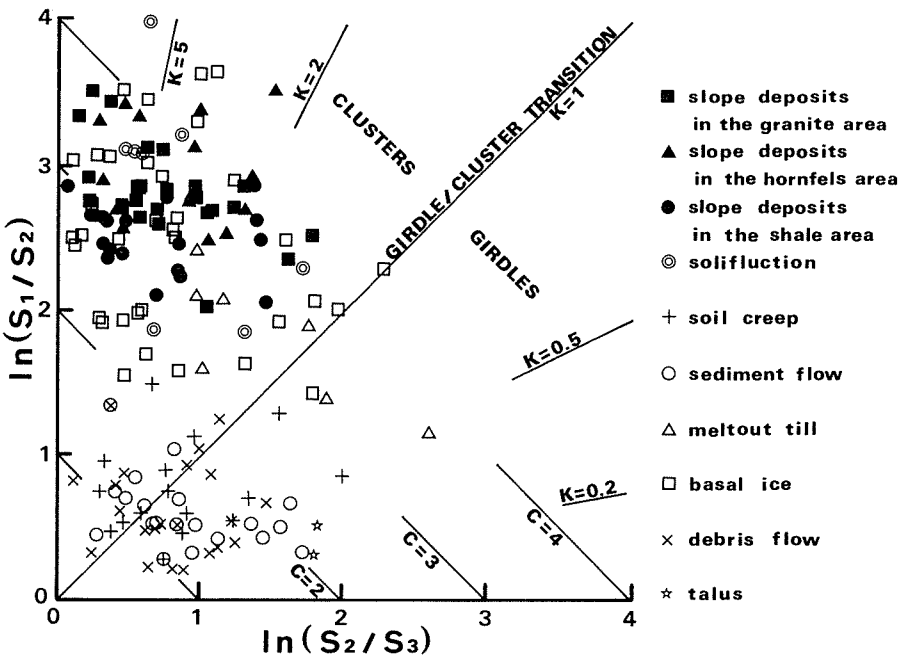

Figure 22 Logarithmic ratio plot of eigen values of slope deposits in this study.
Data source; solifluction: Nelson (1985), soil creep: Mills (1983), sediment flow, meltout till, and basal ice: Lawson (1979), debris flow: Mills (1984, 1986), talus: Giardino and Vitek (1985), and Takada (1987)

Slope deposits in the shale area: S1 ranges from 0.848 to 0.933 (mean value: 0.887; standard deviation: 0.023); C ranges from 2.696 to 4.273 (mean value: 3.241; standard deviation: 0.475); and K ranges from 1.382 to 47.424 (mean value: 7.185; standard deviation: 10.175).

VII−2. Grain Size Distribution of Slope Deposits

Table 15 summarizes the granulometry of slope deposits. Figures 23 and 24 illustrate the grain size distributions in both of all components and matrix, respectively. Figure 25 shows the textural properties of matrix which corresponds to the fractions less than -1ϕ.

Table 15 Granulometmy of slope deposits in the study area.

Loc.	Rock	Gravel (%)	Sand (%)	Silt (%)	Clay (%)	M.p.s. (ϕ)	Skew.	Sort. (ϕ)	Kurto.
2	Gr.	61.41	37.71	0.85	0.03	−2.76	−0.07	3.53	0.31
			(97.72)	(2.23)	(0.08)	(0.82)	(0.21)	(1.35)	(0.63)
3	Gr.	76.42	23.21	0.35	0.02	−2.62	0.22	3.18	0.32
			(89.55)	(1.37)	(0.08)	(0.66)	(0.55)	(1.18)	(0.72)
5	Gr.	69.33	30.07	0.54	0.06	−2.62	0.00	3.08	0.40
			(98.04)	(1.76)	(0.20)	(0.82)	(0.20)	(2.37)	(0.63)
6	Gr.	64.23	34.80	0.92	0.05	−2.25	0.33	2.88	0.38
			(97.29)	(2.57)	(9.14)	(0.72)	(0.20)	(1.25)	(0.76)
7	Gr.	78.36	21.19	0.25	0.21	−2.94	0.25	2.48	0.38
			(97.88)	(1.15)	(0.97)	(0.53)	(0.30)	(1.17)	(0.86)
9	Gr.	63.57	35.14	1.22	0.07	−2.33	−0.07	2.99	0.38
			(96.46)	(3.35)	(0.19)	(0.83)	(0.27)	(1.40)	(0.66)
11	Gr.	71.15	28.26	0.32	0.27	−3.01	0.36	2.91	0.50
			(97.79)	(1.11)	(0.94)	(0.89)	(0.53)	(1.56)	(0.51)
12	Gr.	38.22	59.04	2.29	0.45	−0.30	0.06	2.25	0.70
			(59.56)	(3.71)	(0.73)	(1.20)	(0.24)	(1.73)	(0.38)
13	Gr.	77.41	21.41	1.12	0.06	−2.84	0.19	2.63	0.56
			(94.77)	(4.96)	(0.27)	(1.19)	(0.36)	(1.76)	(0.40)
23	Gr.	55.25	43.54	1.07	0.14	−1.66	−0.20	2.32	0.73
			(97.30)	(2.39)	(0.31)	(0.60)	(0.38)	(1.25)	(0.79)
40	Gr.	63.09	35.61	1.25	0.05	−2.58	∴0.23	2.99	0.34
			(96.47)	(3.39)	(0.13)	(0.64)	(0.36)	(1.28)	(0.79)
42	Gr.	49.08	49.72	1.16	0.04	−2.66	−0.47	3.57	0.22
			(97.64)	(2.28)	(0.08)	(0.58)	(0.15)	(1.15)	(0.82)
43	Gr.	50.71	48.67	0.60	0.02	−2.59	−0.30	3.24	0.28
			(98.74)	(1.22)	(0.04)	(0.38)	(0.26)	(1.03)	(0.56)
45	Gr.	56.03	43.02	0.90	0.05	−2.41	−0.25	3.37	0.30
			(97.84)	(2.05)	(0.11)	(0.68)	(0.11)	(1.20)	(0.74)
47	Gr.	51.16	47.38	1.35	0.11	−2.08	−0.28	3.33	0.37
			(96.98)	(2.79)	(0.23)	(0.83)	(0.17)	(1.33)	(0.68)
50	Gr.	50.25	48.53	1.16	0.66	−1.93	−0.29	3.53	0.28
			(97.55)	(2.33)	(0.12)	(1.09)	(0.15)	(1.43)	(0.57)
57	Gr.	60.21	39.04	0.62	0.23	−2.34	0.19	3.88	0.28
			(98.01)	(1.41)	(0.58)	(1.42)	(0.16)	(1.49)	(0.50)
Mean		60.93	38.02	0.94	0.11	−2.35	−0.33	3.07	0.40
			(97.33)	(2.36)	(0.31)	(0.82)	(0.24)	(1.35)	(0.65)
Standard Deviation		±10.95	±10.60	±0.48	±0.11	±0.62	±0.25	±0.45	±0.14
			(±0.99)	(±1.02)	(±0.30)	(±0.26)	(±0.11)	(±0.19)	(±0.14)

Loc.	Rock	Gravel (%)	Sand (%)	Silt (%)	Clay (%)	M.p.s. (ϕ)	Skew.	Sort. (ϕ)	Kurto.
15	Ho.	41.88	49.63	6.35	2.14	−0.58	0.10	3.04	0.79
			(85.39)	(10.92)	(3.69)	(1.60)	(0.22)	(2.07)	(1.00)
17	Ho.	45.51	47.20	6.42	0.87	−0.93	0.00	4.10	0.38
			(86.62)	(11.79)	(1.59)	(1.97)	(−0.05)	(1.96)	(0.89)
19	Ho.	28.46	62.66	7.24	1.64	−1.09	−0.52	3.80	0.33
			(87.59)	(10.12)	(2.29)	(2.02)	(0.25)	(1.55)	(1.34)
23	Ho.	47.27	45.62	5.04	2.07	−0.75	0.09	3.91	0.37
			(86.52)	(9.56)	(3.92)	(1.89)	(−0.07)	(2.00)	(1.03)
25	Ho.	36.04	55.07	6.06	2.83	−1.06	−0.19	4.20	0.34
			86.10)	(9.48)	(4.42)	(1.83)	(0.07)	(1.98)	(0.92)
26	Ho.	20.43	70.78	4.44	4.35	−0.47	−0.27	3.68	0.52
			(88.95)	(5.58)	(5.47)	(1.71)	(0.14)	(1.94)	(1.44)
28	Ho.	46.52	45.72	4.93	2.83	−1.37	−0.07	3.36	0.56
			(85.48)	(9.22)	(5.30)	(1.53)	(0.23)	(1.87)	(1.51)
29	Ho.	47.23	46.21	4.98	1.58	−0.92	−0.08	4.11	0.41
			(87.47)	(9.43)	(3.00)	(1.60)	(0.22)	(2.07)	(1.00)
Mean		39.17	52.86	5.68	2.29	−0.90	−0.12	2.78	0.46
			(86.78)	(9.51)	(3.71)	(1.77)	(0.13)	(1.93)	(1.14)
Standard Deviation		±9.41	±8.75	±0.91	±0.99	±0.27	±0.19	±0.38	±0.15
			(±1.14)	(±1.70)	(±1.28)	(±0.17)	(±0.12)	(±0.15)	(±0.23)

Loc.	Rock	Gravel (%)	Sand (%)	Silt (%)	Clay (%)	M.p.s. (ϕ)	Skew.	Sort. (ϕ)	Kurto.
10	Sh.	48.16	42.39	8.89	0.56	−1.21	0.28	3.25	0.58
			(81.77)	(17.15)	(1.08)	(2.06)	(0.12)	(2.33)	(0.60)
30	Sh.	65.07	26.44	7.96	0.53	−1.95	0.14	3.10	0.51
			75.70)	(22.79)	(1.51)	(2.65)	(0.45)	(2.61)	(−0.03)
31	Sh.	41.55	48.17	9.34	0.94	−0.33	0.00	3.92	0.49
			(82.40)	(14.99)	(1.61)	(2.18)	(−0.11)	(2.26)	(0.69)
34	Sh.	63.73	30.71	4.90	0.66	−1.66	0.20	3.77	0.42
			(84.66)	(13.51)	(1.83)	(1.66)	(0.46)	(2.21)	(0.53)
35	Sh.	71.26	22.71	5.36	0.67	−2.28	0.55	2.96	0.66
			(79.02)	(18.66)	(2.32)	(2.15)	(0.33)	(2.48)	(0.49)
36	Sh.	65.18	29.26	4.62	0.94	−1.75	0.17	3.84	0.39
			(84.02)	(13.28)	(2.70)	(1.86)	(−0.08)	(2.14)	(0.76)
38	Sh.	61.03	32.80	5.41	0.76	−1.95	0.06	3.45	0.51
			(84.15)	(13.89)	(1.96)	(1.72)	(0.25)	(2.05)	(0.73)
41	Sh.	54.60	33.68	11.13	0.59	−1.59	0.13	3.21	0.62
			(74.18)	(24.51)	(1.31)	(2.77)	(0.18)	(2.45)	(0.48)
65	Sh.	24.27	60.75	13.18	1.80	−0.61	−0.26	3.38	0.58
			(80.22)	(17.40)	(2.38)	(2.54)	(0.14)	(2.20)	(0.68)
Mean		54.98	36.32	7.87	0.83	−1.48	0.14	3.43	0.53
			(80.22)	(17.46)	(1.86)	(2.18)	(0.19)	(2.30)	(0.55)
Standard Deviation		±13.96	±11.34	±2.86	±0.37	±0.61	±0.21	±0.32	±0.08
				(±3.55)	(±3.77)	(±0.50)	(±0.19)	(±0.17)	(±0.23)

M.p.s : mean particle size, Skew. : skewness. Sort. : sorting, Kurto. : kurtosis. Values in perentheses refer to the fraction less than-1.00 ϕ.

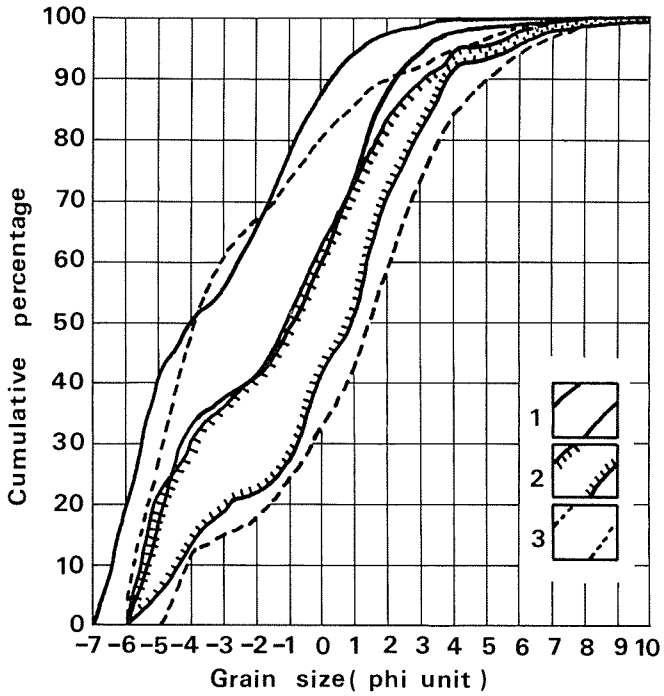

Figure 23 Grain size distribution of slope deposits in the study area.
1: the granite area, 2: the hornfels area, 3: the shale area.

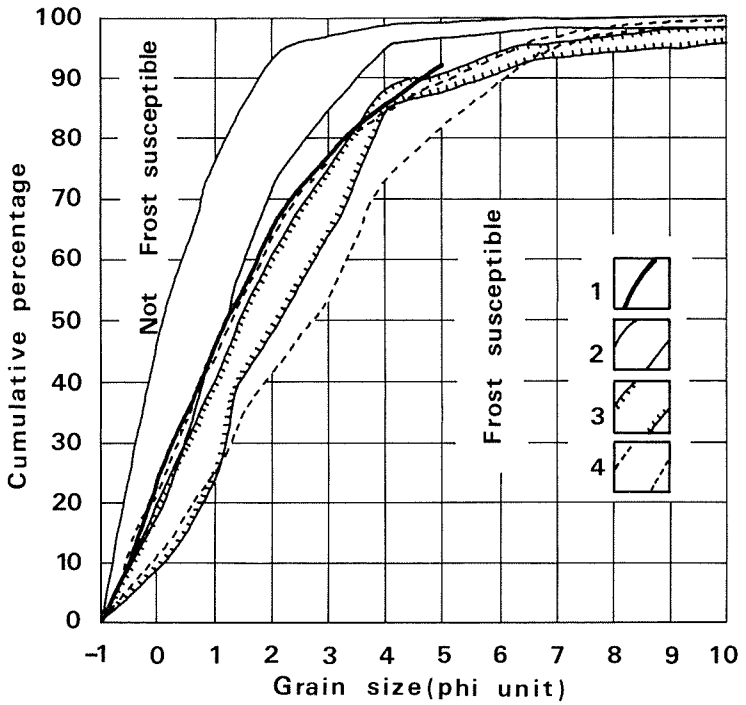

Figure 24 Grain size distribution of matrix of slope deposits in the study area.
1: limit of frost susceptibility (Beskow, 1935), 2: matrix of slope deposits in the granite area, 3: matrix of slope deposits in the hornfels area, 4: matrix of slope deposits in the shale area.

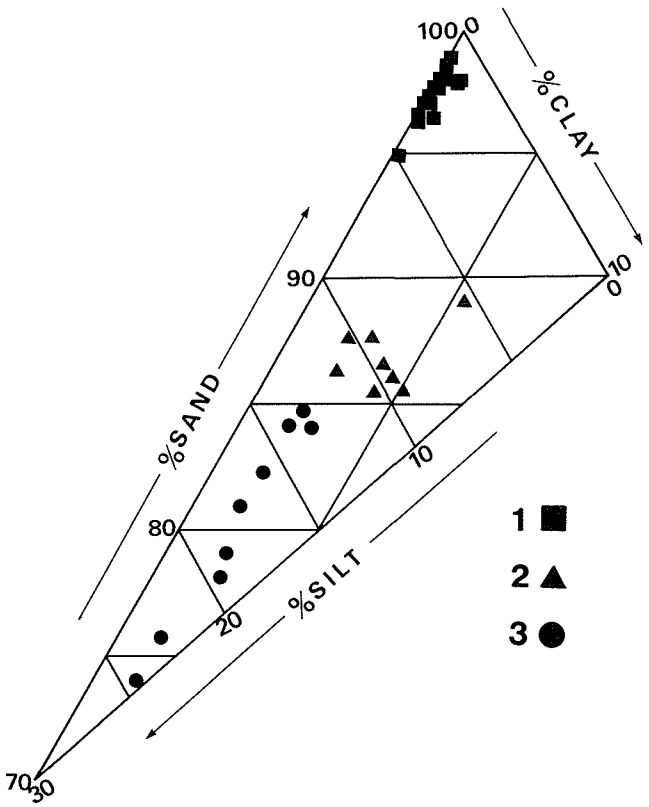

Figure 25 Textural properties of matrix of slope deposits in the study area.
1: the granite area, 2: the hornfels area, 3: the shale area.

They indicate that the slope deposits of the granite area are almost completely composed of gravel (mean content: 60.93%) and sand (mean content: 38.02%), and that the matrix lacks silt (mean content: 2.36%) and clay (mean content: 0.31%). Such a granulometry is considered to be general for the granite area, since the standard deviation for each sedimentary parameter mentioned above is very low, except for clay contents in the matrix.

In contrast to this, the slope deposits in the hornfels area show a lower percentage of gravel content (mean: 39.17%) than in the granite area. Their matrix shows, on the other hand, a high percentage of silt content (mean: 9.51%) and clay content (mean: 3.71%) compared with those in the granite area.

The gravel and sand contents of the slope deposits in the shale area are similar to those in the granite area (mean: 54.98% and 36.72%, respectively). On the other hand, the silt content (mean: 17.46%) and clay content (mean value: 1.86%) in matrix are similar to those in the hornfels area. The slope deposits in the shale area is therefore characterized by a high silt content in the matrix showing over 13%. The sedimentary characteristics of slope deposits in the hornfels and shale areas are also considered to be general because of the low standard deviation of each parameter.

VII—3. Clast Size and Shape of Slope Deposits and Bedrock Joint Density

Table 16 summarizes Av.M.A., Av.A., roundness, and axial ratios of b/a and c/b of slope deposits by different tephra horizons.

Figure 26 shows characteristics of clast size for different lithologic types based on the data listed on Table 16. Both Av.M.A. and Av.A. are larger in the granite area than in the hornfels and shale areas.

Table 16 Clast size and shape of slope deposits in study area.

Loc.	Rock	Size and shape of gravel					Horizon
		Av.M.A. (cm)	Av.A. (cm)	Round.	b/a	c/b	
2	Gr.	27.8	8.7	176.9	0.71	0.59	under Ta-d
3	Gr.	51.1	14.0	122.9	0.63	0.60	under Ta-d
5	Gr.	112.3	16.7	149.4	0.63	0.63	under Ta-d
6	Gr.	49.8	8.0	138.3	0.71	0.64	under Ta-d
7	Gr.	39.6	9.8	144.4	0.64	0.61	under Ta-d
9	Gr.	43.8	9.6	113.5	0.58	0.56	under Ta-d
11	Gr.	32.8	8.8	190.2	0.61	0.67	under Ta-d
12	Gr.	27.2	11.2	173.8	0.69	0.54	under Ta-d
13	Gr.	29.7	9.7	120.7	0.71	0.54	under Ta-d
24	Gr.	22.2	7.9	121.8	0.69	0.65	under Ta-d
40	Gr.	32.8	8.8	190.2	0.61	0.67	under Ta-d
42	Gr.	56.5	11.4	138.2	0.63	0.53	under Ta-d
43	Gr.	34.3	8.7	122.7	0.73	0.63	under Ta-d
45	Gr.	38.5	13.2	124.7	0.72	0.62	under Ta-d
47	Gr.	95.5	11.6	131.5	0.61	0.59	under Ta-d
50	Gr.	32.9	8.5	122.8	0.69	0.57	under Ta-d
57	Gr.	54.5	14.3	122.9	0.66	0.59	under Ta-d
15	Ho.	18.0	4.0	122.9	0.66	0.57	under To-c2
17	Ho.	17.8	4.4	104.5	0.63	0.52	under To-c2
19	Ho.	16.5	4.1	138.2	0.69	0.42	under To-c2
23	Ho.	23.3	6.9	150.5	0.61	0.58	under To-c2
25	Ho.	17.4	5.3	140.1	0.57	0.58	under To-c2
26	Ho.	17.6	7.3	164.3	0.59	0.58	under buried soil
28	Ho.	18.6	5.5	88.9	0.63	0.55	under To-c2
29	Ho.	21.6	8.0	164.7	0.68	0.49	under To-c2
10	Sh.	15.3	5.6	92.1	0.70	0.74	under To-c2
30	Sh.	10.3	3.9	91.0	0.70	0.72	under To-c2
31	Sh.	11.1	3.5	103.6	0.76	0.75	under To-c2
34	Sh.	12.6	6.0	115.7	0.73	0.69	under Ta-d
35	Sh.	16.4	9.3	105.7	0.73	0.69	under To-c2
36	Sh.	11.4	4.9	75.1	0.61	0.72	under To-c2
38	Sh.	14.9	5.3	119.1	0.71	0.71	under To-c2
41	Sh.	21.4	5.5	109.8	0.67	0.62	under To-c2
65	Sh.	11.1	3.7	108.6	0.73	0.71	under To-c2

Av.M.A. : average length of maximum long axis (cm) , Av.A. : average long axis (cm), Round. : roundnss, b/a, c/b : average of the ratio of b-axis length against a-axis length, and c-axis length against b-axis length, respectively.

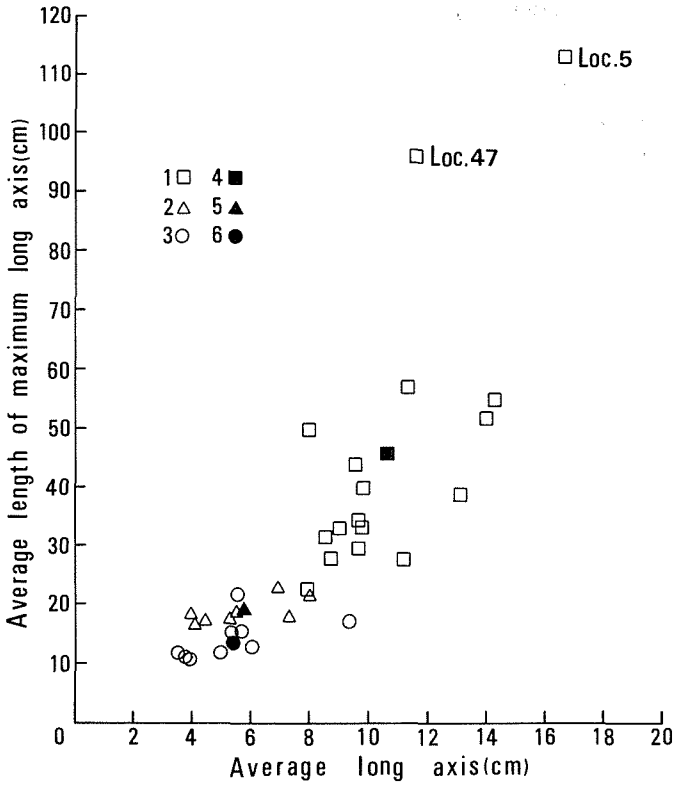

Figure 26 Characteristics of clast size in different lithologic types.
1: clasts contained in slope deposits derived from granite, 2: clasts contained in slope deposits derived from hornfels, 3: clasts contained in slope deposits derived from shale, 4: mean value of legend 1, 5: mean value of legend 2, 6: mean value of legend 3.

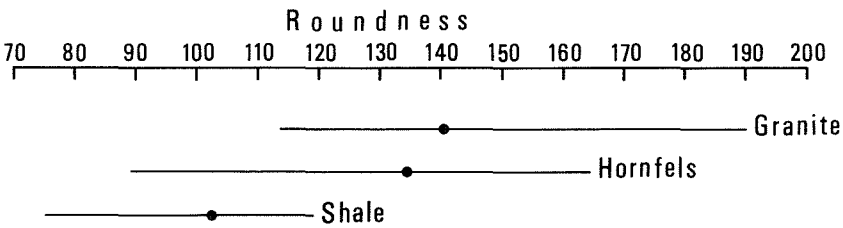

Figure 27 Ranges of roundness of clasts contained in slope deposits. Solid circles show a mean value of roundness in each sample.

Table 17 Bedrock joint density of different lithologic types.

Rock	Loc. No.	Joint Density	Average
Granite	44	5.2	7.9
	48	10.6	
Hornfels	18	23.4	25.4
	20	27.4	
Shale	10	31.8	39.7
	37	47.6	

Figure 27 shows the mean and range of roundness of the clasts by the different lithologic types. All values are less than 200, which coincide with those which are generally regarded as periglacial origin (e.g. King, 1966).

Table 17 shows a bedrock joint density for the different lithologic types. The averages of joint density is the largest for shale but the smallest for granite. This result is in accordance with the clast size data shown in Figure 26, and strongly suggests that clasts were mainly derived from the bedrock surface along joint plane in the past.

VII−4. Discussion

VII−4−1. Main geomorphic processes transporting slope deposits

Table 18 shows the correlation between the fabric strength of each type and slope angle, altitude and other textural properties. The regression coefficient among the above-mentioned variables was calculated on the data listed in Tables 13 and 15. The values of regression coefficient are quite small, indicating that the variables mentioned above do not have a great influence on macro fabrics in the study area. This result supports the idea that the fabric strength of the slope deposits is mainly determined by the process which trnsport the clasts on the slope.

Figures 21 and 22 give the base of discussion for transporting processes. The two-dimensional fabric analysis revealed that the ranges of V.Mg. of slope deposits in the hornfels area coincide with those of solifluction deposits (Figure 21). The mean values of V.Mg.with a 99% confidence are plotted in the range of solifluction deposits. However, the ranges of V.Mg. for the slope deposits in the granite and shale areas are partly overlapped with those for non-periglacial slope deposits. This fact suggests that the two-dimensional fabric analysis is not sufficient for the determination of periglacial and non-periglacial slope processes.

The logarithmic ratio plot give a much better result for the separation of periglacial and non-periglacial deposits (Figure 22). The slope deposits in the study area are plotted in a zone with C larger than 2.5, and K larger than 1.3 in Figure 22. Nelson (1985) pointed out that solifluction deposits have a higher C value than non-periglacial deposits, and that they are plotted in cluster. The plots of solifluction deposits indicated by Nelson (1985) are entirely identical with those of slope deposits in the study area. This fact indicates that the macro fabrics of slope deposits in the study area are determined by the periglacial

Table 18 Correlation between fabric strength of slope deposits in each rock type and other variables.

		Slope Angle	Alti-tude	% Sand+ Silt+ Clay	% Silt+ Clay	% Silt in Matrix	% Silt+ Clay in Matrix
V.Mg.	Gr.	.533	.153	.032	−.136	−.116	−.173
	Ho.	−.041	.305	−.752	−.399	.922	.680
	Sh.	−.295	−.004	.629	.526	.005	−.078
S_1	Gr.	.467	.286	.255	.0439	−.131	−.162
	Ho.	.330	.382	−.381	−.142	.694	.389
	Sh.	−.289	−.084	.703	.524	−.175	−.229
C	Gr.	.578	.592	.146	−.012	.156	−.127
	Ho.	.382	.528	−.294	−.236	.601	.159
	Sh.	−.269	−.206	.448	.229	−.383	−.399

Values mean regression coefficients among two variables. Data listed in Tables 13 and 15 were utilized for these calculations.

solifluction.

VII−4−2. Changes of fabric strength at different stages of mass movement

Figure 28 shows the changes of V.Mg. in different tephra horizons. In this figure, period B coincides with Stage 2 in the granite area, and coincides with Stage 3 in the hornfels and shale areas, respectively. Mean value of V.Mg. of the slope deposits in the granite area varies from 85.4 to 82.4 from Stages 1 to 2, and that of S1 varies equally from 0.921 to 0.919, with the change of that of C from 3.628 to 3.538. By Welch's statistical test, the decrease of each fabric strength is significant (Table 19).

Similarly, the changes in mean values of each fabric strength in the hornfels area from Stages 3 to 4 are as follows: V.Mg.: 88.5→85.4, S1: 0.930→0.927, C: 3.980→3.768. This decrease is also significant by Welch's statistical test (Table 19).

In contrast to the results of the granite and hornfels areas, the change in mean value of each fabric strength in the shale area from Stages 3 to 4 is rejected by Welch's statistical test (Table 19). The change in each fabric strength is as follows:

V.Mg.: 72.8→61.0, S1: 0.897→0.874, C: 3.284→3.010.

VII−4−3. Relationship of clasts in slope deposits and those derived directly from the rock wall

Table 20 compares the particle size and shape between the clasts derived directly from rock wall and those constructing the study slopes. As for the former, 200 clasts were selected at random at two sites, and a total of 400 clasts was measured for each rock type. The axis ratio of 400 clasts in each rock type is summarized in regression equations listed in the table.

On the other hand, data of 50 clasts in each slope deposit are averaged for each rock type, and the regression equations are also calculated. Table 20 indicates that the axis

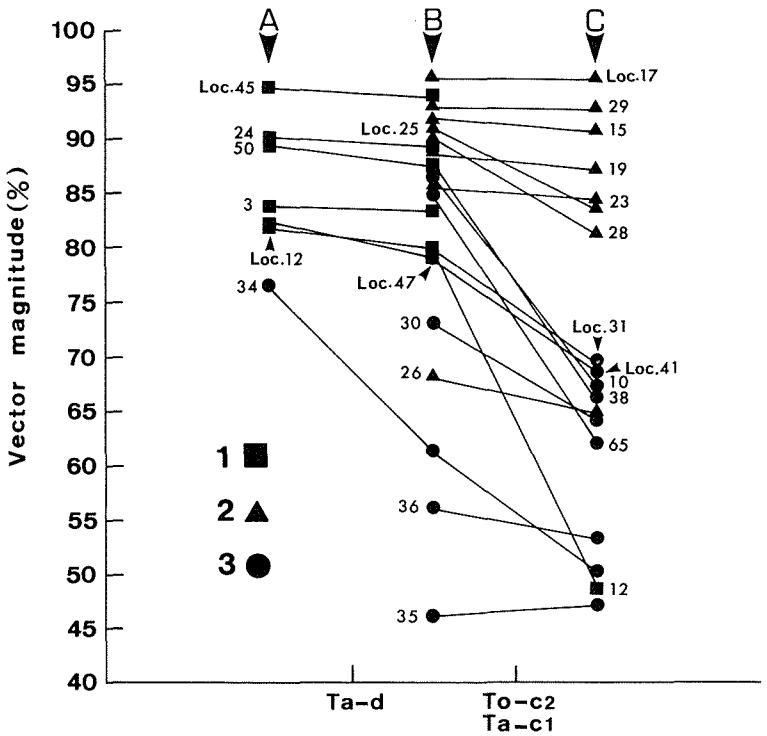

Figure 28 Changes in vector magnitude(%) in different stages of mass movement determined by tephra layers.
1: slope deposits in the granite area, 2: slope deposits in the hornfels area, 3: slope deposits in the shale area.

Table 19 Welch's statistical test for population means of fabric strength in different layers separated by tephra layers.

Rock / Fabric strength	Granite	Hornfels	Shale
Vector magnitude	$H_0: \mu1=\mu2$ $H_1: \mu1>\mu2$ $T=0.665$ with $DF=7$ $t7(.05)=1.895$ ∴significant H_0	$H_0: \mu3=\mu4$ $H_1: \mu3>\mu4$ $T=0.700$ with $DF=14$ $t14(.05)=1.761$ ∴significant H_0	$H_0: \mu3=\mu4$ $H_1: \mu3>\mu4$ $T=2.082$ with $DF=13$ $t13(.05)=1.771$ ∴reject H_0
SI value	$H_0: \mu1=\mu2$ $H_1: \mu1>\mu2$ $T=0.202$ with $DF=8$ $t8(.05)=1.860$ ∴significant H_0	$H_0: \mu3=\mu4$ $H_1: \mu3>\mu4$ $T=0.242$ with $DF=17$ $t17(.05)=1.740$ ∴significant H_0	$H_0: \mu3=\mu4$ $H_1: \mu3>\mu4$ $T=2.082$ with $DF=11$ $t11(.05)=1.796$ ∴reject H_0
C value	$H_0: \mu1=\mu2$ $H_1: \mu1>\mu2$ $T=0.440$ with $DF=7$ $t7(.05)=1.895$ ∴significant H_0	$H_0: \mu3=\mu4$ $H_1: \mu3>\mu4$ $T=0.826$ with $DF=13$ $t13(.05)=1.771$ ∴significant H_0	$H_0: \mu3=\mu4$ $H_1: \mu3>\mu4$ $T=1.135$ with $DF=12$ $t12(.05)=1.782$ ∴significant H_0

H_0 : statistical hypothesis, H_1 : alternative hypothesis, $\mu1-\mu4$: population mean of fabric strength in different horizons ($\mu1$: under Ta-d, $\mu2$: over Ta-d, $\mu3$: under To-c2, $\mu4$: over To-c2), T : calculated statistical testing value in each case, DF : calculated degree of freedom. $t7(.05)=1.895$: value shows critical region on t-distribution with deegree of freedom $=7$, level of significance $=0.05$.

Table 20 Relationship between size and shape of clast derived from rock wall along joint plane and in slope deposits for each lithologic type.

Correlation among length of axes			a-axis of measured clasts (cm)	Correlation among length of axes			a-axis of measured clasts (cm)
Axes	Regression Equation	r		Axes	Regression Equation	r	
Granite clasts derived from rock wall (Loc.3, Loc.48)				Granite clasts in slope deposits			
a and b	b=0.525a+2.541	0.85	Min. 6.5 Max.105.0	a and b	b=0.543a+1.542	0.80	Min. 5.0 Max. 51.0
b and c	c=0.435b+2.880	0.75	Av. 33.3 Sx. 26.2	b and c	c=0.413b+1.643	0.74	Av. 13.7 Sx. 6.4
Hornfels clasts derived from rock wall (Loc.18, Loc.20)				Hornfels clasts slope deposits			
a and b	b=0.660a+0.247	0.83	Min. 3.9 Max. 24.4	a and b	b=0.429a+1.287	0.65	Min. 5.0 Max. 21.4
b and c	c=0.508b+0.868	0.76	Av. 10.8 Sx. 2.7	b and c	c=0.299b+1.087	0.55	Av. 7.2 Sx. 3.2
Shale clasts derived from rock wall (Loc.32, Loc.37)				Shale clasts in slope deposits			
a and b	b=0.476a+1.542	0.65	Min. 4.1 Max. 17.7	a and b	b=0.574a+1.079	0.70	Min. 5.0 Max. 17.2
b and c	c=0.241b+1.528	0.40	Av. 8.5 Sx. 3.4	b and c	c=0.464b+1.231	0.50	Av. 7.1 Sx. 2.7

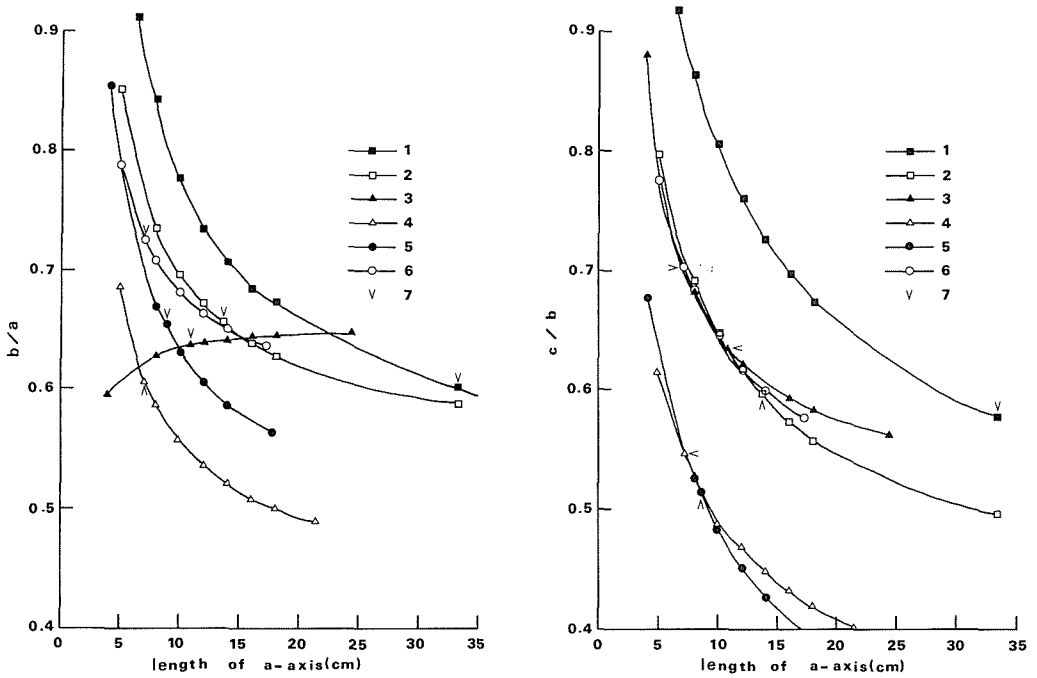

Figure 29 Changes in b/a- and c/b-axis ratios corresponding to the increase in a -axis length of clasts derived from rock wall and of slope deposits.
1: clasts derived from rock wall in the granite area, 2: clasts contained in slope deposits in the granite area, 3: clasts derived from rock wall in the hornfels area, 4: clasts contained in slope deposits in the hornfels area, 5: clasts derived from rock wall in the shale area, 6: clasts contained in slope deposits in the shale area, 7: mean value of a-axis length of clasts in each sample. Values were calculated by regression equations listed in Table 20.

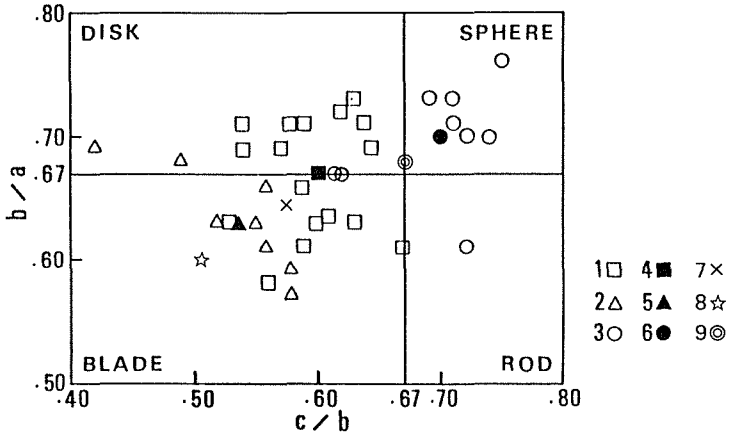

Figure 30 Clast shape indicated by Zingg's diagram.
1: clasts contained in slope deposits in the granite area, 2: clasts contained in slope deposits in the hornfels area, 3: clasts contained in slope deposits in the shale area, 4: mean value of legend 1, 5: mean value of legend 2, 6: mean value of legend 3, 7: mean value of clasts derived from rock wall (granite) of localities 3 and 48, 8: mean value of clasts derived from rock wall (hornfels) of localities 18 and 20, 9: mean value of clasts derived from rock wall (shale) of localities 32 and 37.

growth rates are increasing in the order of a-axis, b-axis and c-axis. In other words, there is a tendency that clasts with a longer a-axis have a lower b/a-axis ratio.

Figure 29 shows the changes in b/a- and c/b-axis ratios corresponding to the increase in a-axis length of clasts directly derived from rock wall and slope deposits. The values in this figure were calculated by means of the regression equation listed in Table 20. It is recognized that b/a- and c/b-axis ratios against the length of a-axis show the similar changes for clasts derived from rock wall and those in slope deposits.

Using the data of axis ratio of clasts at each site listed in Table 15, Figure 30 illustrates the clast shape by Zingg's diagram, in which the mean values of clast derived from the rock wall in each lithologic type (granite; b/a:0.651, c/b:0.588; hornfels; b/a: 0.602, c/b: 0.516; shale; b/a: 0.686, c/b: 0.674) are plotted. Clasts of slope deposits in the shale area are mostly plotted in a zone of Sphere-shape, and those in the hornfels area are mostly in a zone of Blade-shape, while those in the granite area are in a zone intercalated in the above zones. Mean values of b/a and c/b-axis ratios of clasts derived from the rock wall are rather in accordance with those of slope deposits for each rock type, respectively.

From these facts, it is concluded that the weathering characteristics of bedrocks strongly influence a-axis length and shape of clasts in slope deposits in the study area.

VII−4−4. Effects of clast size and shape on the changes in macro fabrics

As illustrated in Figure 28, the fabric strength of slope deposits in the study area shows a greater decrease in the shale area than in the hornfels area. This is probably because

of the difference of clast shape and size of slope deposits in both areas.

The discussion in Chapter VI−3−1 leads to the conclusion that the clasts with a longer a-axis and a lower b/a-axis ratio have a stronger fabric than those with a shorter a-axis and a higher b/a-axis ratio. This conclusion supports the idea that the macro fabric of the Sphere-type or smaller clasts is more easily changed than that of Blade-type or larger clasts, either by non-periglacial slope processes or by an increase in mass movement velocity.

As mentioned in the previous section, the clasts have a shorter a-axis and a higher b/a-axis ratio in the shale area compared with those in the hornfels and granite areas. Therefore, the clasts in the shale area decrease the fabric strength much more easily than those in other bedrocks.

VIII. PERIODS OF MASS MOVEMENT ON MOUNTAIN SLOPES IN THE STUDY AREA

VIII−1. Difference of the Periods of Mass Movement affected by Rock Types and Slope Altitude

Some exposures and columnar sections of the slope deposits in the study area are shown in Figure 31-1 and -2. Many localities show Stage 1 (Locs. 2, 5, 6, 7, 9, 11, 13, 40, 42, 43, 51, 54, 55, 56, 57, 58, 59, 60 and 70) and Stage 2 (Locs. 3, 24, 45, 46, 47, 49, 50, 52, 53, 63, 68 and 72) in the granite area. Slope deposits of Stage 1 are directly overlain by Ta-d.

At Loc.42 in the lowest part of Nissho Pass, Ta-d with 10 cm thick overlie ill-sorted angular debris which is more over 6 m thick. Ta-d, which is overlain by raw humus and humus, is 25 cm thick. Thus, this locality coincides with Stage 1.

The slope deposits at Loc.45 about 300 m east of Loc.43, consist of sub-angular gravel with much sand in a matrix of more than 150 cm thickness, which are intercalated with Ta-d at a depth of 70−80 cm (Photo 7). Thus, this locality coincides with Stage 2.

There are some localities which coincide with Stage 3 (Locs. 4, 39, 60, 61, 62 and 71), Stage 4 (Locs. 12 and 14) and Stage 5 (Locs. 1 and 8).

At Loc.4 east of Mt. Sahorodake, the sediment to a depth of more than 2 m is ill-sorted angular debris which is partly overlain by To-c2 with 3 cm thick (Photo 8). At Loc.39 (Photo 9) north of Mt. Odassyu, the slope deposits, which consist of angular gravels with much sand in matrix, were undercut by fossil valley-fill sediment which is at a depth of about 1 m is To-c2. C-14 age is given from the Kuroboku soil underlying To-c2 (3,000± 170 y.B.P.: NUTA-385). At Loc.62 north of Mt. Pekerebetsudake, the upper 1 m sediment consists of raw humus and Kuroboku soil intercalating thin ash layers, Ta-a and Ta-b, at a depth of 7−8 cm, 74−75.5 cm, respectively. Below that, the sediment consists of sub-angular gravels, which are underlain by Ta-c1, at a depth of 111−112 cm, intercalating To-c2, at depth of 137−139 cm. Thus Locs. 4, 39 and 62 coincide with Stage 3.

At Loc.14 on the east of Karikachi Pass, the upper 14 cm of sediment consists of raw humus and Kuroboku soil, and the lower sediment, which consists of sub-angular gravel

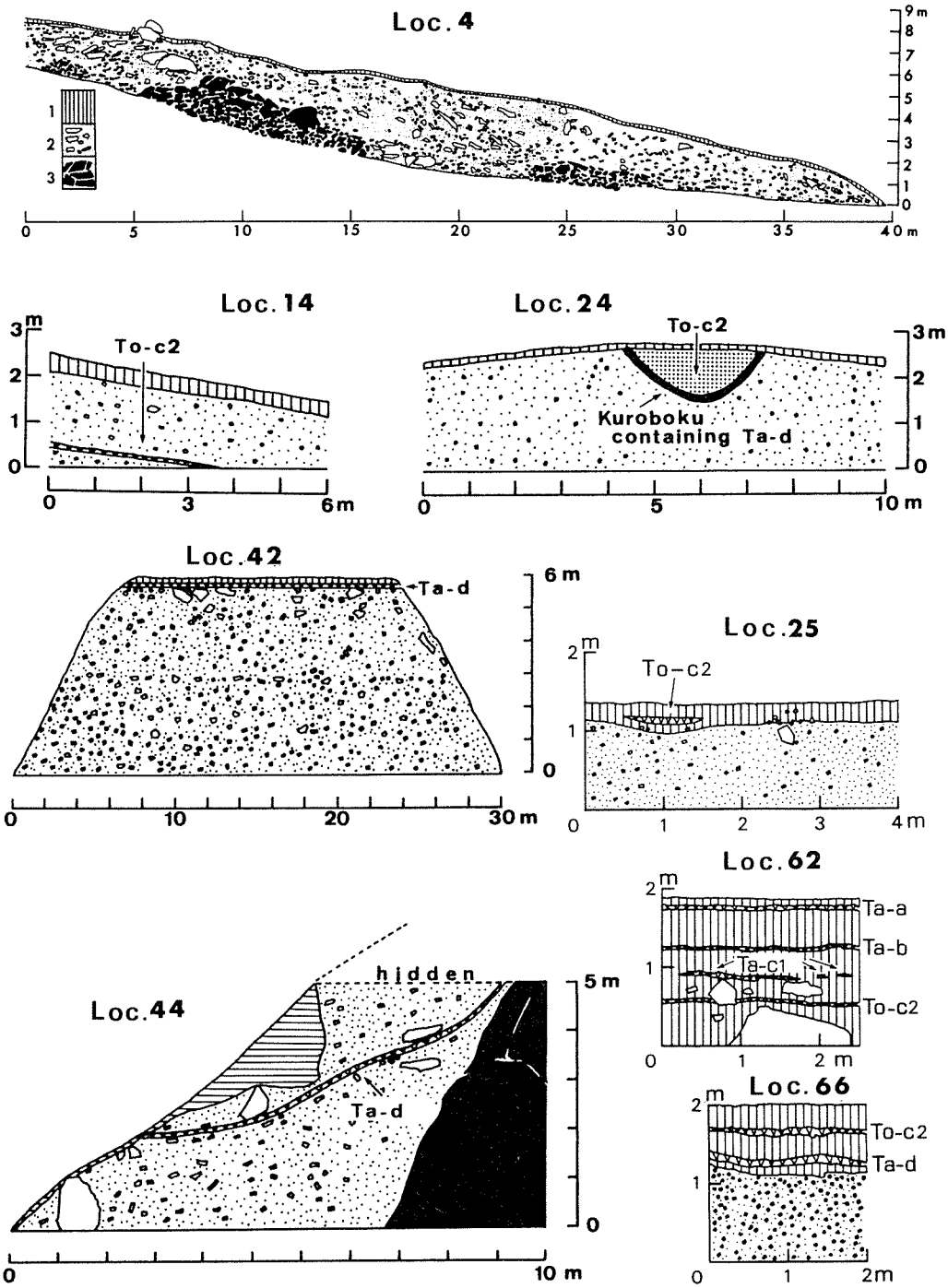

Figure 31 Sketches of exposures and columnar sections of slope deposits in the study area.

1: Kuroboku soil, 2: slope deposits, 3: jointed (in situ) bed rock (for legends see Loc. 4).

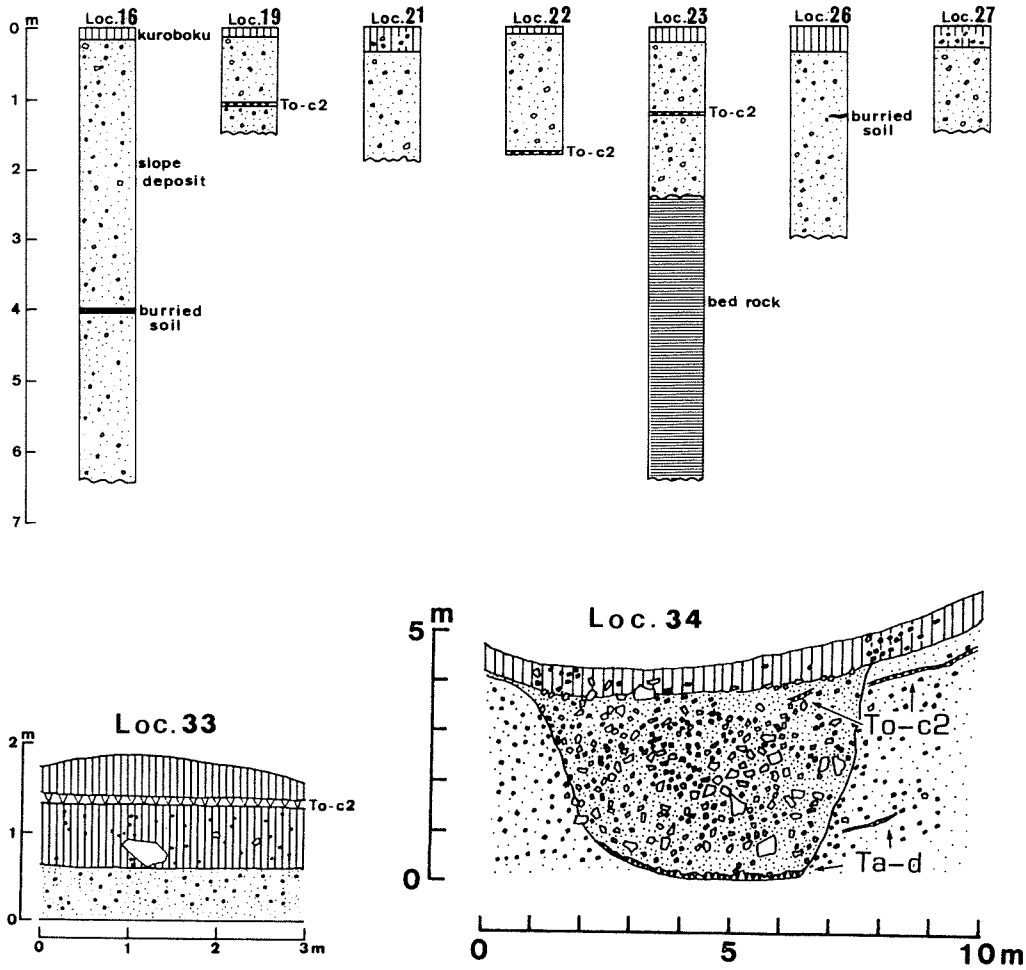

Figure 31-2 Sketches of exposures and columnar sections of slope deposits in the study area.
1: Kuroboku soil, 2: slope deposits, 3: jointed (in situ) bed rock (for legends see Loc. 4).

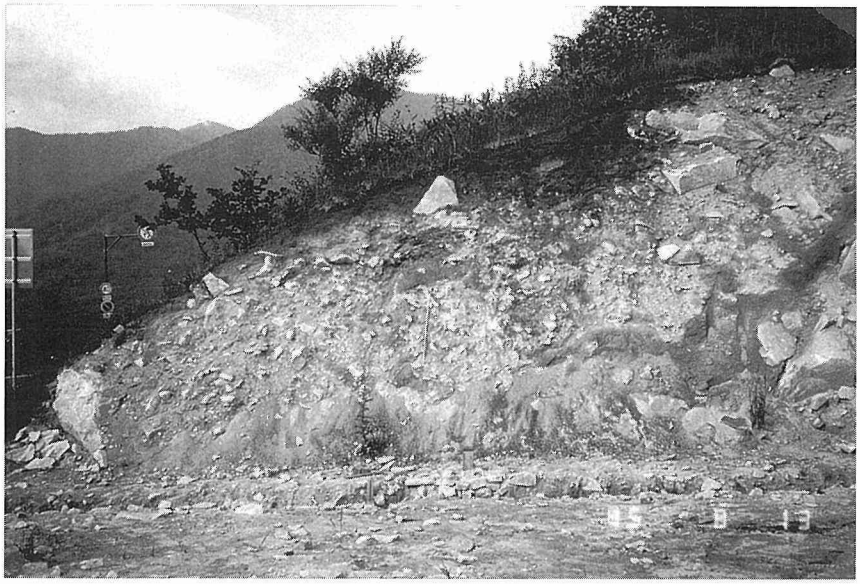

Photo. 7 Section at Loc. 45.
Slope deposits are intercalated with Ta-d at depth of 70−80 cm. Measure is 1 m long.

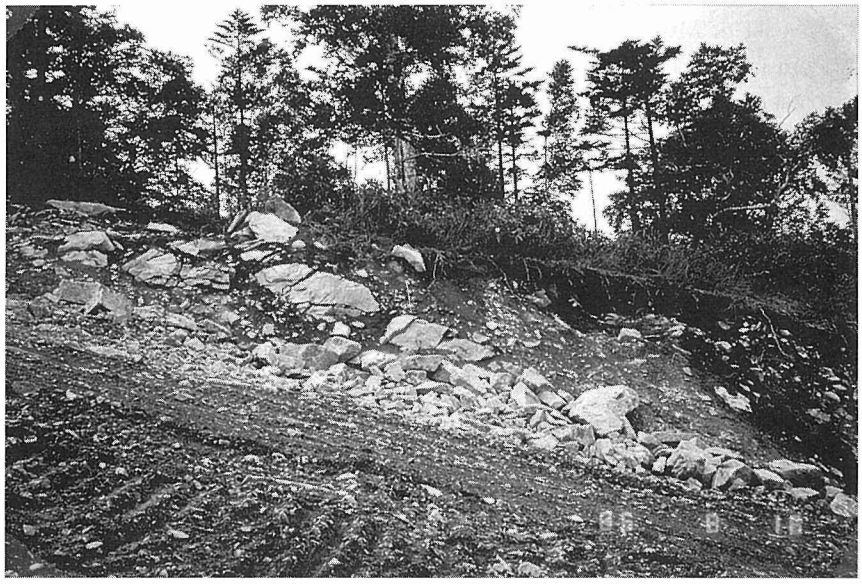

Photo. 8 Section at Loc. 4.
Slope deposits are mainly composed of large angular clasts with sand-rich matrix. Measure is 1 m long.

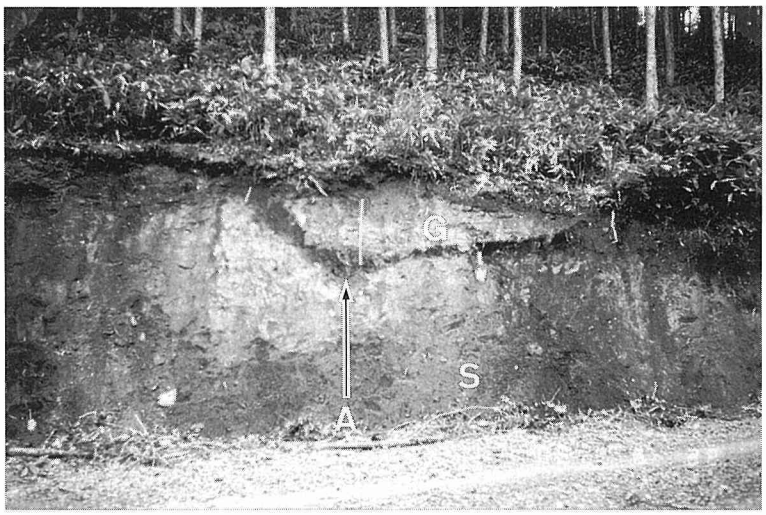

Photo. 9 Section at Loc. 39.
Slope deposits (S), which consist of angular gravels with sandrich matrix, were undercut by fossil gully-fill sediment (G) about 1 m thick. C-14 age is given from point A (3,000−170 y.B.P.: NUTA-385). Measure is 1 m long.

with a slight matrix, is intercalated with To-c2 to a depth of 110−120 cm. Thus Loc.14 coincides with Stage 4.

At Loc.8 east of Mt. Sahorodake, angular gravels are mixed in Kuroboku soil, which is about 25 cm in thickness (Photo 10). Thus Loc.8 coincides with Stage 5.

In contrast to this, most localities in the hornfels area show Stage 4 (Locs. 15, 16, 17, 19, 22, 23, 25, 26, 28 and 29), and a few localities show Stage 5 (Locs. 21 and 27).

At Loc.25 to the south of Karikachi Pass, the upper 25 cm of sediment consists of raw humus and Kuroboku soil partly intercalating To-c2 at a depth of 16−21 cm. It contains many subangular gravels overlying To-c2. At Locs. 16, 19, 21, 22, 23 and 27 south of Karikachi Pass, which are shown in the columnar sections, ill-sorted angular debris is intercalated with To-c2 or buried soil, which were dated as 2,140±35 y.B.P. (KSU-911) in Loc.16 and 2,140±70 y.B.P. (KSU-909) in Loc.26, respectively. Thus, these localities coincide with Stage 4.

In a similar way, most localities in the shale area show Stage 4 (Locs. 10, 30, 31, 34, 35, 36, 38, 41 and 65) and a few localities show other Stages (1: Locs. 66 and 75; 2: Loc.64; 3: Locs. 33 and 67).

At Loc.34 on Mt. Shintoku, slope deposits were undercut by fossil valley-fill sediment, which is at a depth of about 4 m, and which is a debris flow deposits intercalating To-c2, at depth of 115−125 cm. Slope deposits are intercalated with To-c2 and Ta-d at a depth of 74−80 cm and 370−380 cm, respectively (Photo 11).

At Loc.36 on Mt. Shintoku, Kuroboku soil containing many angular gravels is interstratified with To-c2 at a depth of 15−37 cm (Photo 12). Thus, Locs. 34 and 36 coincide

Photo. 10 Section at Loc. 8.
Angular gravels are mixed in Kuroboku soil, which is about 25 cm in thickness.

Photo. 11 Section at Loc. 34.
Slope deposits (S), which are intercalated with To-c2 and Ta-d at depth of 74—80 cm and 370—380 cm respectively, were undercut by fossil gully-fill sediment (G). Measure is 1 m long.

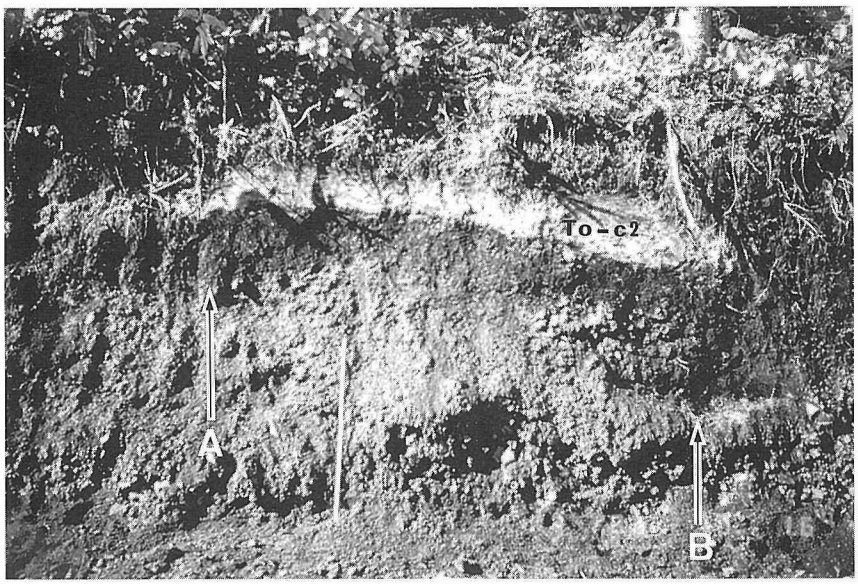

Photo. 12 Section at Loc. 36.
Kuroboku soil is interstratified with To-c2. C-14 ages are given from points A (3, 460−130 y.B.P.:NUTA-146), and B (4,640 130 y.B.P.:NUTA−145). Measure is 1 m long.

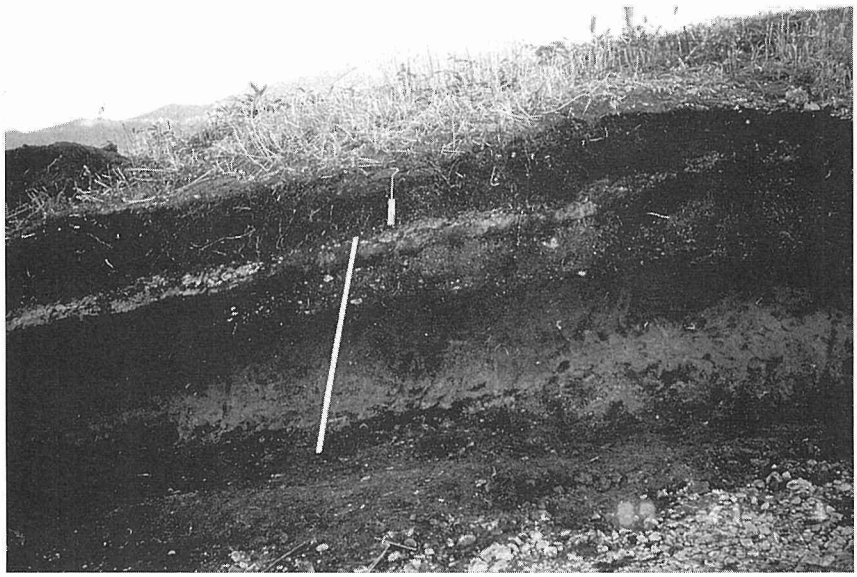

Photo. 13 Section at Loc. 67.
Solifluction lobe containing angular clasts between To-c2 (white ash bed) and Ta -d (reddish-brown one). Measure is 1 m long.

with Stage 4.

At Loc.33 near Loc.34, the upper 80 cm of sediment consists of raw humus and Kuroboku soil intercalating To-c2, at a depth of 55−63 cm. It contains many sub-angular gravels overlying To-c2. At Loc.67 northeast of Mt. Memurodake, a solifluction lobe containing angular gravels is interbedded between Ta-d and To-c2 (Photo 13). Thus, Locs. 33 and 67 coincide with Stage 3.

Figure 32 shows the localities of exposures and the periods of solifluction which are indicated by different symbols related to each stage mentioned in section VI−4−2.

Moreover Figure 33 shows the distributions of exposures defined by their altitude and stage in different rock types. Exposures in the granite area distribute at a higher altitude zone than those in the hornfels and shale areas. This fact results from distributions of each bedrock as mentioned in section V−2. In addition, in the granite area many exposures in the area lower than 1,000 m a.s.l. show Stages 1 and 2, and those in the area higher than 1,000 m a.s.l. show Stage 3, while many exposures in the hornfels and shale areas show Stages 4 and 5.

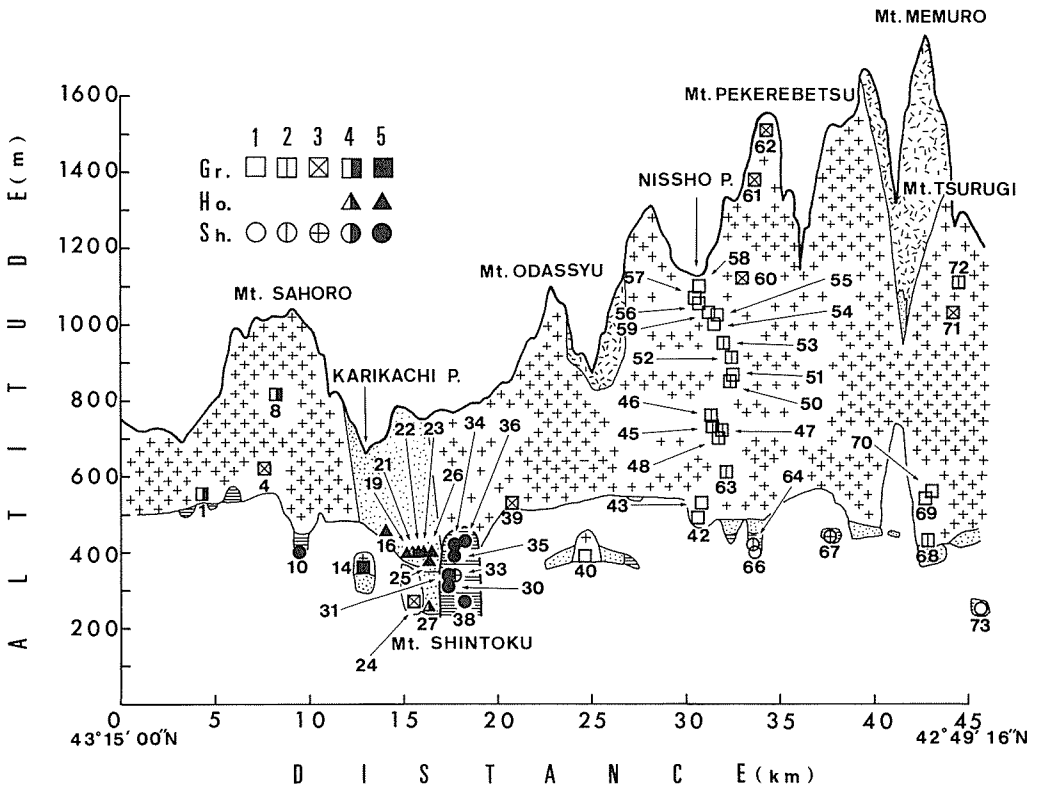

Figure 32 Localities of exposures classified by the stages of mass movement of slope deposits.

Gr.: granitic rocks, Ho.: hornfels, Sh.: shale. Numbers 1 to 73 denote locations. Nos. 1 to 5 correspond to the stages of mass movement illustrated in Figure 19.

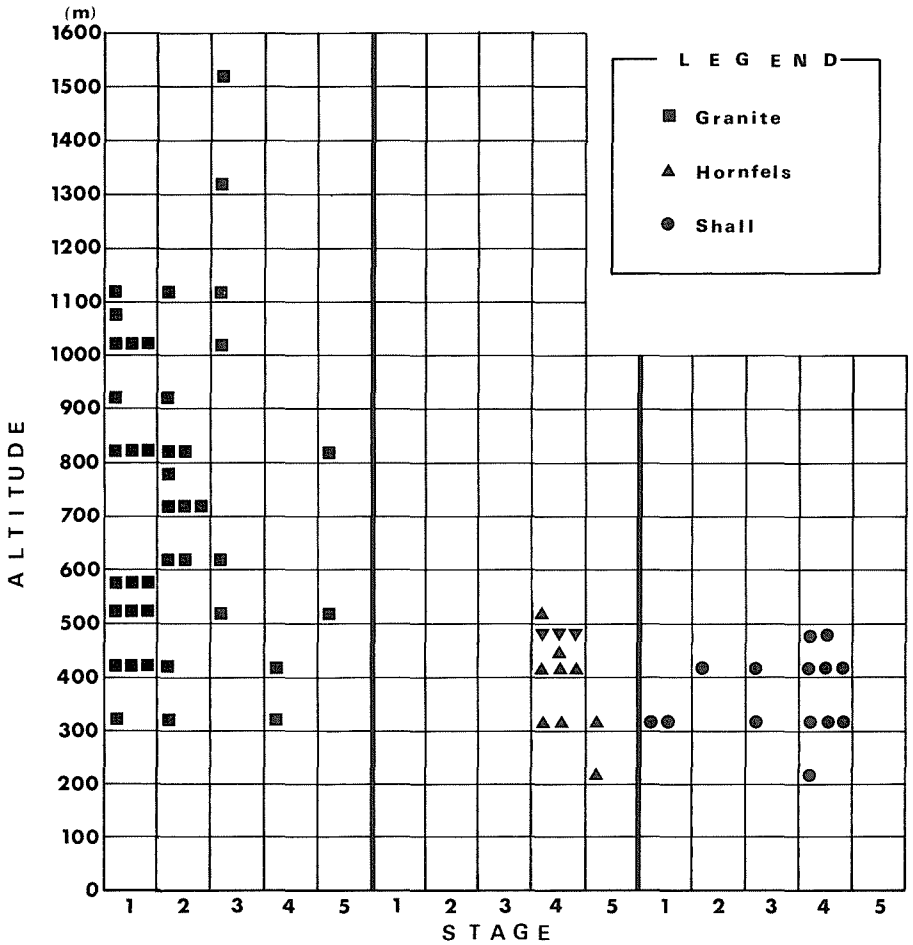

Figure 33 Distributions of localities classified by altitude and stages of mass movement for different lithologic types.
Stages 1 to 5 correspond to those illustrated in Figure 19.

Figure 34 shows the frequency of each stage in different altitude zone separated by 100 m intervals on the basis of the data shown in Figure 31. In the granite area, Stages 1 and 2 show much higher frequency than other stages in the zone lower than 1,000 m a.s.l., and Stage 3 is increasing in frequency according to an increase in altitude in the area higher than 1,000 m a.s.l. From this result it may be inferred that Stages 3, 4 and 5 probably reveal irregular cases in the area lower than 1,000 m a.s.l., and that an altitude of about 1, 000 m a.s.l. probably seems to correspond to the boundary which distinguishes the zone with mainly Stages 1 and 2 from those with mainly Stage 3. To put it different terms, it may be inferred that solifluction ceased in the later time in the higher location according to time -lag in the Holocene in the granite area.

In contrast to this, in the hornfels and shale areas, although all exposures located in

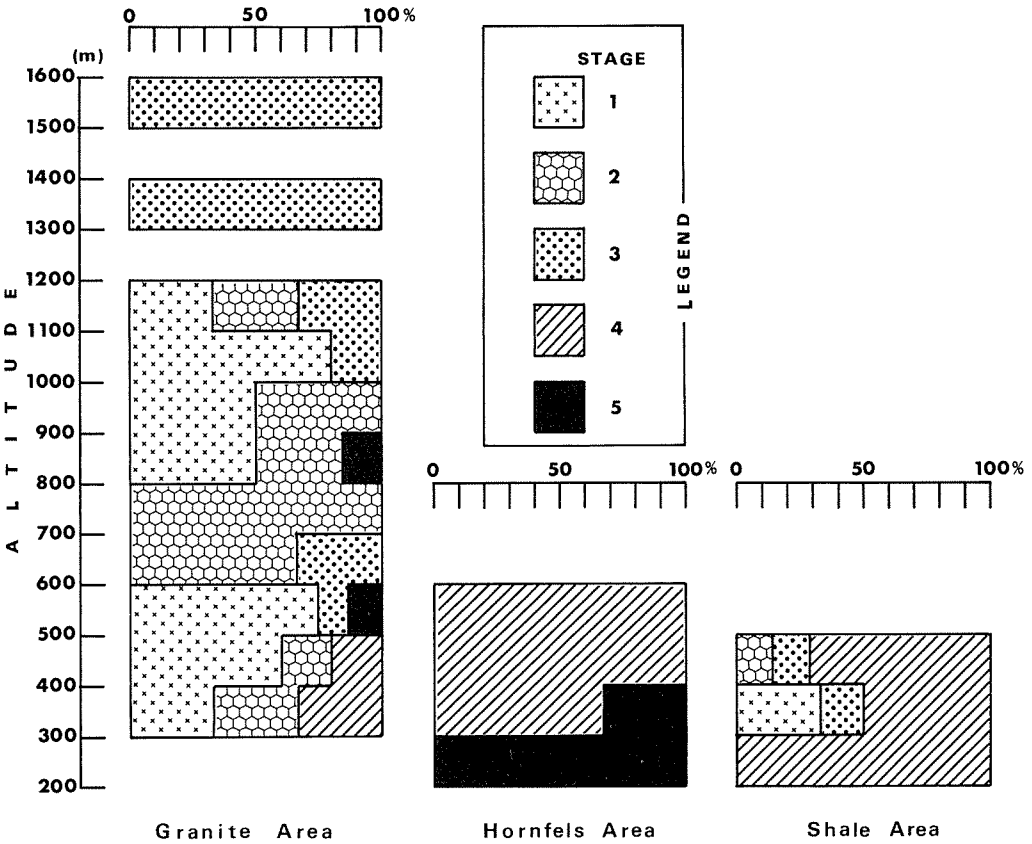

Figure 34 Altitudinal change of frequency of each stage of mass movement for different lithologic types.
Stages 1 to 5 correspond to those illustrated in Figure 19.

areas lower than 600 m a.s.l., Stages 3, 4 and 5 are superior to other stages. The result indicates that solifluction continued until Stages 3, 4 and 5 in many parts of the hornfels and shale areas. The fact that in areas lower than 600 m a.s.l. solifluction continued for a longer time in the hornfels and shale areas than in the granite area may be explained by the finer debris production in the former compared with the later. As mentioned above, the clasts of hornfels and shale are smaller than those of granite. Furthermore, the textural properties of the matrix from granite are not frost-susceptible, while those from hornfels and shale are highly-frost susceptible. Therefore, slope deposits in the hornfels and shale areas were likely to be transported much more easily even by weaker solifluction compared with those in the granite area. The general idea as for the periods of solifluction in the study area is summarized in Figure 35.

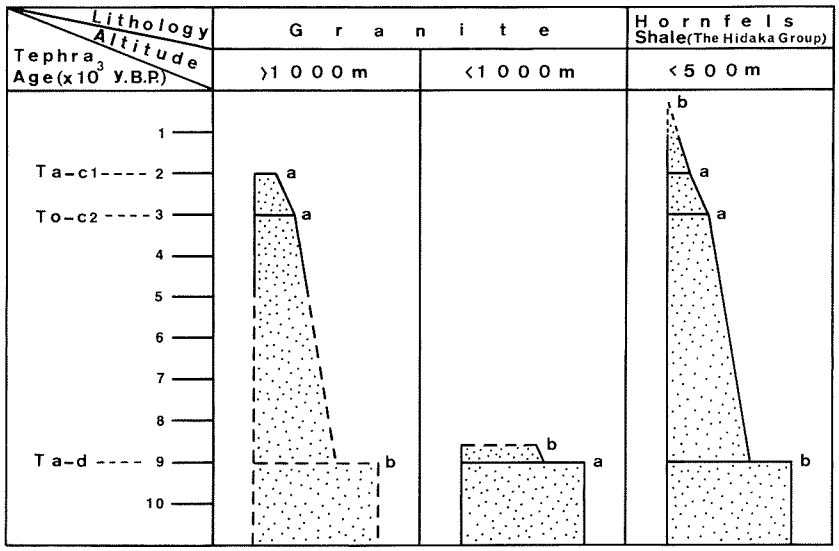

Figure 35 Schematic change of solifluction magnitude on the mountain slopes in the study area.
a: interruption or termination of solifluction, b: estimated.

VIII—2. Discussion

VIII—2—1. Effect of grain size distribution of slope deposits on the period of periglacial mass movement

As mentioned in Chapter VII—2, the slope deposits covered with Ta-d in the granite area are almost completely composed of gravel and sand, and their matrix lacks silt and clay, while those underlain by To-c2 in the hornfels and shale areas contain a much higher percentage of silt and clay than those in the granite area. Furthermore, the textural properties of the matrix in the granite area are not frost-susceptible, while that in the hornfels and shale areas are highly frost-susceptible as shown in Figure 24. This fact suggests that slope deposits in the shale and hornfels areas could be transported much more easily by weaker solifluction.

The reason why periglacial processes continued for a longer time in the hornfels and shale areas than in the granite area can be explained by the difference of grain size distribution and clast size mentioned above. Harris (1987) also pointed out that head deposits with the matrix composed of clay content of more than 25% can give rise to slide with shear plane in England and Wales.

VIII—2—2. Comparison of the periods of mass movement between the study area and other areas

A clear recognition of the fossil periglacial slope deposits, by using the logarithmic

ratio plot method, has never been done in the previous studies in Japan.

However, a few studies have safely claimed the formation of the fossil periglacial slope by solifluction in the Holocene. For example, Higaki (1987) indicated that the solifluction ceased in the later time in the Holocene in the higher location in the Kitakami Highland. Iso (1974) also pointed out the fact that a little solifluction continued in the Holocene on steeper mountain slopes in the area mentioned above. Higaki (1987) recognized that mass movement by solifluction continued until 5,000 y.B.P. on the summit area of Mt. Hayachine in the Kitakami Highland. I also indicated the possibility that "gentle slope II" in Mt. Syokanbetsudake was formed by solifluction in the Holocene (Yamamoto, 1987). These data support the idea that the solifluction was active in the Holocene in the particular areas, such as higher altitude belts or specific rock areas where slope deposits are composed of much finer and more frost-susceptible debris.

The results of the present study reinforce this idea: the Holocene periglacial mass movement was active until about 2,000 y.B.P. only above 1,000 m in altitude in the granite area, where the slope deposits are not frost-susceptible. On the other hand, it was active until quasi-present age even under 500 m in altitude in the hornfels and shale areas where the slope deposits are frost-susceptible.

IX. CONCLUSIONS

IX—1. Macro Fabrics of Periglacial Slope Deposits

The comparison between Vector Magnitude and S1 for macro fabric data of slope and other deposits gathered from various sources revealed that the three-dimensional fabric analysis is more effective than the two-dimensional one to distinguish the periglacial slope deposits from other deposits. By the logarithmic ratio plot method, the solifluction deposits, having a higher C value than other deposits such as those of soil creep, debris flow and talus, are plotted in a zone with C, ranging over about 2.5, and K, ranging over about 1.3. These values characterize the solifluction deposits from other non-periglacial deposits, except glacial ones on the logarithmic ratio plot.

The three-dimensional fabric analysis of 2,350 clasts at the site located on the fossil periglacial slope in the Hidaka Mountains clarified some relations between fabric strength and clast size and shape. The main results are: (1) c/b-axis ratio has little effect on its fabric; (2) clasts with a longer a-axis length have stronger fabrics; and (3) clasts of Blade or Rod types have stronger fabrics than those of Disc or Sphere types in a range of shorter a-axis length.

IX—2. Quantitative Characteristics of Slope Deposits in different Bedrock Areas

The exposures of smooth mountain slopes in the Northern Hidaka Mountains, central Hokkaido, were observed, and three-dimensional fabric analysis of clast constructing these slopes was done in order to determine their transporting processes.

All of the slope deposits in the study area are plotted in a zone with C ranging over 2.

5 and K ranging over 1.3 on a logarithmic ratio plot. This result leads to the conclusion that the slope deposits are of periglacial origin, probably transported by solifluction.

The clast size is basically determined by a joint density of bedrock surface: the shale likely produces Sphere-type clasts, while the hornfels produces more Blade-type clasts; the shale clasts are smaller than those of the granite and hornfels.

This fact suggests that the macro fabric of the Sphere-type and smaller clasts is more easily changed than that of Blade-type and larger clasts under the influence of non-periglacial processes or under the influence of an increase in mass movement velocity. Therefore, the fabric strength of slope deposits shows a greater decrease in the shale area than in the hornfels area, after the fall of Ta-d.

The reason why periglacial processes continued for a longer time in the hornfels and shale areas than in the granite area can be explained by the difference of grain size distribution and clast size in the individual rock areas. The slope deposits covered with Ta-d in the granite area are almost completely composed of gravel and sand, and their matrix lack silt and clay. The slope deposits underlain by To-c2 (about 3,000 y.B.P.) in the hornfels and shale areas contain a much higher percentage of silt and clay than those in the granite areas. Furthermore, the textural properties of the matrix of the slope deposits in the granite area are not frost-susceptible, while those of the hornfels and shale areas are highly frost-susceptible. The sediment characteristics of the slope deposits in the shale and hornfels areas suggest that these slope deposits are easily transported even by weaker solifluction.

IX—3. Chronology of Holocene Periglacial Mass Movement in different Bedrock Areas

Observations of more than 70 exposures, cutting gentle and smooth slope in the Northern Hidaka Mountains, revealed that the slope is composed of ill-sorted angular debris which is covered and/or is intercalated with Holocene pumice layers and the Kuroboku soil. Fabric analysis of the slope deposits by means of the logarithmic ratio plot method strongly suggests that the deposits are periglacial origin, most probably transported by solifluction.

The C-14 dates of the pumice layers and the Kuroboku soil enable to determine the periods of solifluction on the slopes as follows:

Stage 1: before the fall of Ta-d pumice (9,000 y.B.P.)

Stage 2: the fall of Ta-d～short periods (not confirmed)

Stage 3: before the fall of To-c2 pumice (3,000 y.B.P.) or Ta-c1 pumice (2,000 y.B.P.)

Stage 4: after the fall of To-c2 or Ta-c1

Stage 5: after the Kuroboku soil (7,000～3,000 y.B.P.)

The periods in which the solifluction ceased are different according to rock types and altitudes as follows:

Granite areas: solifluction ceased mostly at Stage 1 or 2 in the areas lower than about 1,000 m a.s.l., while in the areas above this altitude, the solifluction occurred again shortly in Stage 3.

Hornfels and shale areas: many localities show continuation of the solifluction until

Stages 3, 4 and 5 even in the areas below 500 m a.s.l., while the slope movement ceased in Stage 1 or 2 in some localities.

The fact that the solifluction continued for a longer time in the hornfels and shale areas than in the granite areas can be explained by a finer, frost-susceptible debris -production from the bedrock in the former areas.

Acknowledgments

I wish to thank to Professor Yugo Ono, Graduate School of Environmental Science, Hokkaido University for his many helpful suggestions during the course of this work. I am also indebted to Mr. Hiroshi Yamamoto, Graduate School of Environmental Science, Hokkaido University for his help and discussions. I also grateful for the help of Associate Professor Hidenori Takahashi, Dr. Shin-ichi Urano and the other members of Laboratory of Fundamental Research, Graduate School of Environmental Science, Hokkaido University. Furthermore, I wish to thank to Professor Hiroshi Kadomura, Department of Geography, Faculty of Science, Tokyo Metropolitan University, Professor Ichio Moriya, Department of Geography, Faculty of Letters, Kanazawa University, Professor Ikuo Suzuki, Faculty of Education, Niigata University and Professor Masami Fukuda, Institute of Low Temperature Science, Hokkaido University for their useful suggestions and encouragements. I am also indebted to Dr. Nobuyuki Takahashi, Hokkaigakuen University, and to Dr. Toshio Sone, Institute of Low Temperature Science, Hokkaido University for their kind suggestions and encouragements.

I must not forget Mr. Takashi Moriyama and the Moriyama's for their grate help in the field survey and constant encouragements.

References

Anderson, J. W. and Stephens, M. A.(1972): Test for randomness of directions against equtorial and bimodal alternatives. Biometrika, 59, 613−621.

Andrews, J. T. and King, C. A. M.(1968): Comparative till fabrics and till fabric variability in a till sheet and a drumlin: A small scale study. Yorkshire Geol. Soc. Proc., 36, 435−461.

Asai, T., Uchida, E. and Kawamura, T.(1986): Dictionary of weather. Heibonsya, Tokyo, 528p. (J)

Beskow, G.(1935): Tjälbidningen och tjällyftningen med särskild hansyn till vägar och järnväger. Sver. geol. Unders. Årsbok. 26(3), Ser.C, 1−242.

Curray, J. R.(1956): The analysis of two-dimensional orientation data. Jour. Geol., 64, 117−131.

Drake, L. D.(1974): Till fabric control by clast shape. Geol. Soc. America Bull. 85, 247−250.

Endo, R.(1977): Fossil periglacial phenomena in the Upper Kitakami River. Abstr. Conf. Assoc. Japan. Geogrs., No.12, 22−23. (J)

Gardner, J.(1971): Morphology and sediment characteristics of mountain debris slope in Lake Louise District (Canadian Rockies). Zeitscher. Geomorphol., 15, 390−403.

Giardino, J. R. and Vitek, J. D.(1985): A statistical interpretation of the fabric of a rock glacier. Arct. and Alp. Res., 17, 165−177.

Harris, C.(1972): Processes of soil movement in turf-banked solifluction lobes, Okstindan, northern Norway. Inst. Br. Geogr. Spec. Publ., 4, 155−174.

Harris, C.(1987): Solifluction and related periglacial deposits in England and Wales. Boardman, J.(ed.):

Periglacial process and landforms in Britain and Ireland. Cambridge University Press, Cambridge, 209−223.

Harris, C. and Wright, M. D.(1980): Some last glaciation drifts deposits near Pontypridd, South Wales. Geol. J., 15, 7−20.

Harrison, P. W.(1957): A clay-till fabric: its character and origin. Jour. Geol., 65, 275−308.

Hashimoto, S.(1954): Explanatory text of the geological map of Mikage. Geological Survey of Hokkaido, Hokkaido Development Agency, 1−36. (JE)

Hashimoto, S.(1971): Explanatory text of the geological map of Sahorodake. Geological Survey of Hokkaido, Hokkaido Development Agency, 1−32. (JE)

Higaki, D.(1980): Tephrochronological study of slope deposits in the Northwestern Kitakami Mountains. Sci. Repts. Tohoku Univ., 7the Ser. (Geogr.), 30, 147−156.

Higaki, D.(1987): Chronology of mass movement and slope formation in the Central Kitakami Mountains, Northeast Japan. The Quaternary Research, 26, 27−45. (JE)

Hirakawa, K.(1976): Slopes and its deposits in the Northern Hidaka Mountains, Hokkaido. Abstr. Conf. Assoc. Japan. Geogrs., No.10, 31−32. (J)

Hirakawa, K.(1977): Chronology and evolution of landforms during the Late Quaternary in the Tokachi Plain and adjacent areas, Hokkaido, Japan. Catena, 4, 255−288.

Holmes, C. D.(1941): Till fabric. Geol. Soc. America Bull., 52, 1299−1354.

Inoue, K., Kaneko, K. and Yoshida, M.(1981): Tephrochronological study of Late Pleistocene periglacial phenomena in the Upper Kitakami River Basin, Northeastern Japan. The Quaternary Research, 20, 61−73. (JE)

Iso, N.(1974): Chronology of mass movement in the northwestern part of the Kitakami Mountains. Abstr. Conf. Assoc. Japan. Geogrs., No.6, 110−111. (J)

Iwata, S.(1986): Glacial and periglacial geomorphology: Early stade of the Last Glacial in the Japanese Island. Quaternary Research, Recent Progress of Natural Science in Japan, 11, 45−59.

King, C. A. M.(1966): Techniques in geomorphology. Edward Arnold, London, 342p.

Koaze, T., Nogami, M. and Iwata, S.(1974): Paleoclimatic significance of fossil periglacial phenomena in Hokkaido, Northern Japan. The Quaternary Research, 12, 177−191. (JE)

Kobayashi, K.(1965): Problems of Late Pleistocene history of Central Japan. International Studies on the Quaternary., Geol. Soc. Amer. Spec. Pap., No.84, 367−391.

Kondo, Y.(1985): Distribution and origin of tephra layers in Hokkaido. Urban Kubota, 24, 2−3. (J)

Kondo, Y. and Doi, M.(1987): Distribution, stratigraphy, and chemical composition of ferromagnetic minerals of the Tarumai "c1" ash —A consideration on the relationship between the Tarumai "c1" ash and the Tokachi "c1" ash in the Tokachi Plain—. Pedologist, 31, 108−119. (JE)

Konoya, M., Matsui, K. and Tsuchiya, T.(1969): Explanatory text of the geological map of Shintoku. Geological Survey of Hokkaido, Hokkaido Development Agency, 1−27. (JE)

Kruger, J.(1970): Till fabric in relation to direction of ice movement. Geogl. Tidssker., 69, 133−170.

Krumbein, W.C.(1939): Preferred orientation of pebbles in sedimentary deposits. Jour. Geol., 47, 673−706.

Lawson, D. E.(1979): A comparison of the pebble orientations in ice and deposits of the Matanusuka Glacier, Alaska. Jour. Geol., 87, 629−645.

Machida, H.(1980): Tephra and its implications with regard to Japanese Quaternary period. Assoc. Japan. Geogrs(ed.): Geography of Japan, Teikoku Shoin, 29−53.

McArthur, J. L.(1981): Periglacial slope planation in the southern Pennines, England. Biul. Peryglacjalny, No.28, 85−97.

Mills, H. H.(1977): Basal till fabrics of modern alpine glaciers. Geol. Soc. America Bull., 88, 824−828.

Mills, H. H.(1983): Clast-fabric strength in hill slope colluvium as a function of slope angle. Geogr. Ann., 65(A), 255−262.

Mills, H. H.(1984): Clast orientation in Mount St. Helens debris-flow deposits, North Fork Toutle River,

Washington. Jour. Sediment. Petro., 54, 626−634.
Mills, H. H.(1986): Piedmont-cove deposits of Dellwood quad-rangle, Great Smoky Mountains, North Carolina, U.S.A.: Some aspect of sedimentology and weathering. Biul. Peryglacjalny, No.30, 91−109.
Miyagi, T., Hibino, K. and Kawamura, T.(1979): Processes of hillslope denudation and environmental changes during the Holocene around Sendai, Northeast Japan. The Quaternary Research, 18, 143−154. (JE)
Miyagi, T., Hibino, K., Kawamura, T. and Nakagami, K.(1981): Hillslope development under changing environment since 20,000 years B.P. in Northeast Japan. Sci. Repts. Tohoku Univ., 7the Ser. (Geogr.), 31, 1−14.
Mottershead, D. N.(1971): Coastal head deposits between Start Point and Hope Cove, Devon. Field. Stud., 3, 433−453.
Nakayama, T. and Miyagi, T.(1984): Hillslope development and sediment yield under changing environment since 46,000 years B.P. in the Kawadoi Basin, Northeast Japan. Ann. Tohoku Geogr. Assoc., 36, 25−38. (JE)
Nelson, F. E.(1985): A preliminary investigation of solifluction macrofabrics. Catena, 12, 23−33.
Nogami, M., Koaze, T. and Fukuda, M.(1980): Periglacial environment in Japan: Present and past. GeoJournal, 4, 125−132.
Nomura, R. and Tanaka, S.(1989): Geomorphological processes since the Last Glacial Age in inland Hyogo Prefecture. The Quaternary Research, 27, 219−228. (JE)
Oguchi, T.(1986): A possible effect of periglacial processes on the slope development on the Aso caldera wall, Central Kyushu, Japan. Trans. Japanese Geomor. Union, 7, 185−196. (JE)
Ohmori, H.(1979): A statistical approach to asymmetrie in roughness of mountain slope in Japan from the viewpoint of climatic geomorphology. Bull. Dept. Geogr., Univ. Tokyo, No.11, 77−92.
Ono, Y.(1984): Last Glacial paleoclimate reconstructed from glacial and periglacial landforms in Japan. Geogr. Rev. Japan, 57(Ser.B), 87−100.
Ono, Y. and Hirakawa, K.(1975): Glacial and periglacial morphogenetic environments around the Hidaka Range in the Würmian age. Geogr. Rev. Japan, 48, 1−26. (JE)
Saijo, K.(1987): Alluvial cone formation related to climatic change since Latest Pleistocene time in the Northern Kitakami Mountains, Northeastern Japan. Sci. Repts. Tohoku Univ., 7the Ser. (Geogr.), 37, 67−74.
Sawaguchi, S.(1984): Fossil periglacial phenomena in Late Glacial substage in the Kitakami Mountains. Ann. Tohoku Geogr. Assoc, 36, 240−246. (J)
Scheidegger, A. E.(1965): On the statistics of the orientation of bedding planes, grain axes, and similar sedimentological data. U. S. Geol. Prof. Pap., 525-c, 164−167.
Shakesby, R. A.(1981): Periglacial origin of slope deposits near Woolhope in the Welsh Borderland. Cambria, 8, 1−16.
Shimizu, C.(1983): Fossil periglacial slopes on the Chichibubetsu Mountains, Central Japan. Geor. Rev. Japan, 56, 521−534. (JE)
Shimizu, C.(1989): Vertical change of slope stability from Last Glacial to Early Holocene in the southern part of the Yubari Mountains and the western part of the Hidaka Range, Hokkaido, Japan. The Quaternary Research, 28, 159−170. (JE)
Sugawara, K.(1973): Gentle slopes along the Hiranuka River system, Northern Iwate Prefecture. Sci. Repts. Tohoku Univ. 7th Ser. (Geogr.), 23, 39−51.
Suzuki, H., Nogami, M. and Tabuchi, H.(1964): Some observations of fossil periglacial phenomena. The Quaternary Research, 3, 166−177. (JE)
Takada, M.(1986): Fossil periglacial smooth slopes and fossil nivation hollows along the main ridge in the Mikuni Mountains, Central Japan. Geogr. Rev. Japan, 59(Ser.A), 729−749. (JE)
Takada, M.(1987): Fabric analysis of slope deposits by means of eigen value method. Abstr. Conf. Assoc.

Japan Geogr., No.32, 120−121. (J)

Tamura, T. and Miura, O.(1968): The period of slope-instability observed in tephra in a coastal area from Hachinohe City to Kuzi City, Northeastern Japan. Ann. Tohoku Gepgr. Assoc., 20, 69−73. (JE)

Tamura, T. and Miura, O.(1971): Slope deposits in the northern margin of Kitakami Massif, Northeast Japan. The Quaternary Research, 10, 21−30. (JE)

Tanaka, S., Inoue, S. and Nomura, R.(1982): A study on the mechanism and chronology of colluvial slope formation in the drainage basin of the Sugihara River, the southern part of Hyogo Prefecture. Geogr. Rev. Japan, 55, 525−548. (JE)

Tanaka, S., Nomura, R., Inoue, S., Tanaka, T., Tsuchiya, K., Ogura, H. and Takada, K.(1988): Landforms and block streams in the Mineyama Highland at the central part of Hyogo Prefecture, West Japan. Geogr. Rev. Japan, 61(Ser.A), 851−871. (JE)

Tephra Layers Naming Committee in Hokkaido(1982): Tephra layers fell in Hokkaido. Sasaki, T.(ed.), Hokkai Sekihan Press, Sapporo, 23p. (J)

The Ministry of Agriculture and Forestry and The Meteorological Agency (1978): Meteorological agriculture reports of the decade (Showa 41−50). The branch of Sapporo, Japan Meteorological Association, Sapporo, 732p. (J)

Thomas, G. S. P.(1967): Simplified technique for determining two-dimensional orientation strength of till -fabric data. Northern Universities Geog. Jour., 8, 23−27.

Tsujii, T. and Miki, N.(1988): Vegetation of the Karikachi Highland. Reports of natural environment of the Karikachi Highland, Yubunsya, Tokyo, 17−80. (J)

Tsurumi, E. and Nogami, M.(1965): Gentle slope of Mt. Tsukuba and Mt. Kaba. Geogr. Rev. Japan, 38, 526−530. (J)

Umetsu, Y.(1987): C-14 ages of the Eniwa-a pumice-fall deposit (En-a) and the tarumae-d pumice-fall deposit(Ta-d). Ann. Tohoku Geogr. assoc., 39, 141−143. (JE)

Watson, E.(1969): The slope deposits in the Nant Iago valley, near Cader Idris, Wales. Biul. Peryglacjalny, No.18, 263−271.

Watson, E and S.(1967): The periglacial origin of the drifts at Morfa-bychan, near Aberystwyth. Geol. J., 5, 419−440.

Wako, T.(1961): River terraces and gentle slopes along the Shokotsu River, Northeastern Hokkaido. Sci. Repts. Tohoku Univ., 7th Ser. (Geogr.), 10, 39−49.

Wako, T.(1963): Valley features along the Sarugaishi River — A note on block field, cryopediment, and relict red soil in the Kitakami Mountainland. Sci. Repts. Tohoku Univ., 7th Ser. (Geogr.), 12, 53−69.

Wako, T.(1966): Chronological study on gentle slope formation in Northeast Japan. Sci. Repts. Tohoku Univ., 7th Ser. (Geogr.), 15, 55−94.

Willson, P.(1981): Periglacial valley-fill sediments at Edale, North Derbyshire. East Midlands Geographer, 7, 263−271.

Win Maung and Toyoshima, M.(1989): Slope modification during the Late Pleistocene in the Natori River drainage Basin. Ann. Tohoku Geogr. Assoc., 41, 1−14.

Woodcock, N. H.(1977): Specification of fabric shapes using an eigen value method. Geol. Soc. America Bull., 88, 1231−1236.

Yamamoto, K.(1987): Gentle slopes and fluvial terraces around Mt. Syokanbetsudake, Hokkaido. Ann. Tohoku Geogr. Assoc., 39, 81−97. (JE)

Yamamoto, K.(1989a): Chronology of Holocene periglacial slope deposits in the Northern Hidaka Mountains, Hokkaido, Japan. The Quaternary Research, 28, 139−157. (JE)

Yamamoto, K.(1989b): Clast-fabric strength in periglacial slope deposits as a function of clast size and shape. Jour. Environ. Sci., Hokkaido Univ., 12(2), 187−197.

Yamamoto, K.(1990): Quantitative characteristics of periglacial slope deposits in the Northern Hidaka Mountains, Hokkaido, Japan. Geogr. Rev. Japan, 63(Ser.A), 285−314. (JE)

Yanagimachi, O.(1987): Last Glacial paleoclimate reconstructed from glacial and periglacial landforms in Central Japan. The Quaternary Research, 25, 295−303. (JE)
Zingg, Th.(1935): Beitrag zur Schotteranalyse. Schweizer. Mineralog. u. Petrog. Mitt., 15, 38−140.

(J) : in Japanese
(JE): in Japanese with English abstract